



Observation and measurements of the production of prompt and non-prompt J/ψ mesons in association with a Z boson in pp collisions at $\sqrt{s}=8$ TeV with the ATLAS detector

The Harvard community has made this article openly available. [Please share](#) how this access benefits you. Your story matters

Citation	ATLAS Collaboration. 2015. "Observation and measurements of the production of prompt and non-prompt J/ψ mesons in association with a Z boson in pp collisions at $\sqrt{s}=8$ TeV with the ATLAS detector." The European Physical Journal C 75 (5) (May). doi:10.1140/epjc/s10052-015-3406-9.
Published Version	doi:10.1140/epjc/s10052-015-3406-9
Citable link	http://nrs.harvard.edu/urn-3:HUL.InstRepos:33470153
Terms of Use	This article was downloaded from Harvard University's DASH repository, and is made available under the terms and conditions applicable to Other Posted Material, as set forth at http://nrs.harvard.edu/urn-3:HUL.InstRepos:dash.current.terms-of-use#LAA

Observation and measurements of the production of prompt and non-prompt J/ψ mesons in association with a Z boson in pp collisions at $\sqrt{s} = 8$ TeV with the ATLAS detector

ATLAS Collaboration*

CERN, 1211 Geneva 23, Switzerland

Received: 22 December 2014 / Accepted: 15 April 2015 / Published online: 27 May 2015

© CERN for the benefit of the ATLAS collaboration 2015. This article is published with open access at Springerlink.com

Abstract The production of a Z boson in association with a J/ψ meson in proton–proton collisions probes the production mechanisms of quarkonium and heavy flavour in association with vector bosons, and allows studies of multiple parton scattering. Using 20.3 fb^{-1} of data collected with the ATLAS experiment at the LHC in pp collisions at $\sqrt{s} = 8$ TeV, the first measurement of associated $Z + J/\psi$ production is presented for both prompt and non-prompt J/ψ production, with both signatures having a significance in excess of 5σ . The inclusive production cross-sections for Z boson production (analysed in $\mu^+\mu^-$ or e^+e^- decay modes) in association with prompt and non-prompt $J/\psi (\rightarrow \mu^+\mu^-)$ are measured relative to the inclusive production rate of Z bosons in the same fiducial volume to be $(36.8 \pm 6.7 \pm 2.5) \times 10^{-7}$ and $(65.8 \pm 9.2 \pm 4.2) \times 10^{-7}$ respectively. Normalised differential production cross-section ratios are also determined as a function of the J/ψ transverse momentum. The fraction of signal events arising from single and double parton scattering is estimated, and a lower limit of 5.3 (3.7) mb at 68 (95)% confidence level is placed on the effective cross-section regulating double parton interactions.

1 Introduction

In the Standard Model, a single parton–parton interaction can produce a J/ψ meson in association with a Z boson either through a “prompt” QCD subprocess, or through the production of a Z boson with a b -quark and its subsequent decay into a J/ψ (“non-prompt” production). The same classification into prompt/non-prompt applies to any feed-down into J/ψ production from the decays of excited charmonium states (expected to be approximately 20–30% of the total inclusive rate), depending on the production mechanism for those states. In addition, this final state may also result from the production of a Z boson and a J/ψ (either promptly

or non-promptly produced) from two distinct parton–parton interactions within the same proton–proton collision. Previous searches for the related processes $W + \Upsilon(1S)$ and $Z + \Upsilon(1S)$ by CDF saw no evidence for the associated-production of vector-bosons and quarkonia and set limits on the production rate [1,2]. The production of a prompt J/ψ in association with a W boson was observed previously [3] by the ATLAS experiment.

The mechanisms responsible for the production of prompt J/ψ , and indeed all quarkonia, are not fully understood in hadron collisions. While the rate of hadroproduction of the J/ψ [4–7] and $\psi(2S)$ [7–10], as a function of their transverse momentum, p_T , is now modelled well by predictions in the non-relativistic QCD (NRQCD) [11–13] framework up to transverse momenta of 100 GeV, predictions of related observables such as charmonium spin-alignment [14,15] remain challenging to model simultaneously with the production rate, in part due to the number of free parameters which are not calculable and must be constrained from data. The study of additional observables and new final states provides further constraints on the contributions from colour-singlet [16–22] and colour-octet production processes, and their properties. The production of a gauge boson in association with a J/ψ sets a high energy scale for the scattering process and results in an improvement in the perturbative convergence of the calculations [23,24] that has troubled the accuracy of quarkonium production models in the past [25]. Recent literature [24] has suggested that colour-octet contributions should dominate the total production rate and that next-to-leading-order (NLO) contributions enhance the cross-section over leading-order (LO) predictions, while other groups [23] state that colour-singlet processes may be important.

Contributions to the total $Z + J/\psi$ production rate can come from non-prompt J/ψ originating from the decay of a b -hadron. Measurement of this contribution provides a new opportunity for studying heavy-flavour production in association with a Z boson [26,27]. Beyond the study of

* e-mail: atlas.publications@cern.ch

quarkonium production mechanisms, measurement of the $Z + \text{prompt } J/\psi$ rate may be relevant for the study of ZZ^* production in a kinematic regime complementary to that previously studied at the Large Hadron Collider (LHC) [28, 29] where one on-shell Z boson is produced along with a highly virtual boson that fragments into a $c\bar{c}$ pair. Measurement of $Z + \text{prompt } J/\psi$ production also represents an important background to the search for the rare $Z \rightarrow \ell^+ \ell^- J/\psi$ three-body decay [30–32]. In the future, $Z + \text{prompt } J/\psi$ may prove to be a compelling mode for the study of rare decays of the Higgs boson in quarkonia and associated vector-boson decay modes, proposed in Refs. [33, 34] and more recently in Refs. [35, 36]. Such decays have received renewed attention as a promising mode for the study of Higgs boson charm couplings [37] and its CP properties [38], and also as a possible background to $H \rightarrow ZZ^*$ decay [39]. The production of a Z boson in association with a J/ψ can also contribute to the search for new physics [35, 40–43].

In addition to the production of $Z + J/\psi$ via single parton scattering (SPS) processes, double parton scattering (DPS) interactions [44–50] are expected to constitute a significant proportion of the observed signal. While DPS processes are not distinguishable event-by-event from SPS interactions, azimuthal angular correlations between the Z and the J/ψ are expected to be starkly different for the two processes, allowing information on their relative contributions to be extracted. These data can be used to tune the modelling of multiple interactions in other high-energy hadron–hadron processes.

This paper presents a measurement of the cross-section for the associated-production of Z and J/ψ relative to inclusive Z production. The results are shown as *fiducial* cross-section ratios defined in a restricted phase-space of the muons from J/ψ decay, and also as *inclusive* cross-section ratios after correcting for the J/ψ kinematic acceptance of these muons, for the range of J/ψ transverse momentum 8.5–100 GeV and rapidity $|y_{J/\psi}| < 2.1$. The contributions from prompt and non-prompt J/ψ production are presented separately. The cross-section ratio for single parton scattering is obtained after estimating and subtracting the contribution due to double parton scattering. A lower limit on the effective cross-section regulating double parton interactions is presented. Differential cross-section ratios as a function of the transverse momentum p_T of the J/ψ are shown for prompt and non-prompt production, inclusive and DPS modes.

2 The ATLAS detector

The ATLAS detector [51] is a general-purpose detector with a cylindrical geometry¹ and forward–backward symmetric

¹ ATLAS uses a right-handed coordinate system with its origin at the nominal interaction point (IP) in the centre of the detector and the z -axis

coverage in pseudorapidity η . The detector consists of inner tracking detectors, calorimeters and a muon spectrometer, and has a three-level trigger system. The inner tracking detector (ID) is composed of a silicon pixel detector, a semiconductor microstrip detector (SCT) and a transition radiation tracker (TRT). The ID directly surrounds the beam pipe and is immersed in a 2 T axial magnetic field generated by a superconducting solenoid.

The calorimeter system surrounds the solenoid and consists of a highly granular liquid-argon electromagnetic calorimeter (EM) and a steel/scintillator tile hadronic calorimeter. The EM calorimeter has three layers: the first consists of fine-grained strips in the η direction, the second collects most of the energy deposited in the calorimeter by photon and electron showers, and the third provides measurements of energy deposited in the tails of these showers. Two complementary presampler detectors complete the EM, correcting for energy lost in the material before the calorimeter. This fine segmentation provides electron identification in conjunction with the inner detector in the region $|\eta| < 2.5$.

The muon spectrometer (MS) surrounds the calorimeters and consists of three large air-core superconducting magnets (each with eight coils), which generate a toroidal magnetic field. The MS is instrumented in three layers with detectors (monitored drift tubes and cathode strip chambers) that provide precision muon tracking covering $|\eta| < 2.7$ and fast trigger detectors (resistive plate chambers and thin gap chambers) covering the range $|\eta| < 2.4$.

The ATLAS trigger is a three-level system [52] (Level-1, Level-2 and Event Filter) used to reduce the 20 MHz proton bunch collision rate to a several-hundred Hz event transfer rate recorded to mass storage. The system consists of a Level-1 trigger implemented in hardware and a software-based two-stage High Level Trigger (HLT). The Level-1 system provides a rough measurement of lepton candidate position in “regions of interest” (RoI) with a spatial granularity of $\Delta\phi \times \Delta\eta \approx 0.1 \times 0.1$. These RoI are used to seed HLT algorithms that use higher precision MS, ID and EM measurements to reconstruct lepton trigger objects.

3 Event selection and reconstruction

Events are collected by triggers requiring at least one lepton with $p_T > 24$ GeV. These triggers are highly efficient

Footnote 1 continued

along the beam pipe. The x -axis points from the IP to the centre of the LHC ring, and the y -axis points upward. Cylindrical coordinates (r, ϕ) are used in the transverse plane, ϕ being the azimuthal angle around the beam pipe. The pseudorapidity η is defined in terms of the polar angle θ as $\eta = -\ln \tan(\theta/2)$ and the transverse momentum p_T is defined as $p_T = p \sin \theta$. The rapidity is defined as $y = 0.5 \ln((E + p_z)/(E - p_z))$, where E and p_z refer to energy and longitudinal momentum, respectively. The η – ϕ distance between two particles is defined as $\Delta R = \sqrt{(\Delta\eta)^2 + (\Delta\phi)^2}$.

in collecting $Z \rightarrow \ell^+\ell^-$ decays and were not prescaled during the 2012 data-taking period. Triggered events are required to satisfy certain standardised data-quality requirements, which exclude events taken when temporary faults in detector systems compromise the reconstruction. The total integrated luminosity of proton–proton collisions used in this measurement, after data-quality requirements are applied, is 20.3 fb^{-1} .

The final state of this measurement is $Z(\rightarrow \ell^+\ell^-) + J/\psi(\rightarrow \mu^+\mu^-)$, where $\ell = \mu, e$, and therefore candidate events are required to have two pairs of leptons with opposite charge. Each pair of leptons is then fitted to a common vertex, with the invariant mass of the first pair required to be close to the Z boson mass and that of the second pair to be near the J/ψ mass. For events with more than four leptons, all possible combinations of $\ell^+\ell^-$ and $\mu^+\mu^-$ pairs are considered. In rare cases where ambiguous solutions are found, the pairings giving the dilepton combination with mass closest to the particle (Z or J/ψ) world-average mass are chosen.

3.1 Lepton reconstruction

Muons are identified [53] by tracks (or track segments) reconstructed in the MS, matched to tracks reconstructed in the ID. Track reconstruction in the inner detector uses the measurements from the pixel, SCT and TRT detectors. The “inside-out” reconstruction strategy starts by finding a track candidate in the pixel and SCT detectors and then extends the trajectories of successfully fitted tracks to the TRT to reconstruct a full inner detector track. Outside of the TRT acceptance ($|\eta| > 2.0$) only pixel and SCT information is used.

The muon momentum is calculated by statistically combining the information from the ID and the MS, applying a parameterised correction for the energy loss in the calorimeter. Such muons are referred to as *combined muons*. In some cases it is possible to match an ID track to a signal in the MS, but not possible to perform the combination because the MS track segment contains too few hits. In such cases, the ID track is used as an identified muon candidate. Muons that cross only the first layers of MS chambers, either due to low transverse momentum or because they fall in an area of reduced MS acceptance, can be identified in this less stringent category. The inclusion of these *segment-tagged muons* provides useful additional kinematic acceptance at low p_T for the reconstruction of particles with low invariant mass, such as the J/ψ .

Muons originating from the Z boson are required to be combined muons and have $p_T > 15 \text{ GeV}$ and $|\eta| < 2.5$. For the J/ψ muons, one must be combined and the other can either be combined or segment-tagged. At least one of these two muons must have $p_T > 4 \text{ GeV}$. Muons with $|\eta| > 1.3$ are required to have $p_T > 2.5 \text{ GeV}$ and muons with $|\eta| < 1.3$ must have $p_T > 3.5 \text{ GeV}$.

Electrons are reconstructed [54] from energy deposits in the electromagnetic calorimeter that are matched to a track in the inner detector. Candidate electron tracks are fitted using a dedicated tracking algorithm to account for bremsstrahlung energy losses, and the track pattern recognition and global χ^2 fit take into account the electron track hypothesis as an alternative to the default pion hypothesis. Both electrons coming from the Z boson decay need to have $p_T > 15 \text{ GeV}$, $|\eta| < 2.47$ and satisfy the *loose identification* criteria described in Ref. [54].

In order to reject non-prompt leptons from the decay of heavy quarks, electrons from conversions of bremsstrahlung photons and fake electrons from misidentified jets, the leptons that form the Z boson candidate must satisfy isolation requirements based on tracking information. The scalar sum of the transverse momenta of inner detector tracks inside an η – ϕ cone of size $\Delta R = 0.2$ around the lepton, excluding the track associated with the lepton itself, is required to be no more than 15% of the lepton p_T .

At least one of the Z boson candidate’s leptons must have been responsible for firing the trigger. This criterion is assessed by requiring one of the reconstructed muons (electrons) from the boson to be less than $\Delta R < 0.1(0.15)$ from a relevant muon (electron) trigger object. The offline reconstructed p_T of the candidate matching the trigger must satisfy $p_T > 25 \text{ GeV}$. In addition, triggered muons must satisfy $|\eta| < 2.4$ and electrons must satisfy the *medium identification* criteria, as described in Ref. [54].

3.2 $Z + J/\psi$ candidate selection

Same-flavour, opposite-sign lepton pairs are combined to reconstruct the $Z(\rightarrow \ell^+\ell^-)$ and $J/\psi(\rightarrow \mu^+\mu^-)$ candidates. Candidate $Z + J/\psi$ events are retained if the J/ψ invariant mass falls in the range 2.6–3.6 GeV and the Z boson candidate has an invariant mass within 10 GeV of the Z mass world-average value (m_{PDG}^Z) [55]. In addition, the J/ψ candidate is required to satisfy $p_T > 8.5 \text{ GeV}$ and $|y_{J/\psi}| < 2.1$. The measurements in the di-electron and di-muon decay channels of the Z boson are performed in slightly different phase spaces and combined into a common phase-space for measurement of the fiducial production cross-sections as summarised in Table 1. The inclusive phase-space definition is identical except for the omission of requirements on the leptons from the J/ψ decay.

The Z boson and J/ψ lepton pairs are used to build two dilepton vertices. In the case of the J/ψ candidate the ID tracks alone are used in this vertex fit, whereas for the $Z \rightarrow \mu^+\mu^-$ the combined tracks (which are built from hits in both the ID and the MS) are used. For $Z \rightarrow e^+e^-$ decays, ID tracks corrected by a dedicated tracking algorithm are used, as described above. To reduce contamination from pileup, where a Z boson and a J/ψ are produced from two separate

Table 1 Phase-space definition of the measured fiducial production cross-section following the geometrical acceptance of the ATLAS detector

Z boson selection	
$p_T(\text{trigger lepton}) > 25 \text{ GeV}$,	$p_T(\text{sub-leading lepton}) > 15 \text{ GeV}$
$ \eta(\text{lepton from } Z) < 2.5$	
$ m^Z - 91.1876 \text{ GeV} < 10 \text{ GeV}$	
J/ψ selection	
$2.6 < m^{J/\psi} < 3.6 \text{ GeV}$	
$8.5 < p_T^{J/\psi} < 100 \text{ GeV}$, $ \eta_{J/\psi} < 2.1$	
$p_T(\text{leading muon}) > 4.0 \text{ GeV}$, $ \eta(\text{leading muon}) < 2.5$	
$\left\{ \begin{array}{l} \text{either } p_T(\text{sub-leading muon}) > 2.5 \text{ GeV}, 1.3 \leq \eta(\text{sub-leading muon}) < 2.5 \\ \text{or } p_T(\text{sub-leading muon}) > 3.5 \text{ GeV}, \eta(\text{sub-leading muon}) < 1.3 \end{array} \right\}$	

proton–proton collisions in the same proton–proton bunch crossing, the candidate vertices must not be separated in the z-direction by more than 10 mm.

Figure 1a shows a scatter plot of the masses of candidates satisfying these selections. In total, 290 candidate events are selected, of which 139 are observed with $Z \rightarrow \mu^+\mu^-$ decays and 151 with $Z \rightarrow e^+e^-$ decays.

3.3 Inclusive Z candidate selection

An inclusive Z sample is formed by selecting all events that satisfy the Z part of the Z + J/ψ selection, including the trigger requirements. This sample is used in the measurement of the ratio of the Z + J/ψ to Z cross-sections, and in the estimates of double parton scattering and the pileup background in the associated-production sample.

An estimate of the background in the inclusive Z sample is obtained using a mixture of Monte Carlo (MC) models and data-driven techniques. The NLO generator POWHEG (R1556) [56–58], interfaced to PYTHIA (8.160) [59], is used to model the signal, as well as Drell–Yan contributions away from the Z peak and $Z \rightarrow \tau\tau$ or $W \rightarrow \ell\nu$ backgrounds. These samples use the CT10 PDF set [60] and the ATLAS AU2 tune [61]. The LO multi-leg generator SHERPA v1.4.1 [62] is used as an alternative signal model. Top quark processes involving $t\bar{t}$ or single top production are modelled with the NLO generator MC@NLO (4.03) [63,64], interfaced to HERWIG (6.52) [65] for parton showering and JIMMY (4.31) [66] for the underlying-event modelling with the ATLAS AUET2 tune [67] and the CT10 PDFs. The single-top Wt process is modelled with the ACERMC (3.8) [68] generator, using the CTEQ6L1 PDF set [69] and interfaced to PYTHIA (6.42) [70]. Diboson (WZ, WW and ZZ) production is modelled using the HERWIG (6.52) and Jimmy generators with the ATLAS AUET2 tune and the CTEQ6L1 PDF set. The detector response is modelled using the ATLAS simulation infrastructure [71] based on the GEANT4 toolkit [72]. Background contributions arising from multi-jet events and from misidentified leptons are obtained directly from the

data. This is achieved by inverting the isolation requirements on the leptons, providing a multi-jet background template, which can be used for comparison with the Z + J/ψ sample. The total background in the $m_{\text{PDG}}^Z \pm 10 \text{ GeV}$ window is estimated to be $0.4 \pm 0.4 \%$ (including systematic uncertainties), giving a sample of 16.15 million Z boson candidates after background subtraction, of which 8.20 million are observed with $Z \rightarrow \mu^+\mu^-$ and 7.95 million with $Z \rightarrow e^+e^-$. The di-muon to di-electron ratios of the associated-production Z + J/ψ sample and the inclusive Z sample are compared and found to be consistent within statistical uncertainties (0.92 ± 0.11 and 1.03 ± 0.01 , respectively).

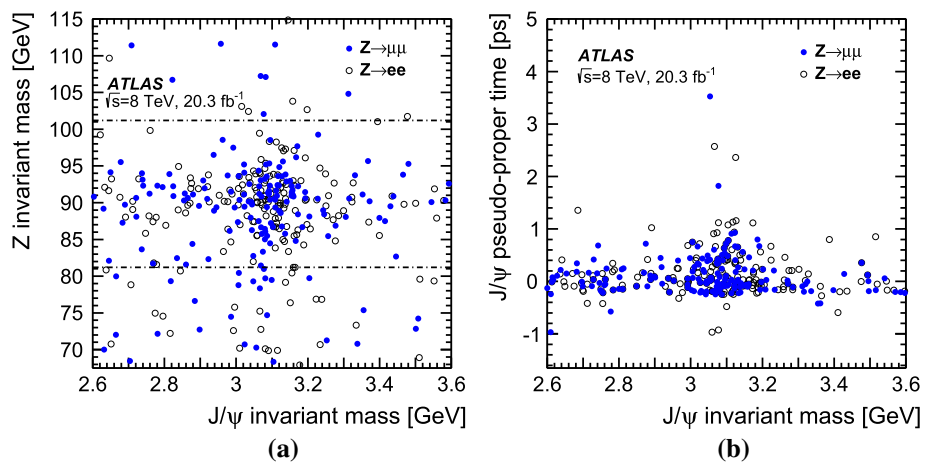
4 Signal and background extraction

The selected Z + J/ψ candidates arise from a variety of signal and background sources. In addition to associated Z boson and J/ψ production from SPS and DPS, Z boson and J/ψ candidates can be produced from pileup. Genuine J/ψ may also be paired with fake Z boson candidates in the same proton–proton collision, or vice-versa. Associated-production candidates may also occur from the production of a Z boson in association with b-quarks, where one of the b-quarks hadronises into a b-hadron that subsequently decays into a J/ψ. This section discusses the means by which the contributions from the prompt and non-prompt signal components are distinguished and separated from the prompt and non-prompt background sources.

4.1 Separation of prompt and non-prompt J/ψ

The $J/\psi \rightarrow \mu^+\mu^-$ candidates originate from prompt and non-prompt production sources, backgrounds with real and fake muon combinations, and real muon pairs producing an invariant mass in the continuum under the J/ψ peak. These various components can be separated into categories using the pseudo-proper time distribution of the J/ψ candidates in combination with the J/ψ invariant mass distribution, where the pseudo-proper time, τ, is defined by:

Fig. 1 Selected $Z + J/\psi$ candidates in **a** Z boson mass versus J/ψ boson mass, with $\ell = e, \mu$ and **b** J/ψ pseudo-proper time versus J/ψ invariant mass, discussed in Sect. 4.1. Z boson candidates decaying to muons are shown with *full circles* and to electrons with *empty circles*. The *horizontal dotted lines* indicate the signal region considered in the analysis



$$\tau := \frac{L_{xy} m^{J/\psi}}{p_T^{J/\psi}} \tag{1}$$

with L_{xy} defined as $L_{xy} = \mathbf{L} \cdot \mathbf{p}_T^{J/\psi} / p_T^{J/\psi}$, \mathbf{L} the vector from the primary vertex to the J/ψ decay vertex, $m^{J/\psi}$ the world-average mass of the J/ψ meson [55], $\mathbf{p}_T^{J/\psi}$ the transverse momentum of the J/ψ and $p_T^{J/\psi} = |\mathbf{p}_T^{J/\psi}|$ its magnitude. The invariant mass and pseudo-proper time of the selected J/ψ candidates produced in association with a Z boson are shown in Fig. 1b.

Promptly produced J/ψ mesons, which are created directly in the hard interaction or feed-down from prompt excited charmonium states produced by the colliding protons, have small pseudo-proper times (distributed around zero due to detector resolution). Background from opposite-sign muon pairs with invariant mass close to the J/ψ mass and short reconstructed pseudo-proper times can mimic prompt J/ψ mesons and forms the prompt background. The second component of the background arises from non-prompt muon pairs, with a vertex displacement that is related to b -hadron decays. Similarly, the signal from non-prompt J/ψ production exhibits a longer pseudo-proper time distribution reflecting the lifetime of b -hadrons, although the distributions of non-prompt signal and background are not necessarily equal. In total, four terms are used for signal and background to fit the pseudo-proper time distribution simultaneously with the invariant mass distribution of the muon pair. The mass regions either side of the J/ψ mass peak are used to constrain the background components.

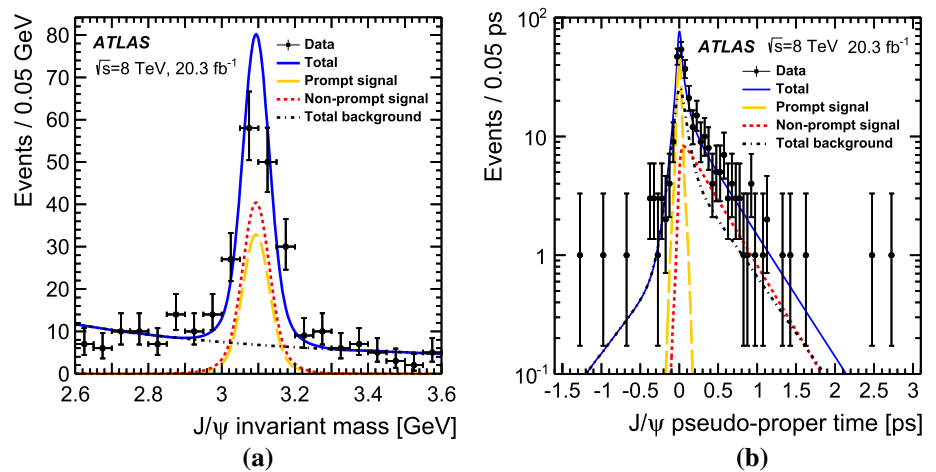
The pseudo-proper time of the signal prompt component is modelled by a double Gaussian distribution. For the background prompt component, a double-sided exponential convolved with the prompt signal function, accounting for resolution effects, is used. The non-prompt signal component is modelled with a single-sided exponential convolved with the prompt signal function and for the non-prompt background component the sum of a single-sided and a double-

sided exponential convolved with the signal function is used. The dimuon invariant mass is modelled with a double Gaussian distribution both for the prompt and non-prompt signal components and exponential functions for the backgrounds (again, prompt and non-prompt). The fit is performed in two separate rapidity regions, the barrel ($|y_{J/\psi}| < 1.0$) and the endcap ($1.0 < |y_{J/\psi}| < 2.1$). The mass resolution is different between the two regions, due to increased multiple scattering and the decrease of the magnetic field integral at high rapidity.

In order to improve the stability of the fit process, the pseudo-proper time and invariant mass of the associated-production J/ψ candidates are fitted simultaneously with a sample of 100 k inclusive J/ψ candidates, selected with the same requirements on the J/ψ and its daughter muons as applied to the $Z + J/\psi$ signal sample (see Table 1). The parameters that determine the shape of the pseudo-proper time and invariant mass distributions are linked between the two samples in this fit, leaving only the normalisations free between the two samples. Figure 2 shows the mass and pseudo-proper time distributions of the J/ψ candidates, produced in association with a Z boson, with the signal and background fits. Applying the fit model to the sample of Z bosons produced in association with a J/ψ candidate results in 56 ± 10 promptly produced J/ψ mesons and 95 ± 12 non-prompt.

After the fit is performed in the J/ψ mass and pseudo-proper time, the sPlot tool [73] is used to assign a weight to each event for each of the components included in the fit model (prompt signal, non-prompt signal, prompt background and non-prompt background). This technique allows the determination of distributions of observables associated with a specific contribution, e.g. prompt J/ψ , while removing the contamination from the other components. As the sPlot technique relies on the assumption that the control variable is uncorrelated with the discriminating variables, the correlations between the J/ψ mass and pseudo-proper time,

Fig. 2 Projections of the unbinned mass and pseudo-proper time maximum-likelihood fit in **a** invariant mass and **b** pseudo-proper time of the associated-production sample. The fit is used to extract the prompt and non-prompt signal fractions and is performed in two rapidity regions: $|y_{J/\psi}| < 1.0$ and $1.0 < |y_{J/\psi}| < 2.1$. The results are combined, presenting the mass and pseudo-proper time of all candidates inside the analysis phase-space



on one side, and the variables that the weights will be applied to, on the other, were checked, and found to be negligible. The invariant mass distribution of Z boson candidates, after application of the sPlot weights, is shown in Fig. 3a, b for prompt J/ψ and non-prompt J/ψ events, respectively.

4.2 Properties of the Z boson candidates

Signal and multi-jet background templates for the dilepton mass were extracted separately for $Z \rightarrow e^+e^-$ and $Z \rightarrow \mu^+\mu^-$ from the POWHEG MC generator described in Sect. 3.3 and the data. The signal templates are parameterised with a Gaussian distribution convolved with a Breit–Wigner function, with an additional Gaussian, with smaller mean value compared to the core Gaussian, to model the radiative tails. The multi-jet templates are modelled with an exponential function. The normalisations of the two templates are extracted from a fit to the sPlot-weighted Z invariant mass distributions (Fig. 3). The numbers of background events estimated in the Z signal region, defined as $m_{\text{PDG}}^Z \pm 10$ GeV, are 0 ± 4 (1 ± 4) and 1 ± 5 (0 ± 5) for the $Z \rightarrow e^+e^-$ ($\mu^+\mu^-$) candidates associated with prompt and non-prompt J/ψ , respectively, supporting the hypothesis that the sample is dominated by genuine $Z + J/\psi$ events. The background estimation procedure was verified with toy MC simulation.

4.3 Pileup background

During the 2012 data-taking period the average number of pp interactions per bunch crossing at ATLAS was 20.7. While the most likely scenario is that all but one of these inelastic collisions are low- p_T background events, there is a certain probability that two or more of these produce a hard scatter. Of these cases, some produce a Z from one scatter, and a J/ψ from another. To exclude as many as possible of these background events, the two dilepton vertices are required to be separated along the z -axis by less than 10 mm. The remain-

ing contamination can be estimated using four ingredients: the spread of the beam spot in z for the data-taking period of relevance; the J/ψ production cross-sections (prompt or non-prompt) from pp collisions at 8 TeV; the number of Z candidates; and the mean number of inelastic interactions per proton–proton bunch crossing, $\langle \mu \rangle$. This latter quantity is calculated from the instantaneous luminosity, \mathcal{L} , as $\langle \mu \rangle = \mathcal{L} \sigma_{\text{inel}} / n_b f_r$, where σ_{inel} is the pp inelastic cross-section (equal to 73 mb [74]), n_b is the number of colliding bunches and f_r is the LHC revolution frequency.

To estimate the mean number of pileup collisions occurring within 10 mm of a given Z vertex, an MC procedure is used. A number of pileup vertices are sampled from the luminosity-weighted distribution of $\langle \mu \rangle$. These vertices are distributed according to a Gaussian function with width 48 ± 3 mm, equal to the measured width of the proton beam spread in the z -coordinate. The number of additional vertices which lie within 10 mm of a randomly selected vertex, is determined to be $N_{\text{extra}} = 2.3 \pm 0.2$.

As it has been verified that the J/ψ reconstruction efficiency is independent of the number of interactions per bunch crossing, the probability for a J/ψ to be produced at a given pileup vertex is

$$P_{J/\psi}^{ij} = \sigma_{J/\psi}^{ij} / \sigma_{\text{inel}} \quad (2)$$

where $\sigma_{J/\psi}^{ij}$ is the cross-section for J/ψ production in the appropriate $p_T(i)$ and rapidity (j) bin. Although $\sigma_{J/\psi}^{ij}$ has not been measured in the fiducial region used in this measurement at centre-of-mass energies of $\sqrt{s} = 8$ TeV, it can be estimated using an existing non-prompt J/ψ fraction measurement at $\sqrt{s} = 7$ TeV [4] and the fixed-order next-to-leading-logarithm [75, 76] (FONLL) prediction for the non-prompt J/ψ cross-section at $\sqrt{s} = 8$ TeV. This extrapolation to 8 TeV is based on the observation [4] that the variation in the ratio of non-prompt to prompt J/ψ production with p_T appears to be independent of the collision energy, and also on

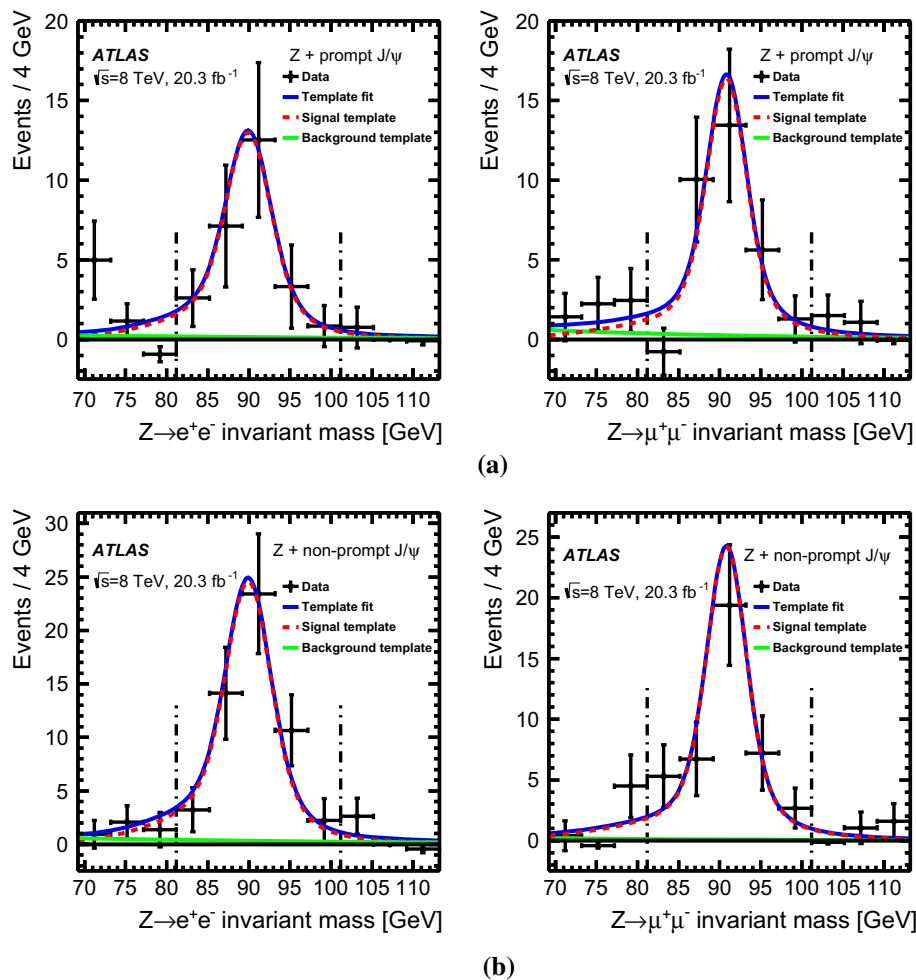


Fig. 3 $Z \rightarrow e^+e^-$ (left) and $Z \rightarrow \mu^+\mu^-$ (right) candidate invariant mass distributions after the application of the sPlot weights coming from the **a** prompt and **b** non-prompt J/ψ component of the fit. Projections of the unbinned maximum likelihood template fit, for the signal and

background components derived from MC simulation and data respectively, are overlaid on the sPlot-weighted distributions. The vertical dot-dashed lines indicate the signal region considered in the analysis

the excellent agreement between the ATLAS measurement and the FONLL predictions of the non-prompt cross-section.

The number of pileup candidates can be evaluated using the number of Z candidates in the fiducial region, N_Z , according to $N_{\text{pileup}}^{ij} = N_{\text{extra}} N_Z P_{J/\psi}^{ij}$, giving a total of $\sum_{i,j} N_{\text{pileup}}^{ij} = 5.2^{+1.8}_{-1.3}$ and $2.7^{+0.9}_{-0.6}$ events in the prompt and non-prompt samples, respectively. The uncertainty on the final result includes contributions from the estimated J/ψ cross-section at $\sqrt{s} = 8$ TeV, the number of inclusive Z events and the number of extra vertices. The dependence of $\langle \mu \rangle$ and $P_{J/\psi}$ on σ_{inel} cancels in the determination of N_{pileup} .

4.4 Double parton scattering

The DPS contribution to the $Z + J/\psi$ sample is counted as part of the signal. The effective cross-section for double parton interactions σ_{eff} measured by ATLAS in $W + 2$ -jet events [77], and the $pp \rightarrow J/\psi$ prompt and non-prompt

cross-sections, are used to estimate the number of signal candidates from this source. Based on the assumptions that σ_{eff} is process-independent, and that the two hard scatters are uncorrelated, for a collision where a Z boson is produced, the probability that a J/ψ is produced in addition due to a second hard process is

$$P_{J/\psi|Z}^{ij} = \sigma_{J/\psi}^{ij} / \sigma_{\text{eff}} \tag{3}$$

where σ_{eff} is taken to be $\sigma_{\text{eff}} = 15 \pm 3$ (stat.) $^{+5}_{-3}$ (sys.) mb according to the ATLAS measurement. The estimated numbers of DPS events in the associated-production $Z + J/\psi$ sample are $11.1^{+5.7}_{-5.0}$ for the prompt component and $5.8^{+2.8}_{-2.6}$ for the non-prompt component. Uncertainties from the J/ψ cross-section at $\sqrt{s} = 8$ TeV, the number of inclusive Z events and the DPS effective cross-section contribute to the total uncertainty.

Figure 4 shows the azimuthal angle between the Z boson and the J/ψ momentum vectors, $\Delta\phi$, after the application of

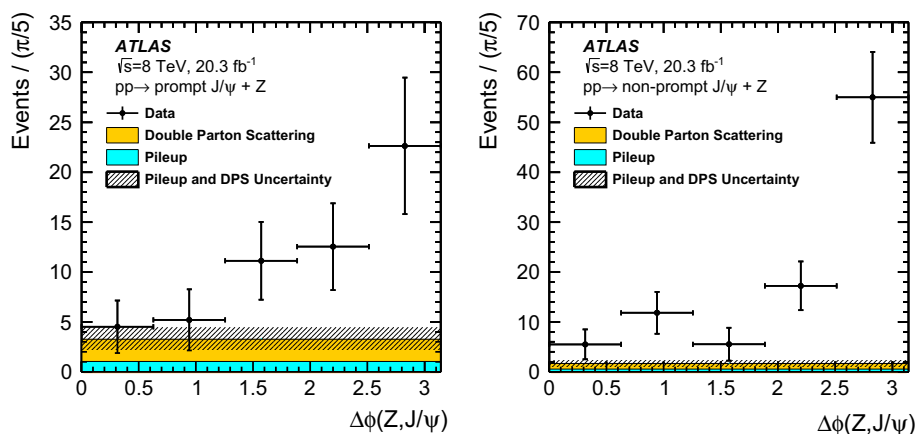


Fig. 4 Azimuthal angle between the Z boson and the J/ψ meson after the application of the sPlot weights to separate the prompt (*left*) and non-prompt (*right*) yield from background contributions. The esti-

sPlot weights to separate the prompt and non-prompt J/ψ signal components from each other and from background sources. The estimated contributions of double parton scattering and pileup to the observed signal yields for prompt and non-prompt production are also overlaid. DPS events are expected to be distributed uniformly in $\Delta\phi$ because the Z and the J/ψ are produced by two independent processes. On the contrary, SPS events are expected to display a back-to-back correlation of the Z and the J/ψ ($\Delta\phi = \pi$) since the two particles come from a single interaction of two partons. This back-to-back behaviour is smeared by the presence of additional gluons in the final state, radiation from the leptons, detector effects and by the intrinsic properties of the protons; the measured data are consistent with a combination of a smeared $\Delta\phi = \pi$ peak from SPS and a flat DPS contribution with σ_{eff} taken from the ATLAS $W + 2$ -jet measurement.

4.5 Detector effects and acceptance corrections

The efficiency for reconstructing muons in the ATLAS detector is very high [53] and depends on the kinematics of the muon. In order to correct the measurements for detector effects, a per-event weight is applied, based on the pseudorapidity and transverse momentum of both muons coming from the J/ψ decay. These weights are extracted using large inclusive $J/\psi \rightarrow \mu^+\mu^-$ and $Z \rightarrow \mu^+\mu^-$ data samples and have been validated with MC simulation [53]. Small inefficiencies resulting from the requirement on separation of Z and J/ψ vertices are corrected using MC simulations.

It was verified using MC simulation that detector resolution effects causing reconstructed Z boson candidates to migrate in and out of the phase space defined in Table 1 do not produce visible effects on the measured relative production rates.

mated DPS (yellow band) and pileup (cyan band) contributions to the observed data are overlaid. The hashed region show the DPS and pileup uncertainties added in quadrature

In addition to corrections applied for reconstruction efficiency (approximately 90% depending on the p_T of the J/ψ), the detector acceptance needs to be taken into account. The spin-alignment profile of the J/ψ meson produced in association with a Z boson might be different from the known profile of inclusive J/ψ mesons [78]. The modified angular distributions of muons from the decay of alternatively-polarised J/ψ mesons can cause changes in acceptance in the fiducial region defined by the selection requirements (see Table 1). For various extreme polarisation states of the J/ψ [79], the J/ψ rate is corrected for muons that fall outside the detector acceptance in transverse momentum and pseudorapidity.

5 Systematic uncertainties

Systematic uncertainties coming from the fit are calculated by varying the probability density functions for the J/ψ mass and pseudo-proper time distributions. In addition to the model described in Sect. 4, an alternative model was used, changing the parameterisation for the mass and lifetime resolution and the shapes of the background components. This model parameterised the mass with a Gaussian function for the J/ψ signal and exponential (or polynomial) functions for the combinatorial background, and parameterised the pseudo-proper time with the sum of a Gaussian and a double-sided exponential function convolved with a Gaussian resolution function for the prompt J/ψ and prompt combinatorial background component, and an exponential function convolved with a Gaussian resolution function for the non-prompt J/ψ and non-prompt combinatorial background. The shape-related parameters are linked between the $Z + J/\psi$ sample and the inclusive J/ψ sample in the model used for the signal extraction. This assumption neglects the possible

Table 2 Summary of experimental systematic uncertainties

Source	Prompt (%)		Non-prompt (%)	
	$ y_{J/\psi} < 1.0$	$1.0 < y_{J/\psi} < 2.1$	$ y_{J/\psi} < 1.0$	$1.0 < y_{J/\psi} < 2.1$
Fit procedure	3	3	4	8
Z boson kinematics	1	1	1	1
$\mu_{J/\psi}$ efficiency	1	1	1	1
Vertex separation	7	16	2	15

difference in kinematics between J/ψ mesons that are produced inclusively and J/ψ mesons produced in association with a Z boson and needs to be taken into account. This effect is evaluated by removing the link between the parameters and repeating the fit, using the main fit model and the alternative considered for the systematic study. The systematic uncertainty associated with the fit procedure was determined with a toy MC simulation technique. A large number of simulated data samples were generated for the two rapidity bins and then fitted with all the available fit procedures. The uncertainties were evaluated from the maximal variation in mean yield extracted from each of the three fit models, relative to the nominal model. This uncertainty was found to be 3% for prompt production and 4–8% (depending on the rapidity of the J/ψ candidate) for non-prompt production.

In the measurement of the cross-section ratios, it is assumed that the efficiency and acceptance for the Z boson are the same when the Z is produced in association with a J/ψ as when it is produced inclusively. In the absence of reliable signal Monte Carlo samples for the SPS or DPS processes, systematic uncertainties that arise from this assumption are calculated using a data-driven approach. The reconstruction and trigger efficiencies calculated for the associated-production data sample and an inclusive Z sample, re-weighted to match the observed $Z + J/\psi$ p_T spectrum, are compared. The non-cancellation of efficiencies and acceptance between inclusively-produced Z bosons and those produced in association with a J/ψ is found to be (1 ± 1) %.

The reconstruction efficiencies of the J/ψ muons used for the correction and calculation of the inclusive cross-section are extracted from $Z \rightarrow \mu^+\mu^-$ and $J/\psi \rightarrow \mu^+\mu^-$ decays using a tag-and-probe method [53]. These efficiencies and their uncertainties depend on the muon pseudorapidity and p_T and are applied to the data in the form of two-dimensional maps. In order to calculate the systematic uncertainty, each bin of the efficiency map is allowed to vary within its uncertainty and the effect on the extracted yield is examined. The systematic uncertainty from the muon reconstruction efficiency is of the order of 1%.

In the selection requirements applied to the dataset, the Z and J/ψ vertices are required to be within 10 mm along

the z-axis. This choice could cause a potential bias in the measurement of the prompt and the non-prompt yield since it affects the pseudo-proper time distribution of the J/ψ . This cut is loosened to 20 mm and the difference in the extracted yield, again assessed using data-driven pseudoexperiments, determined after the pileup subtraction and correction for the expected change in signal efficiency from MC simulations, is taken as a systematic uncertainty. This variation is found to be between 2 and 16%, depending on the rapidity of the J/ψ .

A possible contribution from the decay of $Z \rightarrow \ell^+\ell^- J/\psi$ [30–32] might lead to an enhancement of the measured yields over contributions from $Z + J/\psi$. This possible enhancement is studied by considering the change in the prompt yield after subtracting events for which the mass of the $\ell^+\ell^- J/\psi$ lies within 10 GeV of the world-average value of the Z boson mass; the effect was found to be negligible.

The kinematic acceptance of Z bosons is dependent on the average Z boson polarisation. Due to the high detector acceptance for Z boson decays, the possible effect of modification of the average polarisation of the Z boson in associated production relative to inclusive production is considered negligible in this study.

Uncertainties linked with the luminosity measurement and the Z trigger efficiencies cancel in the ratio of $Z + J/\psi$ to inclusive Z cross-sections. The contributions of all non-negligible systematic uncertainties are summarised in Table 2.

6 Results

The results of the two-dimensional maximum likelihood fit are shown in Table 3 for the two rapidity regions.

The signal significances for both the prompt and non-prompt final states were calculated by performing pseudoexperiments and taking into account the pileup background contribution. Events were generated with a di-muon invariant mass and a pseudo-proper time according to the background-only hypothesis, then fitted with the background-only and signal+background hypotheses, which allowed the likelihood ratio of the two hypotheses to be calculated and compared with the likelihood ratio of the data. Using this

Table 3 Results of the fit with statistical (first) and systematic (second) uncertainties. The total number of background events is measured in the $2.6 < m_{\mu\mu} < 3.6$ GeV window. The last column presents the expected

number of pileup events for the prompt and non-prompt component, and their statistical uncertainty

Process	$ y_{J/\psi} < 1.0$	$1.0 < y_{J/\psi} < 2.1$	Total	
			Events found	From pileup
Prompt signal	$24 \pm 6 \pm 2$	$32 \pm 8 \pm 5$	$56 \pm 10 \pm 5$	$5.2^{+1.8}_{-1.3}$
Non-prompt signal	$54 \pm 9 \pm 3$	$41 \pm 8 \pm 7$	$95 \pm 12 \pm 8$	$2.7^{+0.9}_{-0.6}$
Background	$61 \pm 11 \pm 6$	$77 \pm 13 \pm 7$	$138 \pm 17 \pm 9$	

method, the background-only hypothesis for both the prompt and non-prompt final states was excluded at 5σ significance. To allow for an assessment of the significance beyond that possible using pseudoexperiments, the significance was extracted as $\sqrt{-2 \times \ln \mathcal{L}}$, where \mathcal{L} is the likelihood ratio of the background-only and signal plus background hypotheses. Both methods yielded consistent results, the outcome being that the background-only hypothesis is excluded at 5σ significance for the $Z +$ prompt J/ψ final state, and 9σ significance for the non-prompt J/ψ signature.

After background subtraction, significant signals for the associated-production of $Z +$ prompt J/ψ and $Z +$ non-prompt J/ψ are observed. The background-subtracted $Z +$ prompt J/ψ and $Z +$ non-prompt J/ψ candidate yields are corrected for detector efficiency effects, and production cross-sections are determined in a restricted fiducial volume given by the criteria in Table 1. The measured $Z + J/\psi$ cross-sections are normalised by the inclusive Z production cross-section determined in the same Z boson fiducial volume as the $Z + J/\psi$ measurement, benefiting from the cancellation of some systematic uncertainties to allow a more precise determination of production cross-sections.

6.1 Fiducial cross-section ratio measurements

The fiducial cross-section ratio, as described in Table 1 (normalised to the inclusive Z boson cross-section), $R_{Z+J/\psi}^{\text{fid}}$, is measured without applying corrections for the incomplete geometric acceptance for the J/ψ decay muons, nor for the Z boson acceptance and is defined as²:

$$R_{Z+J/\psi}^{\text{fid}} = \mathcal{B}(J/\psi \rightarrow \mu^+\mu^-) \frac{\sigma_{\text{fid}}(pp \rightarrow Z + J/\psi)}{\sigma_{\text{fid}}(pp \rightarrow Z)}$$

$$= \frac{1}{N(Z)} \sum_{p_T \text{ bins}} [N^{\text{ec}}(Z + J/\psi) - N_{\text{pileup}}^{\text{ec}}],$$

where $\mathcal{B}(J/\psi \rightarrow \mu^+\mu^-)$ is the branching ratio for the decay $J/\psi \rightarrow \mu^+\mu^-$ [55], $N^{\text{ec}}(Z + J/\psi)$ is the yield of $Z +$

(prompt/non-prompt) J/ψ events after corrections for J/ψ muon reconstruction efficiency, $N(Z)$ is the background-subtracted yield of inclusive Z events and $N_{\text{pileup}}^{\text{ec}}$ is the efficiency-corrected expected pileup background contribution in the fiducial J/ψ acceptance. For prompt and non-prompt production, the cross-section ratios were measured to be:

$$\text{prompt: } {}^{\text{p}}R_{Z+J/\psi}^{\text{fid}} = (36.8 \pm 6.7 \pm 2.5) \times 10^{-7}$$

$$\text{non-prompt: } {}^{\text{np}}R_{Z+J/\psi}^{\text{fid}} = (65.8 \pm 9.2 \pm 4.2) \times 10^{-7}$$

for $8.5 \text{ GeV} < p_T^{J/\psi} < 100 \text{ GeV}$ and $|y_{J/\psi}| < 2.1$, where the first uncertainty is statistical and the second is systematic in origin. The results are summarised in Fig. 5. Production of a $J/\psi \rightarrow \mu^+\mu^-$ meson in association with a Z boson occurs approximately ten times per million Z bosons produced in the fiducial volume defined in Table 1.

The differential fiducial cross-section ratios $dR_{Z+J/\psi}^{\text{fid}}/dy$ for prompt and non-prompt $Z + J/\psi$ production are also determined in two bins, for central J/ψ rapidities ($|y_{J/\psi}| < 1$) and forward J/ψ rapidities ($1 < |y_{J/\psi}| < 2.1$), and are reported in Table 4.

6.2 Inclusive cross-section ratio measurements

Theoretical predictions for the production rates of J/ψ are often presented within a limited J/ψ phase-space, but without any kinematic requirements on the decay products. To allow comparison of theoretical and experimentally measured production rates, corrections derived from simulation are applied to the measured fiducial cross-sections to account for the geometrical acceptance loss due to the muon p_T and η requirements detailed in Table 1. These corrections are dependent on the p_T and rapidity of the J/ψ meson and on the angular distribution of the dilepton system in the decay of prompt J/ψ . The angular distribution is dependent on the spin-alignment state of the produced J/ψ mesons. While the spin-alignment has been measured for inclusive prompt J/ψ production [78] and found to be consistent with an isotropic angular distribution hypothesis, J/ψ produced

² The equation used is slightly different to that used in the $W + J/\psi$ analysis [3], which was normalised to unit rapidity.

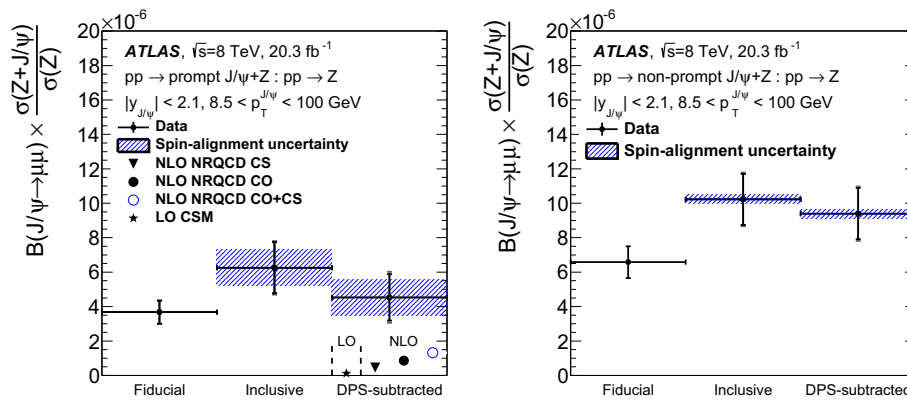


Fig. 5 Production cross-sections ratios of J/ψ in association with a Z boson, relative to inclusive Z production, for prompt and non-prompt J/ψ production. The first point indicates the total integrated cross-section ratio measured in the defined fiducial volume, the second point shows the same quantity corrected for detector acceptance effects on the J/ψ reconstruction, and the third point illustrates the corrected

cross-section ratio after subtraction of the double parton scattering contribution as discussed in the text. The *inner error bars* represent statistical uncertainties and the *outer error bars* represent statistical and systematic uncertainties added in quadrature. Also shown are LO [23] and NLO [24] predictions for the inclusive SPS production rates in the colour-singlet (CS) and colour-octet (CO) formalisms

Table 4 The fiducial, inclusive (SPS + DPS) and DPS-subtracted differential cross-section ratio $dR_{Z+J/\psi}/dy$ as a function of $y_{J/\psi}$ for prompt and non-prompt J/ψ

$y_{J/\psi}$	Fiducial ($\times 10^{-7}$) value \pm (stat) \pm (syst)	Inclusive ($\times 10^{-7}$) value \pm (stat) \pm (syst) \pm (spin)	DPS-subtracted ($\times 10^{-7}$) value \pm (stat) \pm (syst) \pm (spin)
Prompt cross-section ratio			
$ y_{J/\psi} < 1.0$	$7.6 \pm 2.1 \pm 0.5$	$13.9 \pm 4.6 \pm 0.8 \pm 3.4$	$9.4 \pm 4.6 \pm 1.1 \pm 3.4$
$1.0 < y_{J/\psi} < 2.1$	$9.8 \pm 2.2 \pm 1.3$	$15.8 \pm 4.5 \pm 2.1 \pm 3.5$	$12.0 \pm 4.5 \pm 2.7 \pm 3.5$
Non-prompt cross-section ratio			
$ y_{J/\psi} < 1.0$	$18.0 \pm 3.3 \pm 0.6$	$29.9 \pm 5.0 \pm 0.9 \pm 1.1$	$27.8 \pm 5.0 \pm 1.0 \pm 1.1$
$1.0 < y_{J/\psi} < 2.1$	$13.5 \pm 2.9 \pm 1.9$	$19.3 \pm 5.0 \pm 2.1 \pm 0.8$	$17.5 \pm 5.0 \pm 2.1 \pm 0.8$

in association with a Z boson may have a different polarisation, leading to different decay kinematics. The central value is determined assuming unpolarised decays, with the effect of the most extreme polarisation scenarios assigned as a systematic uncertainty. The largest change in acceptance obtained considering the extreme polarisation scenarios is used as an additional systematic uncertainty in the determination of inclusive production cross-section for prompt J/ψ production, and is equal to $\pm 24\%$ for $|y_{J/\psi}| < 1.0$ and $\pm 23\%$ for $1.0 < |y_{J/\psi}| < 2.1$. The range of variation for non-prompt production was reduced to about 10% of the full range as suggested by the measurement of the J/ψ polarisation in b -decays [80] and the uncertainty was found to be $\pm 3\%$ for $|y_{J/\psi}| < 1.0$ and $\pm 2\%$ for $1.0 < |y_{J/\psi}| < 2.1$.

The acceptance-corrected inclusive production cross-section ratio, $R_{Z+J/\psi}^{\text{incl}}$, is defined as:

$$R_{Z+J/\psi}^{\text{incl}} = \mathcal{B}(J/\psi \rightarrow \mu^+ \mu^-) \frac{\sigma_{\text{incl}}(pp \rightarrow Z + J/\psi)}{\sigma_{\text{incl}}(pp \rightarrow Z)}$$

$$= \frac{1}{N(Z)} \sum_{p_T \text{ bins}} [N^{\text{ec+ac}}(Z + J/\psi) - N_{\text{pileup}}^{\text{ec+ac}}],$$

where $N^{\text{ec+ac}}(Z + J/\psi)$ is the yield of $Z +$ (prompt/non-prompt) J/ψ events after J/ψ acceptance corrections and efficiency corrections for both muons from the J/ψ decay, $N_{\text{pileup}}^{\text{ec+ac}}$ is the expected pileup contribution in the full J/ψ decay phase-space, and other variables are the same as for $R_{Z+J/\psi}^{\text{fid}}$. The production cross-section ratio is measured to be:

$$\text{prompt: } R_{Z+J/\psi}^{\text{incl}} = (63 \pm 13 \pm 5 \pm 10) \times 10^{-7}$$

$$\text{non-prompt: } R_{Z+J/\psi}^{\text{incl}} = (102 \pm 15 \pm 5 \pm 3) \times 10^{-7}$$

for $8.5 \text{ GeV} < p_T^{J/\psi} < 100 \text{ GeV}$ and $|y_{J/\psi}| < 2.1$, where the first uncertainty is statistical, the second uncertainty is systematic, and the third uncertainty is due to the unknown J/ψ spin-alignment in $Z + J/\psi$ production.

The differential fiducial cross-section ratios $dR_{Z+J/\psi}^{\text{incl}}/dy$ for prompt and non-prompt $Z + J/\psi$ production are also determined in two bins, for central J/ψ rapidities ($|y_{J/\psi}| < 1$) and forward J/ψ rapidities ($1 < |y_{J/\psi}| < 2.1$), and are reported in Table 4.

6.3 Comparison with theoretical calculations and double parton scattering contributions

Double parton scattering interactions are expected to contribute significantly to the measured inclusive production cross-sections. Using the relation in Eq. 3 and a σ_{eff} value of 15 ± 3 (stat.) $_{-3}^{+5}$ (syst.) mb, an estimate of the double parton scattering component of the observed signal for both prompt and non-prompt production can be derived in any kinematic interval of the measurement. Subtracting this DPS contribution from $R_{Z+J/\psi}^{\text{incl}}$ gives an estimate $R_{Z+J/\psi}^{\text{DPS sub}}$ of the single parton scattering cross-section ratio for prompt J/ψ production:

$$^{\text{p}}R_{Z+J/\psi}^{\text{DPS sub}} = (45 \pm 13 \pm 6 \pm 10) \times 10^{-7}$$

and non-prompt J/ψ production:

$$^{\text{np}}R_{Z+J/\psi}^{\text{DPS sub}} = (94 \pm 15 \pm 5 \pm 3) \times 10^{-7}$$

for $8.5 \text{ GeV} < p_{\text{T}}^{J/\psi} < 100 \text{ GeV}$ and $|y_{J/\psi}| < 2.1$, where the first uncertainty is statistical, the second uncertainty is systematic, taking into account uncertainties from the DPS estimate, and the third uncertainty is due to the unknown J/ψ spin-alignment in $Z + J/\psi$ production. Figure 5 summarises the fiducial, inclusive and DPS-subtracted cross-section ratios for prompt and non-prompt production and Table 4 presents the differential cross-section ratios in the central and forward J/ψ rapidity intervals. The DPS fraction is $(29 \pm 9)\%$ for the $Z +$ prompt J/ψ signal and $(8 \pm 2)\%$ for the non-prompt signal, in the kinematic region studied in this measurement.

The production cross-section ratios for $Z +$ prompt J/ψ production are compared to LO colour-singlet [23] predictions, as well as the contributions from colour-singlet (CS) and colour-octet (CO) processes in the non-relativistic QCD (NRQCD) formalism [24].

All theoretical calculations consider only single parton scattering processes in which the J/ψ mesons are produced directly from the parton interaction, without any feed-down from excited charmonium states. To allow direct comparison to the measured DPS-subtracted cross-section ratios, these predictions are normalised to NNLO calculations of the Z boson fiducial production cross-section (533.4 pb), determined using FEWZ [81, 82].

LO colour-singlet mechanism (CSM) predictions for the production cross-section (normalised to the inclusive Z production rate) vary between $(11.6 \pm 3.2) \times 10^{-8}$ (from Ref. [23]) and $(46.2_{-6.5}^{+6.0}) \times 10^{-8}$ (from Ref. [24]). The NLO NRQCD prediction [24] for the colour-singlet rate is $(45.7_{-9.6}^{+10.5}) \times 10^{-8}$. NRQCD colour-octet contributions to the normalised production rate (that should be added to the corresponding colour-singlet rates to provide the total NRQCD prediction) shown in Fig. 5 are predicted to be

$(25.1_{-3.5}^{+3.3}) \times 10^{-8}$ at LO and $(86_{-18}^{+20}) \times 10^{-8}$ at NLO accuracy, approximately a factor of two larger than the contribution from colour-singlet production at the same order in the perturbative expansion. Uncertainties in the predictions arise from a variation of the renormalisation and factorisation scales up and down by a factor of two from their nominal values, and uncertainties on the charm quark mass. The variation in the predictions for the colour-singlet rate at LO from different groups arises from a different choice of scale for the central prediction, either taking the Z mass, m_Z , or the J/ψ transverse mass, $m_{\text{T}}^{J/\psi} = \sqrt{(m^{J/\psi})^2 + (p_{\text{T}}^{J/\psi})^2}$, the appropriateness of which is the subject of some discussion [23, 24]. The CO predictions presented here use the values for the NRQCD long-distance matrix elements as discussed in Ref. [24], but do not include uncertainties related to the determination of these matrix elements [83].

The effective cross-section regulating multiple parton interactions is expected to be a dynamical quantity dependent on the probed scale of the interactions, and thus should be x -dependent (where $x \equiv p_{\text{parton}}/p_{\text{beam}}$) [84]. Recent theoretical studies [85] have suggested that vector-boson production in association with jets may have σ_{eff} values as high as 15–25 mb. In this paper, the ATLAS $W + 2$ -jet measurement of $\sigma_{\text{eff}} = 15 \pm 3$ (stat.) $_{-3}^{+5}$ (syst.) mb is used to estimate the DPS contribution, and is found to be consistent, within the still sizeable uncertainties, with the observed rates and the plateau observed at small azimuthal separations between the produced Z bosons and J/ψ , illustrated in Fig. 4.

The small $\Delta\phi(Z, J/\psi)$ region is sensitive to DPS contributions and can be used to limit the maximum allowed double parton scattering contribution to the observed signal, which corresponds to a lower limit on σ_{eff} , by conservatively assuming that all observed signal in the first bin ($\Delta\phi(Z, J/\psi) < \pi/5$ region) is due to DPS. As the estimated relative signal contribution from DPS processes is largest in prompt production, the data from $Z +$ prompt J/ψ provides the most stringent limit on the rate of DPS interactions. The data uncertainties and uncertainties inherent in the DPS estimate allow a lower limit $\sigma_{\text{eff}} > 5.3$ mb (3.7 mb) at 68% (95%) confidence level to be extracted from the $Z +$ prompt J/ψ data.

A model-independent upper limit on σ_{eff} cannot be extracted from these data, as such a limit corresponds to a minimum rate of DPS contribution at small $\Delta\phi(Z, J/\psi)$. While SPS contributions are largest at wide angles, a significant SPS contribution is possible at low angles due to high-order processes [86].

6.4 Differential production cross-section measurements

Extending upon the measurement of the total inclusive production ratios $R_{Z+J/\psi}^{\text{incl}}$ and determination of the DPS con-

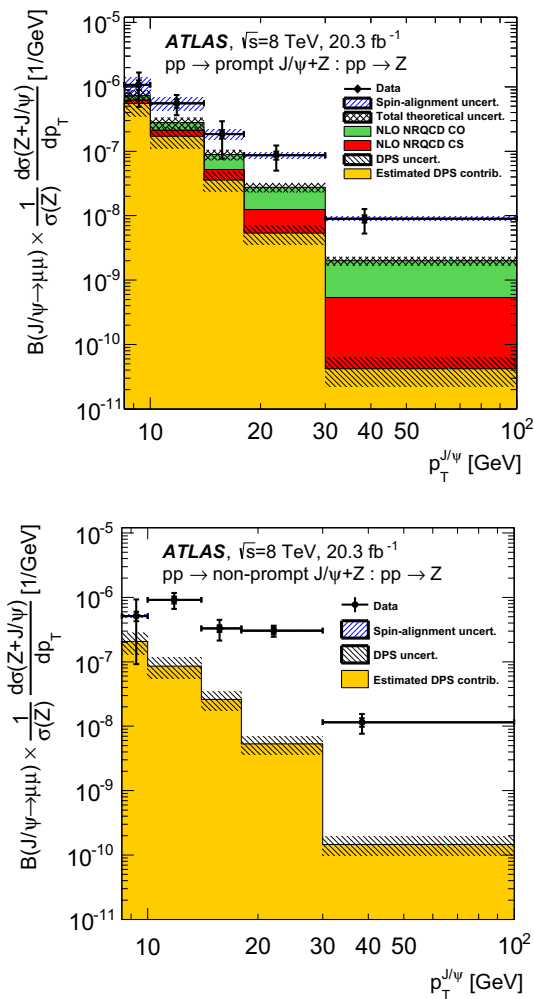


Fig. 6 Production cross-section of J/ψ in association with a Z boson as a function of the p_T of prompt J/ψ , and non-prompt J/ψ , normalised to the inclusive Z cross-section. Overlaid on the measurement is the contribution to the total signal originating from double parton scattering (DPS) interactions. Theoretical predictions at NLO accuracy for the SPS contributions from colour-singlet (CS) and colour-octet (CO) processes are added to the DPS estimate and presented in comparison to the data as solid bands

tribution, the differential cross-section ratio $dR_{Z+J/\psi}^{incl}/dp_T$ is measured as a function of the transverse momentum of the J/ψ for both the prompt and non-prompt signals, using the sPlot weights obtained from the fit procedure. The differential DPS contribution (using $\sigma_{eff} = 15$ mb) is shown together with the inclusive cross-section ratio in each kinematic interval in Fig. 6 and in Table 5. The observed p_T dependence is significantly harder than for inclusive J/ψ production [4].

The measured differential production cross-section ratio for prompt J/ψ production is compared to NLO colour-singlet and colour-octet predictions. As these predictions are for single parton scattering rates, the estimated DPS contribution is added to the theoretical predictions to allow like-

for-like comparison between theory and data. Theory predicts that colour-octet contributions exceed the production rate from singlet processes by approximately a factor of two, with colour-octet processes becoming increasingly dominant for higher p_T of the J/ψ . The combination of DPS and NLO NRQCD contributions tends to underestimate the production rate observed in data, with the discrepancy increasing with transverse momentum and reaching a factor of 4–5 at $p_T^{J/\psi} > 18$ GeV. A significant SPS contribution to $Z +$ non-prompt J/ψ production rate from $Z + b$ -jet production, where the jet contains a J/ψ meson, is expected but has not been evaluated for this article. The data presented here offer the opportunity to test $Z + b$ -jet production at low transverse momentum.

7 Conclusions

This paper documents the first observation and measurement of both associated $Z +$ prompt J/ψ and $Z +$ non-prompt J/ψ production, with the background-only hypothesis being excluded at 5σ significance for prompt $Z + J/\psi$ production and at 9σ significance for non-prompt J/ψ production, using 20.3 fb $^{-1}$ of proton–proton collisions recorded in the ATLAS detector at the LHC, at a centre-of-mass energy of 8 TeV.

Fiducial cross-sections of the production rate of the two final states were measured as ratios to the inclusive Z boson production rate in the same fiducial volume, and found to be $(36.8 \pm 6.7 \pm 2.5) \times 10^{-7}$ and $(65.8 \pm 9.2 \pm 4.2) \times 10^{-7}$ for Z bosons produced in association with a prompt and non-prompt J/ψ , respectively, where the first uncertainty is statistical and the second is systematic. Ratios, corrected for the limited geometrical acceptance for the muons from the J/ψ decay in the J/ψ fiducial volume, are also presented. For prompt production this correction factor depends on the spin-alignment state of J/ψ produced in association with a Z boson, which may differ from the spin-alignment observed in inclusive J/ψ production. The measured $Z +$ prompt J/ψ production rates are compared to theoretical predictions at LO and NLO for colour-singlet and colour-octet prompt production processes. A higher production rate is predicted through colour-octet transitions than through colour-singlet processes, but the expected production rate from the sum of singlet and octet contributions is lower than the data by a factor of 2 to 5 in the $p_T^{J/\psi}$ range studied.

Measurements of the azimuthal angle between the Z boson and J/ψ meson suggest that both single and double parton scattering contributions may be present in the data. Using the effective cross-section regulating double parton scattering rates as measured by ATLAS in the $W + 2$ -jet final state, the fraction of the inclusive production rate arising from double parton scattering interactions is estimated to

Table 5 The inclusive (SPS + DPS) cross-section ratio $dR_{Z+J/\psi}^{\text{incl}}/dp_T$ for prompt and non-prompt J/ψ . Estimated DPS contributions for each bin, based on the assumptions made in this study, are presented

$p_T^{J/\psi}$ (GeV)	Inclusive prompt ratio ($\times 10^{-7}/\text{GeV}$) value \pm (stat) \pm (syst) \pm (spin)			Estimated DPS ($\times 10^{-7}/\text{GeV}$) assuming $\sigma_{\text{eff}} = 15 \text{ mb}$
(8.5, 10)	10.8 ± 5.6	± 1.9	± 3.1	5.5 ± 2.1
(10, 14)	5.6 ± 1.9	± 0.8	± 1.2	1.7 ± 0.6
(14, 18)	1.9 ± 1.1	± 0.1	± 0.3	0.4 ± 0.1
(18, 30)	0.87 ± 0.37	± 0.12	± 0.09	0.05 ± 0.02
(30, 100)	0.090 ± 0.037	± 0.012	± 0.006	0.0004 ± 0.0002
$p_T^{J/\psi}$ (GeV)	Inclusive non-prompt ratio ($\times 10^{-7}/\text{GeV}$) value \pm (stat) \pm (syst) \pm (spin)			Estimated DPS ($\times 10^{-7}/\text{GeV}$) assuming $\sigma_{\text{eff}} = 15 \text{ mb}$
(8.5, 10)	5.1 ± 4.2	± 0.9	± 0.3	2.07 ± 0.77
(10, 14)	9.2 ± 2.5	± 1.2	± 0.3	0.85 ± 0.30
(14, 18)	3.3 ± 1.2	± 0.4	± 0.1	0.26 ± 0.09
(18, 30)	3.04 ± 0.59	± 0.04	± 0.04	0.05 ± 0.02
(30, 100)	0.115 ± 0.039	± 0.002	± 0.001	0.0015 ± 0.0005

be $(29 \pm 9) \%$ for prompt production and $(8 \pm 2) \%$ for non-prompt production. An independent limit on the maximum rate of double parton scattering contributing to the signal is set, corresponding to a lower limit on the effective cross-section of 5.3 mb (3.7 mb) at 68 % (95 %) confidence level. The measured production cross-section ratios of inclusive $Z +$ prompt J/ψ and $Z +$ non-prompt J/ψ production, and the estimated contribution from double parton scattering, are shown differentially in five intervals of the J/ψ p_T , with the differential production rates compared to NLO predictions from colour-singlet and colour-octet processes.

Acknowledgments We thank CERN for the very successful operation of the LHC, as well as the support staff from our institutions without whom ATLAS could not be operated efficiently. We acknowledge the support of ANPCyT, Argentina; YerPhI, Armenia; ARC, Australia; BMWFW and FWF, Austria; ANAS, Azerbaijan; SSTC, Belarus; CNPq and FAPESP, Brazil; NSERC, NRC and CFI, Canada; CERN; CONICYT, Chile; CAS, MOST and NSFC, China; COLCIENCIAS, Colombia; MSMT CR, MPO CR and VSC CR, Czech Republic; DNRF, DNSRC and Lundbeck Foundation, Denmark; EPLANET, ERC and NSRF, European Union; IN2P3-CNRS, CEA-DSM/IRFU, France; GNSF, Georgia; BMBF, DFG, HGF, MPG and AvH Foundation, Germany; GSRT and NSRF, Greece; RGC, Hong Kong SAR, China; ISF, MINERVA, GIF, I-CORE and Benozzi Center, Israel; INFN, Italy; MEXT and JSPS, Japan; CNRST, Morocco; FOM and NWO, Netherlands; BRF and RCN, Norway; MNiSW and NCN, Poland; GRICES and FCT, Portugal; MNE/IFA, Romania; MES of Russia and NRC KI, Russian Federation; JINR; MSTB, Serbia; MSSR, Slovakia; ARRS and MIZŠ, Slovenia; DST/NRF, South Africa; MINECO, Spain; SRC and Wallenberg Foundation, Sweden; SER, SNSF and Cantons of Bern and Geneva, Switzerland; NSC, Taiwan; TAEK, Turkey; STFC, the Royal Society and Leverhulme Trust, United Kingdom; DOE and NSF, United States of America. The crucial computing support from all WLCG partners is acknowledged gratefully, in particular from CERN and the ATLAS Tier-1 facilities at TRIUMF (Canada), NDGF (Denmark, Norway, Sweden), CC-IN2P3 (France), KIT/GridKA (Germany), INFN-CNAF (Italy), NL-T1 (Netherlands), PIC (Spain), ASGC (Taiwan), RAL (UK) and BNL (USA) and in the Tier-2 facilities worldwide.

Open Access This article is distributed under the terms of the Creative Commons Attribution 4.0 International License (<http://creativecommons.org/licenses/by/4.0/>), which permits unrestricted use, distribution, and reproduction in any medium, provided you give appropriate credit to the original author(s) and the source, provide a link to the Creative Commons license, and indicate if changes were made. Funded by SCOAP³.

References

1. CDF Collaboration, F. Abe et al., Search for associated production of Υ and vector boson in $p\bar{p}$ collisions at $\sqrt{s} = 1.8 \text{ TeV}$. Phys. Rev. Lett. **90**, 221803 (2003)
2. CDF Collaboration, T.A. Aaltonen et al., Search for production of an $\Upsilon(1S)$ meson in association with a W or Z boson using the full 1.96 TeV proton anti-proton collision data set at CDF. [arXiv:1412.4827](https://arxiv.org/abs/1412.4827) [hep-ex]
3. ATLAS Collaboration, Measurement of the production cross section of prompt J/ψ mesons in association with a W^\pm boson in pp collisions at $\sqrt{s} = 7 \text{ TeV}$ with the ATLAS detector. JHEP **1404**, 172 (2014). [arXiv:1401.2831](https://arxiv.org/abs/1401.2831) [hep-ex]
4. ATLAS Collaboration, Measurement of the differential cross-sections of inclusive, prompt and non-prompt J/ψ production in proton-proton collisions at $\sqrt{s} = 7 \text{ TeV}$. Nucl. Phys. B **850**, 387–444 (2011). [arXiv:1104.3038](https://arxiv.org/abs/1104.3038) [hep-ex]
5. LHCb Collaboration, R. Aaij et al., Measurement of J/ψ production in pp collisions at $\sqrt{s} = 7 \text{ TeV}$. Eur. Phys. J. C **71**, 1645 (2011). [arXiv:1103.0423](https://arxiv.org/abs/1103.0423) [hep-ex]
6. ALICE Collaboration, B. Abelev et al., Measurement of prompt J/ψ and beauty hadron production cross sections at mid-rapidity in pp collisions at $\sqrt{s} = 7 \text{ TeV}$. JHEP **1211**, 065 (2012). [arXiv:1205.5880](https://arxiv.org/abs/1205.5880) [hep-ex]
7. CMS Collaboration, J/ψ and $\psi(2S)$ production in pp collisions at $\sqrt{s} = 7 \text{ TeV}$. JHEP **1202**, 011 (2012). [arXiv:1111.1557](https://arxiv.org/abs/1111.1557) [hep-ex]
8. ATLAS Collaboration, Measurement of the production cross-section of $\psi(2S) \rightarrow J/\psi(\rightarrow \mu^+\mu^-)\pi^+\pi^-$ in pp collisions at $\sqrt{s} = 7 \text{ TeV}$ at ATLAS. JHEP **1409**, 79 (2014). [arXiv:1407.5532](https://arxiv.org/abs/1407.5532) [hep-ex]
9. LHCb Collaboration, R. Aaij et al., Measurement of $\psi(2S)$ meson production in pp collisions at $\sqrt{s} = 7 \text{ TeV}$. Eur. Phys. J. C **72**, 2100 (2012). [arXiv:1204.1258](https://arxiv.org/abs/1204.1258) [hep-ex]

10. ALICE Collaboration, B.B. Abelev et al., Measurement of quarkonium production at forward rapidity in pp collisions at $\sqrt{s} = 7$ TeV. *Eur. Phys. J. C* **74**, 2974 (2014). [arXiv:1403.3648](#) [nucl-ex]
11. W. Caswell, G. Lepage, Effective lagrangians for bound state problems in QED, QCD, and other field theories. *Phys. Lett. B* **167**, 437 (1986)
12. G.T. Bodwin, E. Braaten, G.P. Lepage, Rigorous QCD analysis of inclusive annihilation and production of heavy quarkonium. *Phys. Rev. D* **51**, 1125 (1995). [arXiv:hep-ph/9407339](#) [hep-ph]
13. Y.-Q. Ma, K. Wang, K.-T. Chao, $J/\psi(\psi')$ production at the Tevatron and LHC at $\mathcal{O}(\alpha_s^4 v^4)$ in nonrelativistic QCD. *Phys. Rev. Lett.* **106**, 042002 (2011). [arXiv:1009.3655](#) [hep-ph]
14. N. Brambilla et al., Heavy quarkonium: progress, puzzles, and opportunities. *Eur. Phys. J. C* **71**, 1534 (2011). [arXiv:1010.5827](#) [hep-ph]
15. Quarkonium Working Group, N. Brambilla et al., Heavy quarkonium physics—Section 5. CERN Yellow Report CERN-2005-005 (2004). [arXiv:hep-ph/0412158](#) [hep-ph]
16. J. Owens, E. Reya, M. Gluck, Detailed quantum chromodynamic predictions for high- p_T processes. *Phys. Rev. D* **18**, 1501 (1978)
17. V. Kartvelishvili, A. Likhoded, S. Slabospitsky, D meson and ψ meson production in hadronic interactions. *Sov. J. Nucl. Phys.* **28**, 678 (1978)
18. V.D. Barger, W.-Y. Keung, R. Phillips, On ψ and Υ production via gluons. *Phys. Lett. B* **91**, 253 (1980)
19. C.-H. Chang, Hadronic production of J/ψ associated with a gluon. *Nucl. Phys. B* **172**, 425–434 (1980)
20. E.L. Berger, D.L. Jones, Inelastic photoproduction of J/ψ and Υ by gluons. *Phys. Rev. D* **23**, 1521–1530 (1981)
21. R. Baier, R. Ruckl, On inelastic leptoproduction of heavy quarkonium states. *Nucl. Phys. B* **201**, 1 (1982)
22. R. Baier, R. Ruckl, Hadronic collisions: a quarkonium factory. *Z. Phys. C* **19**, 251 (1983)
23. B. Gong, J.-P. Lansberg, C. Lorce, J. Wang, Next-to-leading-order QCD corrections to the yields and polarisations of J/ψ and Υ directly produced in association with a Z boson at the LHC. *JHEP* **1303**, 115 (2013). [arXiv:1210.2430](#) [hep-ph]
24. S. Mao et al., QCD corrections to J/ψ plus Z^0 -boson production at the LHC. *JHEP* **1102**, 071 (2011). [arXiv:1102.0398](#) [hep-ph]
25. J. Lansberg, On the mechanisms of heavy-quarkonium hadroproduction. *Eur. Phys. J. C* **61**, 693–703 (2009). [arXiv:0811.4005](#) [hep-ph]
26. ATLAS Collaboration, Measurement of the cross-section for b -jets produced in association with a Z boson at $\sqrt{s} = 7$ TeV with the ATLAS detector. *Phys. Lett. B* **706**, 295–313 (2012). [arXiv:1109.1403](#) [hep-ex]
27. CMS Collaboration, Measurement of the production cross sections for a Z boson and one or more b jets in pp collisions at $\sqrt{s} = 7$ TeV. *JHEP* **1406**, 120 (2014). [arXiv:1402.1521](#) [hep-ex]
28. ATLAS Collaboration, Measurement of ZZ production in pp collisions at $\sqrt{s} = 7$ TeV and limits on anomalous ZZZ and $ZZ\gamma$ couplings with the ATLAS detector. *JHEP* **1303**, 128 (2013). [arXiv:1211.6096](#) [hep-ex]
29. CMS Collaboration, Measurement of the pp to ZZ production cross section and constraints on anomalous triple gauge couplings in four-lepton final states at $\sqrt{s} = 8$ TeV. [arXiv:1406.0113](#) [hep-ex]
30. E. Braaten, K. Cheung, T.C. Yuan, Z^0 decay into charmonium via charm quark fragmentation. *Phys. Rev. D* **48**, 4230–4235 (1993). [arXiv:hep-ph/9302307](#) [hep-ph]
31. S. Fleming, Electromagnetic production of quarkonium in Z^0 decay. *Phys. Rev. D* **48**, 1914–1916 (1993). [arXiv:hep-ph/9304270](#) [hep-ph]
32. S. Fleming, J/ψ production from electromagnetic fragmentation in Z^0 decay. *Phys. Rev. D* **50**, 5808–5815 (1994). [arXiv:hep-ph/9403396](#) [hep-ph]
33. M. Doroshenko, V. Kartvelishvili, E. Chikovani, S. Esakiya, Vector quarkonium in decays of heavy Higgs particles. *Sov. J. Nucl. Phys.* **46**, 493–495 (1987)
34. V. Kartvelishvili, E. Chikovani, S. Esakiya, The production and decays of heavy quark bound states in strong and electroweak interactions (in Russian). *Fiz. Elem. Chast. Atom. Yadra* **19**, 139–179 (1988)
35. M. Gonzalez-Alonso, G. Isidori, The $h \rightarrow 4l$ spectrum at low m_{34} : standard model vs. light new physics. *Phys. Lett.* **B733**, 359–365 (2014). [arXiv:1403.2648](#) [hep-ph]
36. M.A. Diaz, T.J. Weiler, Decays of a fermiophobic Higgs. [arXiv:hep-ph/9401259](#) [hep-ph]
37. G. Bodwin et al., Higgs boson decays to quarkonia and the $H\bar{c}c$ coupling. *Phys. Rev. D* **88**, 053003 (2013). [arXiv:1306.5770](#) [hep-ph]
38. B. Bhattacharya, A. Datta, D. London, Probing new physics in Higgs couplings to fermions using an angular analysis. *Phys. Lett. B* **736**, 421–427 (2014). [arXiv:1407.0695](#) [hep-ph]
39. D.-N. Gao, A note on Higgs decays into Z boson and $J/\psi(\Upsilon)$. *Phys. Lett. B* **737**, 366–368 (2014). [arXiv:1406.7102](#) [hep-ph]
40. H. Davoudiasl, H.-S. Lee, W.J. Marciano, ‘Dark’ Z implications for parity violation, rare meson decays, and Higgs physics. *Phys. Rev. D* **85**, 115019 (2012). [arXiv:1203.2947](#) [hep-ph]
41. D. Curtin et al., Exotic decays of the 125 GeV Higgs boson. *Phys. Rev. D* **90**, 075004 (2014). [arXiv:1312.4992](#) [hep-ph]
42. A. Falkowski, R. Vega-Morales, Exotic Higgs decays in the golden channel. [arXiv:1405.1095](#) [hep-ph]
43. J.D. Clarke, R. Foot, R.R. Volkas, Phenomenology of a very light scalar ($100 \text{ MeV} < m_h < 10 \text{ GeV}$) mixing with the SM Higgs. *JHEP* **1402**, 123 (2014). [arXiv:1310.8042](#) [hep-ph]
44. N. Paver, D. Treleani, Multi-quark scattering and large p_T jet production in hadronic collisions. *Nuovo Cim. A* **70**, 215 (1982)
45. T. Sjostrand, P.Z. Skands, Multiple interactions and the structure of beam remnants. *JHEP* **03**, 053 (2004). [arXiv:hep-ph/0402078](#) [hep-ph]
46. V. Korotkikh, A. Snigirev, Double parton correlations versus factorized distributions. *Phys. Lett. B* **594**, 171–176 (2004). [arXiv:hep-ph/0404155](#) [hep-ph]
47. J.R. Gaunt, W.J. Stirling, Double parton distributions incorporating perturbative QCD evolution and momentum and quark number sum rules. *JHEP* **03**, 005 (2010). [arXiv:0910.4347](#) [hep-ph]
48. P. Bartalini et al., Multi-parton interactions at the LHC. [arXiv:1111.0469](#) [hep-ph]
49. K. Golec-Biernat, E. Lewandowska, Electroweak boson production in double parton scattering. *Phys. Rev. D* **90**, 094032 (2014). [arXiv:1407.4038](#) [hep-ph]
50. J.R. Gaunt, R. Maciula, A. Szczurek, Conventional versus single-ladder-splitting contributions to double parton scattering production of two quarkonia, two Higgs bosons and $c\bar{c}c\bar{c}$. *Phys. Rev. D* **90**, 054017 (2014). [arXiv:1407.5821](#) [hep-ph]
51. ATLAS Collaboration, The ATLAS Experiment at the CERN Large Hadron Collider. *JINST* **3**, S08003 (2008)
52. ATLAS Collaboration, Performance of the ATLAS muon trigger in pp collisions at $\sqrt{s} = 8$ TeV. [arXiv:1408.3179](#) [hep-ex]
53. ATLAS Collaboration, Measurement of the muon reconstruction performance of the ATLAS detector using 2011 and 2012 LHC proton–proton collision data. *Eur. Phys. J. C* **74**, 3130 (2014). [arXiv:1407.3935](#) [hep-ex]
54. ATLAS Collaboration, Electron and photon energy calibration with the ATLAS detector using LHC Run 1 data. *Eur. Phys. J. C* **74**, 3071 (2014). [arXiv:1407.5063](#) [hep-ex]
55. J. Beringer et al., Particle Data Group, Review of particle physics (RPP). *Phys. Rev. D* **86**, 010001 (2012)
56. P. Nason, A new method for combining NLO QCD with shower Monte Carlo algorithms. *JHEP* **0411**, 040 (2004). [arXiv:hep-ph/0409146](#) [hep-ph]

57. S. Frixione, P. Nason, G. Ridolfi, A positive-weight next-to-leading-order Monte Carlo for heavy flavour hadroproduction. *JHEP* **0709**, 126 (2007). [arXiv:0707.3088](#) [hep-ph]
58. S. Frixione, P. Nason, C. Oleari, Matching NLO QCD computations with Parton Shower simulations: the POWHEG method. *JHEP* **0711**, 070 (2007). [arXiv:0709.2092](#) [hep-ph]
59. T. Sjostrand, S. Mrenna, P.Z. Skands, A brief introduction to PYTHIA 8.1. *Comput. Phys. Commun.* **178**, 852–867 (2008). [arXiv:0710.3820](#) [hep-ph]
60. H.-L. Lai et al., New parton distributions for collider physics. *Phys. Rev. D* **82**, 074024 (2010). [arXiv:1007.2241](#) [hep-ph]
61. ATLAS Collaboration, ATLAS tunes of PYTHIA 6 and Pythia 8 for MC11, ATL-PHYS-PUB-2011-009 (2011). <https://cds.cern.ch/record/1363300>
62. T. Gleisberg et al., Event generation with SHERPA 1.1. *JHEP* **0902**, 007 (2009). [arXiv:0811.4622](#) [hep-ph]
63. S. Frixione, B.R. Webber, Matching NLO QCD computations and Parton Shower simulations. *JHEP* **0206**, 029 (2002). [arXiv:hep-ph/0204244](#) [hep-ph]
64. S. Frixione, P. Nason, B.R. Webber, Matching NLO QCD and parton showers in heavy flavour production. *JHEP* **0308**, 007 (2003). [arXiv:hep-ph/0305252](#) [hep-ph]
65. G. Corcella et al., HERWIG 6: an event generator for hadron emission reactions with interfering gluons (including supersymmetric processes). *JHEP* **0101**, 010 (2001). [arXiv:hep-ph/0011363](#) [hep-ph]
66. J. Butterworth, J.R. Forshaw, M. Seymour, Multiparton interactions in photoproduction at HERA. *Z. Phys.* **C72**, 637–646 (1996). [arXiv:hep-ph/9601371](#) [hep-ph]
67. ATLAS Collaboration, New ATLAS event generator tunes to 2010 data, ATL-PHYS-PUB-2011-008 (2011). <https://cds.cern.ch/record/1345343>
68. B.P. Kersevan, E. Richter-Was, The Monte Carlo event generator AcerMC versions 2.0 to 3.8 with interfaces to PYTHIA 6.4, HERWIG 6.5 and ARIADNE 4.1. *Comput. Phys. Commun.* **184**, 919 (2013). [arXiv:hep-ph/0405247](#) [hep-ph]
69. J. Pumplin et al., New generation of parton distributions with uncertainties from global QCD analysis. *JHEP* **0207**, 012 (2002). [arXiv:hep-ph/0201195](#) [hep-ph]
70. T. Sjostrand, S. Mrenna, P.Z. Skands, PYTHIA 6.4 physics and manual. *JHEP* **0605**, 026 (2006). [arXiv:hep-ph/0603175](#) [hep-ph]
71. ATLAS Collaboration, The ATLAS simulation infrastructure. *Eur. Phys. J. C* **70**, 823 (2010). [arXiv:1005.4568](#) [physics.ins-det]
72. GEANT4 Collaboration, S. Agostinelli et al., GEANT4: a simulation toolkit. *Nucl. Instrum. Meth. A* **506**, 250–303 (2003)
73. M. Pivk, F.R. Le Diberder, sPlot: a statistical tool to unfold data distributions. *Nucl. Instrum. Meth. A* **555**, 356–369 (2005). [arXiv:physics/0402083](#) [physics.data-an]
74. ATLAS Collaboration, Luminosity determination in pp collisions at $\sqrt{s} = 7$ TeV using the ATLAS detector at the LHC. *Eur. Phys. J. C* **71**, 1630 (2011). [arXiv:1101.2185](#) [hep-ex]
75. M. Cacciari, M. Greco, P. Nason, The p_T spectrum in heavy flavour hadroproduction. *JHEP* **9805**, 007 (1998). [arXiv:hep-ph/9803400](#) [hep-ph]
76. M. Cacciari et al., Theoretical predictions for charm and bottom production at the LHC. *JHEP* **1210**, 137 (2012). [arXiv:1205.6344](#) [hep-ph]
77. ATLAS Collaboration, Measurement of hard double-parton interactions in $W(\rightarrow l\nu)+2$ jet events at $\sqrt{s}=7$ TeV with the ATLAS detector. *New J. Phys.* **15**, 033038 (2013). [arXiv:1301.6872](#) [hep-ex]
78. CMS Collaboration, Measurement of the prompt J/ψ and $\psi(2S)$ polarizations in pp collisions at $\sqrt{s} = 7$ TeV. *Phys. Lett. B* **727**, 381–402 (2013). [arXiv:1307.6070](#) [hep-ex]
79. P. Faccioli, C. Lourenco, J. Seixas, H.K. Wohri, Towards the experimental clarification of quarkonium polarization. *Eur. Phys. J. C* **69**, 657–673 (2010). [arXiv:1006.2738](#) [hep-ph]
80. CDF Collaboration, A. Abulencia et al., Polarization of J/ψ and $\psi(2S)$ mesons produced in $p\bar{p}$ collisions at $\sqrt{s} = 1.96$ TeV. *Phys. Rev. Lett.* **99**, 132001 (2007). [arXiv:0704.0638](#) [hep-ex]
81. R. Gavin, Y. Li, F. Petriello, S. Quackenbush, FEWZ 2.0: a code for hadronic Z production at next-to-next-to-leading order. *Comput. Phys. Commun.* **182**, 2388–2403 (2011). [arXiv:1011.3540](#) [hep-ph]
82. R. Gavin, Y. Li, F. Petriello, S. Quackenbush, W physics at the LHC with FEWZ 2.1. *Comput. Phys. Commun.* **184**, 209–214 (2013). [arXiv:1201.5896](#) [hep-ph]
83. M. Butenschoen, B.A. Kniehl, World data of J/ψ production consolidate NRQCD factorization at NLO. *Phys. Rev. D* **84**, 051501 (2011). [arXiv:1105.0820](#) [hep-ph]
84. CDF Collaboration, F. Abe et al., Double parton scattering in $\bar{p}p$ collisions at $\sqrt{s} = 1.8$ TeV. *Phys. Rev. D* **56**, 3811–3832 (1997)
85. B. Blok, Y. Dokshitzer, L. Frankfurt, M. Strikman, Perturbative QCD correlations in multi-parton collisions. *Eur. Phys. J. C* **74**, 2926 (2014). [arXiv:1306.3763](#) [hep-ph]
86. J.-P. Lansberg, H.-S. Shao, Production of $J/\psi + \eta_c$ versus $J/\psi + J/\psi$ at the LHC: importance of Real α_s^2 Corrections. *Phys. Rev. Lett.* **111**, 122001 (2013). [arXiv:1308.0474](#) [hep-ph]

ATLAS Collaboration

G. Aad⁸⁵, B. Abbott¹¹³, J. Abdallah¹⁵², S. Abdel Khalek¹¹⁷, O. Abdinov¹¹, R. Aben¹⁰⁷, B. Abi¹¹⁴, M. Abolins⁹⁰, O. S. AbouZeid¹⁵⁹, H. Abramowicz¹⁵⁴, H. Abreu¹⁵³, R. Abreu³⁰, Y. Abulaiti^{147a,147b}, B. S. Acharya^{165a,165b,a}, L. Adamczyk^{38a}, D. L. Adams²⁵, J. Adelman¹⁰⁸, S. Adomeit¹⁰⁰, T. Adye¹³¹, T. Agatonovic-Jovin¹³, J. A. Aguilar-Saavedra^{126a,126f}, M. Agustoni¹⁷, S. P. Ahlen²², F. Ahmadov^{65,b}, G. Aielli^{134a,134b}, H. Akerstedt^{147a,147b}, T. P. A. Åkesson⁸¹, G. Akimoto¹⁵⁶, A. V. Akimov⁹⁶, G. L. Alberghi^{20a,20b}, J. Albert¹⁷⁰, S. Albrand⁵⁵, M. J. Alconada Verzini⁷¹, M. Aleksa³⁰, I. N. Aleksandrov⁶⁵, C. Alexa^{26a}, G. Alexander¹⁵⁴, G. Alexandre⁴⁹, T. Alexopoulos¹⁰, M. Alhroob¹¹³, G. Alimonti^{91a}, L. Alio⁸⁵, J. Alison³¹, B. M. M. Allbrooke¹⁸, L. J. Allison⁷², P. P. Allport⁷⁴, A. Aloisio^{104a,104b}, A. Alonso³⁶, F. Alonso⁷¹, C. Alpigiani⁷⁶, A. Altheimer³⁵, B. Alvarez Gonzalez⁹⁰, M. G. Alviggi^{104a,104b}, K. Amako⁶⁶, Y. Amaral Coutinho^{24a}, C. Amelung²³, D. Amidei⁸⁹, S. P. Amor Dos Santos^{126a,126c}, A. Amorim^{126a,126b}, S. Amoroso⁴⁸, N. Amram¹⁵⁴, G. Amundsen²³, C. Anastopoulos¹⁴⁰, L. S. Ancu⁴⁹, N. Andari³⁰, T. Andeen³⁵, C. F. Anders^{58b}, G. Anders³⁰, K. J. Anderson³¹, A. Andreazza^{91a,91b}, V. Andrei^{58a}, X. S. Anduaga⁷¹, S. Angelidakis⁹, I. Angelozzi¹⁰⁷, P. Anger⁴⁴, A. Angerami³⁵, F. Anghinolfi³⁰, A. V. Anisenkov^{109,c}, N. Anjos¹², A. Annovi^{124a,124b}, M. Antonelli⁴⁷, A. Antonov⁹⁸, J. Antos^{145b}, F. Anulli^{133a}, M. Aoki⁶⁶, L. Aperio Bella¹⁸, G. Arabidze⁹⁰, Y. Arai⁶⁶, J. P. Araque^{126a}, A. T. H. Arce⁴⁵, F. A. Arduh⁷¹, J-F. Arguin⁹⁵, S. Argyropoulos⁴², M. Arik^{19a}, A. J. Armbruster³⁰, O. Arnaez³⁰, V. Arnal⁸², H. Arnold⁴⁸, M. Arratia²⁸, O. Arslan²¹, A. Artamonov⁹⁷, G. Artoni²³, S. Asai¹⁵⁶, N. Asbah⁴², A. Ashkenazi¹⁵⁴, B. Åsman^{147a,147b}, L. Asquith¹⁵⁰, K. Assamagan²⁵, R. Astalos^{145a}, M. Atkinson¹⁶⁶, N. B. Atlay¹⁴², B. Auerbach⁶, K. Augsten¹²⁸, M. Aurousseau^{146b}, G. Avolio³⁰, B. Axen¹⁵, G. Azuelos^{95,d}, M. A. Baak³⁰, A. E. Baas^{58a}, C. Bacci^{135a,135b}, H. Bachacou¹³⁷, K. Bachas¹⁵⁵, M. Backes³⁰, M. Backhaus³⁰, P. Bagiacchi^{133a,133b}, P. Bagnaia^{133a,133b}, Y. Bai^{33a}, T. Bain³⁵, J. T. Baines¹³¹, O. K. Baker¹⁷⁷, P. Balek¹²⁹, T. Balestri¹⁴⁹, F. Balli⁸⁴, E. Banas³⁹, Sw. Banerjee¹⁷⁴, A. A. E. Bannoura¹⁷⁶, H. S. Bansil¹⁸, L. Barak¹⁷³, S. P. Baranov⁹⁶, E. L. Barberio⁸⁸, D. Barberis^{50a,50b}, M. Barbero⁸⁵, T. Barillari¹⁰¹, M. Barisonzi^{165a,165b}, T. Barklow¹⁴⁴, N. Barlow²⁸, S. L. Barnes⁸⁴, B. M. Barnett¹³¹, R. M. Barnett¹⁵, Z. Barnovska⁵, A. Baroncelli^{135a}, G. Barone⁴⁹, A. J. Barr¹²⁰, F. Barreiro⁸², J. Barreiro Guimarães da Costa⁵⁷, R. Bartoldus¹⁴⁴, A. E. Barton⁷², P. Bartos^{145a}, A. Bassalat¹¹⁷, A. Basye¹⁶⁶, R. L. Bates⁵³, S. J. Batista¹⁵⁹, J. R. Batley²⁸, M. Battaglia¹³⁸, M. Baucé^{133a,133b}, F. Bauer¹³⁷, H. S. Bawa^{144,e}, J. B. Beacham¹¹¹, M. D. Beattie⁷², T. Beau⁸⁰, P. H. Beauchemin¹⁶², R. Beccherle^{124a,124b}, P. Bechtel²¹, H. P. Beck^{17,f}, K. Becker¹²⁰, S. Becker¹⁰⁰, M. Beckingham¹⁷¹, C. Becot¹¹⁷, A. J. Beddall^{19c}, A. Beddall^{19c}, V. A. Bednyakov⁶⁵, C. P. Bee¹⁴⁹, L. J. Beemster¹⁰⁷, T. A. Beermann¹⁷⁶, M. Beger²⁵, K. Behr¹²⁰, C. Belanger-Champagne⁸⁷, P. J. Bell⁴⁹, W. H. Bell⁴⁹, G. Bella¹⁵⁴, L. Bellagamba^{20a}, A. Bellerive²⁹, M. Bellomo⁸⁶, K. Belotskiy⁹⁸, O. Beltramello³⁰, O. Benary¹⁵⁴, D. Benchechroun^{136a}, M. Bender¹⁰⁰, K. Bendtz^{147a,147b}, N. Benekos¹⁰, Y. Benhammou¹⁵⁴, E. Benhar Nocchioli⁴⁹, J. A. Benitez Garcia^{160b}, D. P. Benjamin⁴⁵, J. R. Bensinger²³, S. Bentvelsen¹⁰⁷, D. Berge¹⁰⁷, E. Bergeas Kuutmann¹⁶⁷, N. Berger⁵, F. Berghaus¹⁷⁰, J. Beringer¹⁵, C. Bernard²², N. R. Bernard⁸⁶, C. Bernius¹¹⁰, F. U. Bernlochner²¹, T. Berry⁷⁷, P. Berta¹²⁹, C. Bertella⁸³, G. Bertoli^{147a,147b}, F. Bertolucci^{124a,124b}, C. Bertsche¹¹³, D. Bertsche¹¹³, M. I. Besana^{91a}, G. J. Besjes¹⁰⁶, O. Bessidskaia Bylund^{147a,147b}, M. Bessner⁴², N. Besson¹³⁷, C. Betancourt⁴⁸, S. Bethke¹⁰¹, A. J. Bevan⁷⁶, W. Bhimji⁴⁶, R. M. Bianchi¹²⁵, L. Bianchini²³, M. Bianco³⁰, O. Biebel¹⁰⁰, S. P. Bieniek⁷⁸, M. Biglietti^{135a}, J. Bilbao De Mendizabal⁴⁹, H. Bilokon⁴⁷, M. Bindi⁵⁴, S. Binet¹¹⁷, A. Bingul^{19c}, C. Bini^{133a,133b}, C. W. Black¹⁵¹, J. E. Black¹⁴⁴, K. M. Black²², D. Blackburn¹³⁹, R. E. Blair⁶, J.-B. Blanchard¹³⁷, J. E. Blanco⁷⁷, T. Blazek^{145a}, I. Bloch⁴², C. Blocker²³, W. Blum^{83,*}, U. Blumenschein⁵⁴, G. J. Bobbink¹⁰⁷, V. S. Bobrovnikov^{109,c}, S. S. Bocchetta⁸¹, A. Bocchi⁴⁵, C. Bock¹⁰⁰, C. R. Boddy¹²⁰, M. Boehler⁴⁸, J. A. Bogaerts³⁰, A. G. Bogdanichikov¹⁰⁹, C. Boehm^{147a}, V. Boisvert⁷⁷, T. Bold^{38a}, V. Boldea^{26a}, A. S. Boldyrev⁹⁹, M. Bomben⁸⁰, M. Bona⁷⁶, M. Boonekamp¹³⁷, A. Borisov¹³⁰, G. Borissov⁷², S. Borroni⁴², J. Bortfeldt¹⁰⁰, V. Bortolotto^{60a}, K. Bos¹⁰⁷, D. Boscherini^{20a}, M. Bosman¹², J. Boudreau¹²⁵, J. Bouffard², E. V. Bouhova-Thacker⁷², D. Boumediene³⁴, C. Bourdarios¹¹⁷, N. Bousson¹¹⁴, S. Boutouil^{136d}, A. Boveia³⁰, J. Boyd³⁰, I. R. Boyko⁶⁵, I. Bozic¹³, J. Bracinik¹⁸, A. Brandt⁸, G. Brandt¹⁵, O. Brandt^{58a}, U. Bratzler¹⁵⁷, B. Brau⁸⁶, J. E. Brau¹¹⁶, H. M. Braun^{176,*}, S. F. Brazzale^{165a,165c}, K. Brendlinger¹²², A. J. Brennan⁸⁸, L. Brenner¹⁰⁷, R. Brenner¹⁶⁷, S. Bressler¹⁷³, K. Bristow^{146c}, T. M. Bristow⁴⁶, D. Britton⁵³, F. M. Brochu²⁸, I. Brock²¹, R. Brock⁹⁰, J. Bronner¹⁰¹, G. Brooijmans³⁵, T. Brooks⁷⁷, W. K. Brooks^{32b}, J. Brosamer¹⁵, E. Brost¹¹⁶, J. Brown⁵⁵, P. A. Bruckman de Renstrom³⁹, D. Bruncko^{145b}, R. Bruneliere⁴⁸, A. Bruni^{20a}, G. Bruni^{20a}, M. Bruschi^{20a}, L. Bryngemark⁸¹, T. Buanes¹⁴, Q. Buat¹⁴³, F. Bucci⁴⁹, P. Buchholz¹⁴², A. G. Buckley⁵³, S. I. Buda^{26a}, I. A. Budagov⁶⁵, F. Buehrer⁴⁸, L. Bugge¹¹⁹, M. K. Bugge¹¹⁹, O. Bulekov⁹⁸, H. Burckhart³⁰, S. Burdin⁷⁴, B. Burghgrave¹⁰⁸, S. Burke¹³¹, I. Burmeister⁴³, E. Busato³⁴, D. Büscher⁴⁸, V. Büscher⁸³, P. Bussey⁵³, C. P. Buszello¹⁶⁷, J. M. Butler²², A. I. Butt³, C. M. Buttar⁵³, J. M. Butterworth⁷⁸, P. Butti¹⁰⁷, W. Buttinger²⁸, A. Buzatu⁵³, S. Cabrera Urbán¹⁶⁸, D. Caforio¹²⁸, O. Cakir^{4a}, P. Calafiura¹⁵, A. Calandri¹³⁷, G. Calderini⁸⁰, P. Calfayan¹⁰⁰, L. P. Caloba^{24a}, D. Calvet³⁴, S. Calvet³⁴

R. Camacho Toro⁴⁹, S. Camarda⁴², D. Cameron¹¹⁹, L. M. Caminada¹⁵, R. Caminal Armadans¹², S. Campana³⁰, M. Campanelli⁷⁸, A. Campoverde¹⁴⁹, V. Canale^{104a,104b}, A. Canepa^{160a}, M. Cano Bret⁷⁶, J. Cantero⁸², R. Cantrill^{126a}, T. Cao⁴⁰, M. D. M. Capeans Garrido³⁰, I. Caprini^{26a}, M. Caprini^{26a}, M. Capua^{37a,37b}, R. Caputo⁸³, R. Cardarelli^{134a}, T. Carli³⁰, G. Carlino^{104a}, L. Carminati^{91a,91b}, S. Caron¹⁰⁶, E. Carquin^{32a}, G. D. Carrillo-Montoya^{146c}, J. R. Carter²⁸, J. Carvalho^{126a,126c}, D. Casadei⁷⁸, M. P. Casado¹², M. Casolino¹², E. Castaneda-Miranda^{146b}, A. Castelli¹⁰⁷, V. Castillo Gimenez¹⁶⁸, N. F. Castro^{126a}, P. Catastini⁵⁷, A. Catinaccio³⁰, J. R. Catmore¹¹⁹, A. Cattai³⁰, G. Cattani^{134a,134b}, J. Caudron⁸³, V. Cavaliere¹⁶⁶, D. Cavalli^{91a}, M. Cavalli-Sforza¹², V. Cavasinni^{124a,124b}, F. Ceradini^{135a,135b}, B. C. Cerio⁴⁵, K. Cerny¹²⁹, A. S. Cerqueira^{24b}, A. Cerri¹⁵⁰, L. Cerrito⁷⁶, F. Cerutti¹⁵, M. Cerv³⁰, A. Cervelli¹⁷, S. A. Cetin^{19b}, A. Chafaq^{136a}, D. Chakraborty¹⁰⁸, I. Chalupkova¹²⁹, P. Chang¹⁶⁶, B. Chapleau⁸⁷, J. D. Chapman²⁸, D. Charfeddine¹¹⁷, D. G. Charlton¹⁸, C. C. Chau¹⁵⁹, C. A. Chavez Barajas¹⁵⁰, S. Cheatham¹⁵³, A. Chegwidan⁹⁰, S. Chekanov⁶, S. V. Chekulaev^{160a}, G. A. Chelkov^{65g}, M. A. Chelstowska⁸⁹, C. Chen⁶⁴, H. Chen²⁵, K. Chen¹⁴⁹, L. Chen^{33d,h}, S. Chen^{33c}, X. Chen^{33f}, Y. Chen⁶⁷, H. C. Cheng⁸⁹, Y. Cheng³¹, A. Cheplakov⁶⁵, E. Cheremushkina¹³⁰, R. Cherkaoui El Moursli^{136e}, V. Chernyatin^{25*}, E. Cheu⁷, L. Chevalier¹³⁷, V. Chiarella⁴⁷, J. T. Childers⁶, A. Chilingarov⁷², G. Chiodini^{73a}, A. S. Chisholm¹⁸, R. T. Chislett⁷⁸, A. Chitan^{26a}, M. V. Chizhov⁶⁵, S. Chouridou⁹, B. K. B. Chow¹⁰⁰, D. Chromek-Burckhart³⁰, M. L. Chu¹⁵², J. Chudoba¹²⁷, J. J. Chwastowski³⁹, L. Chytka¹¹⁵, G. Ciapetti^{133a,133b}, A. K. Ciftci^{4a}, D. Cincă⁵³, V. Cindro⁷⁵, A. Ciocio¹⁵, Z. H. Citron¹⁷³, M. Citterio^{91a}, M. Ciubancan^{26a}, A. Clark⁴⁹, P. J. Clark⁴⁶, R. N. Clarke¹⁵, W. Cleland¹²⁵, C. Clement^{147a,147b}, Y. Coadou⁸⁵, M. Cobal^{165a,165c}, A. Coccaro¹³⁹, J. Cochran⁶⁴, L. Coffey²³, J. G. Cogan¹⁴⁴, B. Cole³⁵, S. Cole¹⁰⁸, A. P. Colijn¹⁰⁷, J. Collot⁵⁵, T. Colombo^{58c}, G. Compostella¹⁰¹, P. Conde Muiño^{126a,126b}, E. Coniavitis⁴⁸, S. H. Connell^{146b}, I. A. Connelly⁷⁷, S. M. Consonni^{91a,91b}, V. Consorti⁴⁸, S. Constantinescu^{26a}, C. Conta^{121a,121b}, G. Conti³⁰, F. Conventi^{104a,i}, M. Cooke¹⁵, B. D. Cooper⁷⁸, A. M. Cooper-Sarkar¹²⁰, K. Copic¹⁵, T. Cornelissen¹⁷⁶, M. Corradi^{20a}, F. Corriveau^{87j}, A. Corso-Radu¹⁶⁴, A. Cortes-Gonzalez¹², G. Cortiana¹⁰¹, M. J. Costa¹⁶⁸, D. Costanzo¹⁴⁰, D. Côté⁸, G. Cottin²⁸, G. Cowan⁷⁷, B. E. Cox⁸⁴, K. Cranmer¹¹⁰, G. Cree²⁹, S. Crépe-Renaudin⁵⁵, F. Crescioli⁸⁰, W. A. Cribbs^{147a,147b}, M. Crispin Ortuzar¹²⁰, M. Cristinziani²¹, V. Croft¹⁰⁶, G. Crosetti^{37a,37b}, T. Cuhadar Donszelmann¹⁴⁰, J. Cummings¹⁷⁷, M. Curatolo⁴⁷, C. Cuthbert¹⁵¹, H. Cziri¹⁴², P. Czodrowski³, S. D'Auria⁵³, M. D'Onofrio⁷⁴, M. J. Da Cunha Sargedas De Sousa^{126a,126b}, C. Da Via⁸⁴, W. Dabrowski^{38a}, A. Dafinca¹²⁰, T. Dai⁸⁹, O. Dale¹⁴, F. Dallaire⁹⁵, C. Dallapiccola⁸⁶, M. Dam³⁶, A. C. Daniells¹⁸, M. Danninger¹⁶⁹, M. Dano Hoffmann¹³⁷, V. Dao⁴⁸, G. Darbo^{50a}, S. Darmora⁸, J. Dassoulas³, A. Dattagupta⁶¹, W. Davey²¹, C. David¹⁷⁰, T. Davidek¹²⁹, E. Davies^{120,k}, M. Davies¹⁵⁴, O. Davignon⁸⁰, P. Davison⁷⁸, Y. Davygora^{58a}, E. Dawe¹⁴³, I. Dawson¹⁴⁰, R. K. Daya-Ishmukhametova⁸⁶, K. De⁸, R. de Asmundis^{104a}, S. De Castro^{20a,20b}, S. De Cecco⁸⁰, N. De Groot¹⁰⁶, P. de Jong¹⁰⁷, H. De la Torre⁸², F. De Lorenzi⁶⁴, L. De Nooij¹⁰⁷, D. De Pedis^{133a}, A. De Salvo^{133a}, U. De Sanctis¹⁵⁰, A. De Santo¹⁵⁰, J. B. De Vivie De Regie¹¹⁷, W. J. Dearnaley⁷², R. Debbé²⁵, C. Debenedetti¹³⁸, D. V. Dedovich⁶⁵, I. Deigaard¹⁰⁷, J. Del Peso⁸², T. Del Prete^{124a,124b}, F. Deliot¹³⁷, C. M. Delitzsch⁴⁹, M. Deliyergiyev⁷⁵, A. Dell'Acqua³⁰, L. Dell'Asta²², M. Dell'Orso^{124a,124b}, M. Della Pietra^{104a,i}, D. della Volpe⁴⁹, M. Delmastro⁵, P. A. Delsart⁵⁵, C. Deluca¹⁰⁷, D. A. DeMarco¹⁵⁹, S. Demers¹⁷⁷, M. Demichev⁶⁵, A. Demilly⁸⁰, S. P. Denisov¹³⁰, D. Derendarz³⁹, J. E. Derkaoui^{136d}, F. Derue⁸⁰, P. Dervan⁷⁴, K. Desch²¹, C. Deterre⁴², P. O. Deviveiros³⁰, A. Dewhurst¹³¹, S. Dhaliwal¹⁰⁷, A. Di Ciaccio^{134a,134b}, L. Di Ciaccio⁵, A. Di Domenico^{133a,133b}, C. Di Donato^{104a,104b}, A. Di Girolamo³⁰, B. Di Girolamo³⁰, A. Di Mattia¹⁵³, B. Di Micco^{135a,135b}, R. Di Nardo⁴⁷, A. Di Simone⁴⁸, R. Di Sipio^{20a,20b}, D. Di Valentino²⁹, C. Diaconu⁸⁵, F. A. Dias⁴⁶, M. A. Diaz^{32a}, E. B. Diehl⁸⁹, J. Dietrich¹⁶, T. A. Dietzsch^{58a}, S. Diglio⁸⁵, A. Dimitrievska¹³, J. Dingfelder²¹, F. Dittus³⁰, F. Djama⁸⁵, T. Djobava^{51b}, J. I. Djuvsland^{58a}, M. A. B. do Vale^{24c}, D. Dobos³⁰, M. Dobre^{26a}, C. Doglioni⁴⁹, T. Doherty⁵³, T. Dohmae¹⁵⁶, J. Dolejsi¹²⁹, Z. Dolezal¹²⁹, B. A. Dolgoshein^{98*}, M. Donadelli^{24d}, S. Donati^{124a,124b}, P. Dondero^{121a,121b}, J. Donini³⁴, J. Dopke¹³¹, A. Doria^{104a}, M. T. Dova⁷¹, A. T. Doyle⁵³, M. Dris¹⁰, E. Dubreuil³⁴, E. Duchovni¹⁷³, G. Duckeck¹⁰⁰, O. A. Ducu^{26a}, D. Duda¹⁷⁶, A. Dudarev³⁰, L. Duflo¹¹⁷, L. Duguid⁷⁷, M. Dührssen³⁰, M. Dunford^{58a}, H. Duran Yildiz^{4a}, M. Düren⁵², A. Durglishvili^{51b}, D. Duschinger⁴⁴, M. Dwuznik^{38a}, M. Dyndal^{38a}, W. Edson², N. C. Edwards⁴⁶, W. Ehrenfeld²¹, T. Eifert³⁰, G. Eigen¹⁴, K. Einsweiler¹⁵, T. Ekelof¹⁶⁷, M. El Kacimi^{136c}, M. Ellert¹⁶⁷, S. Elles⁵, F. Ellinghaus⁸³, A. A. Elliot¹⁷⁰, N. Ellis³⁰, J. Elmsheuser¹⁰⁰, M. Elsing³⁰, D. Emelianov¹³¹, Y. Enari¹⁵⁶, O. C. Endner⁸³, M. Endo¹¹⁸, R. Engelmann¹⁴⁹, J. Erdmann⁴³, A. Ereditato¹⁷, D. Eriksson^{147a}, G. Ernis¹⁷⁶, J. Ernst², M. Ernst²⁵, S. Errede¹⁶⁶, E. Ertel⁸³, M. Escalier¹¹⁷, H. Esch⁴³, C. Escobar¹²⁵, B. Esposito⁴⁷, A. I. Etienne¹³⁷, E. Etzion¹⁵⁴, H. Evans⁶¹, A. Ezhilov¹²³, L. Fabbri^{20a,20b}, G. Facini³¹, R. M. Fakhruddinov¹³⁰, S. Falciano^{133a}, R. J. Falla⁷⁸, J. Faltova¹²⁹, Y. Fang^{33a}, M. Fanti^{91a,91b}, A. Farbin⁸, A. Farilla^{135a}, T. Farooque¹², S. Farrell¹⁵, S. M. Farrington¹⁷¹, P. Farthouat³⁰, F. Fassi^{136e}, P. Fassnacht³⁰, D. Fassouliotis⁹, A. Favareto^{50a,50b}, L. Fayard¹¹⁷, P. Federic^{145a}, O. L. Fedin^{123,l}, W. Fedorko¹⁶⁹, S. Feigl³⁰, L. Feligioni⁸⁵, C. Feng^{33d}, E. J. Feng⁶, H. Feng⁸⁹, A. B. Fenyuk¹³⁰, P. Fernandez Martinez¹⁶⁸, S. Fernandez Perez³⁰, S. Ferrag⁵³, J. Ferrando⁵³, A. Ferrari¹⁶⁷, P. Ferrari¹⁰⁷, R. Ferrari^{121a}, D. E. Ferreira de Lima⁵³,

A. Ferrer¹⁶⁸, D. Ferrere⁴⁹, C. Ferretti⁸⁹, A. Ferretto Parodi^{50a,50b}, M. Fiascaris³¹, F. Fiedler⁸³, A. Filipčič⁷⁵, M. Filipuzzi⁴², F. Filthaut¹⁰⁶, M. Fincke-Keeler¹⁷⁰, K. D. Finelli¹⁵¹, M. C. N. Fiolhais^{126a,126c}, L. Fiorini¹⁶⁸, A. Firan⁴⁰, A. Fischer², J. Fischer¹⁷⁶, W. C. Fisher⁹⁰, E. A. Fitzgerald²³, M. Flechl⁴⁸, I. Fleck¹⁴², P. Fleischmann⁸⁹, S. Fleischmann¹⁷⁶, G. T. Fletcher¹⁴⁰, G. Fletcher⁷⁶, T. Flick¹⁷⁶, A. Floderus⁸¹, L. R. Flores Castillo^{60a}, M. J. Flowerdew¹⁰¹, A. Formica¹³⁷, A. Forti⁸⁴, D. Fournier¹¹⁷, H. Fox⁷², S. Fracchia¹², P. Francavilla⁸⁰, M. Franchini^{20a,20b}, D. Francis³⁰, L. Franconi¹¹⁹, M. Franklin⁵⁷, M. Fraternali^{121a,121b}, D. Freeborn⁷⁸, S. T. French²⁸, F. Friedrich⁴⁴, D. Froidevaux³⁰, J. A. Frost¹²⁰, C. Fukunaga¹⁵⁷, E. Fullana Torregrosa⁸³, B. G. Fulsom¹⁴⁴, J. Fuster¹⁶⁸, C. Gabaldon⁵⁵, O. Gabizon¹⁷⁶, A. Gabrielli^{20a,20b}, A. Gabrielli^{133a,133b}, S. Gadatsch¹⁰⁷, S. Gadomski⁴⁹, G. Gagliardi^{50a,50b}, P. Gagnon⁶¹, C. Galea¹⁰⁶, B. Galhardo^{126a,126c}, E. J. Gallas¹²⁰, B. J. Gallop¹³¹, P. Gallus¹²⁸, G. Galster³⁶, K. K. Gan¹¹¹, J. Gao^{33b,85}, Y. S. Gao^{144.e}, F. M. Garay Walls⁴⁶, F. Garbersen¹⁷⁷, C. García¹⁶⁸, J. E. García Navarro¹⁶⁸, M. Garcia-Sciveres¹⁵, R. W. Gardner³¹, N. Garelli¹⁴⁴, V. Garonne³⁰, C. Gatti⁴⁷, G. Gaudio^{121a}, B. Gaur¹⁴², L. Gauthier⁹⁵, P. Gauzzi^{133a,133b}, I. L. Gavrilenko⁹⁶, C. Gay¹⁶⁹, G. Gaycken²¹, E. N. Gazis¹⁰, P. Ge^{33d}, Z. Gece¹⁶⁹, C. N. P. Gee¹³¹, D. A. A. Geerts¹⁰⁷, Ch. Geich-Gimbel²¹, C. Gemme^{50a}, A. Gemmell⁵³, M. H. Genest⁵⁵, S. Gentile^{133a,133b}, M. George⁵⁴, S. George⁷⁷, D. Gerbaudo¹⁶⁴, A. Gershon¹⁵⁴, H. Ghazlane^{136b}, N. Ghodbane³⁴, B. Giacobbe^{20a}, S. Giagu^{133a,133b}, V. Giangiobbe¹², P. Giannetti^{124a,124b}, F. Gianotti³⁰, B. Gibbard²⁵, S. M. Gibson⁷⁷, M. Gilchriese¹⁵, T. P. S. Gillam²⁸, D. Gillberg³⁰, G. Gilles³⁴, D. M. Gingrich^{3,d}, N. Giokaris⁹, M. P. Giordani^{165a,165c}, F. M. Giorgi^{20a}, F. M. Giorgi¹⁶, P. F. Giraud¹³⁷, D. Giugni^{91a}, C. Giuliani⁴⁸, M. Giulini^{58b}, B. K. Gjelsten¹¹⁹, S. Gkaitatzis¹⁵⁵, I. Gkialas¹⁵⁵, E. L. Gkougkousis¹¹⁷, L. K. Gladilin⁹⁹, C. Glasman⁸², J. Glatzer³⁰, P. C. F. Glaysher⁴⁶, A. Glazov⁴², G. L. Glonti⁶², M. Goblirsch-Kolb¹⁰¹, J. R. Goddard⁷⁶, J. Godlewski³⁹, S. Goldfarb⁸⁹, T. Golling⁴⁹, D. Golubkov¹³⁰, A. Gomes^{126a,126b,126d}, R. Gonçalves^{126a}, J. Goncalves Pinto Firmino Da Costa¹³⁷, L. Gonella²¹, S. González de la Hoz¹⁶⁸, G. Gonzalez Parra¹², S. Gonzalez-Sevilla⁴⁹, L. Goossens³⁰, P. A. Gorbounov⁹⁷, H. A. Gordon²⁵, I. Gorelov¹⁰⁵, B. Gorini³⁰, E. Gorini^{73a,73b}, A. Gorišek⁷⁵, E. Gornicki³⁹, A. T. Goshaw⁴⁵, C. Gössling⁴³, M. I. Gostkin⁶⁵, M. Gouighri^{136a}, D. Goujdami^{136c}, M. P. Goulette⁴⁹, A. G. Goussiou¹³⁹, H. M. X. Grabas¹³⁸, L. Graber⁵⁴, I. Grabowska-Bold^{38a}, P. Grafström^{20a,20b}, K.-J. Grahm⁴², J. Gramling⁴⁹, E. Gramstad¹¹⁹, S. Grancagnolo¹⁶, V. Grassi¹⁴⁹, V. Gratchev¹²³, H. M. Gray³⁰, E. Graziani^{135a}, Z. D. Greenwood^{79,m}, K. Gregersen⁷⁸, I. M. Gregor⁴², P. Grenier¹⁴⁴, J. Griffiths⁸, A. A. Grillo¹³⁸, K. Grimm⁷², S. Grinstein^{12,n}, Ph. Gris³⁴, Y. V. Grishkevich⁹⁹, J.-F. Grivaz¹¹⁷, J. P. Grohs⁴⁴, A. Grohsjean⁴², E. Gross¹⁷³, J. Grosse-Knetter⁵⁴, G. C. Grossi^{134a,134b}, Z. J. Grout¹⁵⁰, L. Guan^{33b}, J. Guenther¹²⁸, F. Guescini⁴⁹, D. Guest¹⁷⁷, O. Gueta¹⁵⁴, E. Guido^{50a,50b}, T. Guillemin¹¹⁷, S. Guindon², U. Gul⁵³, C. Gumpert⁴⁴, J. Guo^{33e}, S. Gupta¹²⁰, P. Gutierrez¹¹³, N. G. Gutierrez Ortiz⁵³, C. Gutsche⁷⁸, N. Guttman¹⁵⁴, C. Guyot¹³⁷, C. Gwenlan¹²⁰, C. B. Gwilliam⁷⁴, A. Haas¹¹⁰, C. Haber¹⁵, H. K. Hadavand⁸, N. Haddad^{136e}, P. Haefner²¹, S. Hageböck²¹, Z. Hajduk³⁹, H. Hakobyan¹⁷⁸, M. Haleem⁴², J. Haley¹¹⁴, D. Hall¹²⁰, G. Halladjian⁹⁰, G. D. Hallewell⁸⁵, K. Hamacher¹⁷⁶, P. Hamal¹¹⁵, K. Hamano¹⁷⁰, M. Hamer⁵⁴, A. Hamilton^{146a}, S. Hamilton¹⁶², G. N. Hamity^{146c}, P. G. Hamnett⁴², L. Han^{33b}, K. Hanagaki¹¹⁸, K. Hanawa¹⁵⁶, M. Hance¹⁵, P. Hanke^{58a}, R. Hanna¹³⁷, J. B. Hansen³⁶, J. D. Hansen³⁶, P. H. Hansen³⁶, K. Hara¹⁶¹, A. S. Hard¹⁷⁴, T. Harenberg¹⁷⁶, F. Hariri¹¹⁷, S. Harkusha⁹², R. D. Harrington⁴⁶, P. F. Harrison¹⁷¹, F. Hartjes¹⁰⁷, M. Hasegawa⁶⁷, S. Hasegawa¹⁰³, Y. Hasegawa¹⁴¹, A. Hasib¹¹³, S. Hassani¹³⁷, S. Haug¹⁷, R. Hauser⁹⁰, L. Hauswald⁴⁴, M. Havranek¹²⁷, C. M. Hawkes¹⁸, R. J. Hawkings³⁰, A. D. Hawkins⁸¹, T. Hayashi¹⁶¹, D. Hayden⁹⁰, C. P. Hays¹²⁰, J. M. Hays⁷⁶, H. S. Hayward⁷⁴, S. J. Haywood¹³¹, S. J. Head¹⁸, T. Heck⁸³, V. Hedberg⁸¹, L. Heelan⁸, S. Heim¹²², T. Heim¹⁷⁶, B. Heinemann¹⁵, L. Heinrich¹¹⁰, J. Hejbal¹²⁷, L. Helary²², M. Heller³⁰, S. Hellman^{147a,147b}, D. Hellmich²¹, C. Helsens³⁰, J. Henderson¹²⁰, R. C. W. Henderson⁷², Y. Heng¹⁷⁴, C. Hengler⁴², A. Henrichs¹⁷⁷, A. M. Henriques Correia³⁰, S. Henrot-Versille¹¹⁷, G. H. Herbert¹⁶, Y. Hernández Jiménez¹⁶⁸, R. Herrberg-Schubert¹⁶, G. Herten⁴⁸, R. Hertenberger¹⁰⁰, L. Hervas³⁰, G. G. Hesketh⁷⁸, N. P. Hessey¹⁰⁷, R. Hickling⁷⁶, E. Higón-Rodríguez¹⁶⁸, E. Hill¹⁷⁰, J. C. Hill²⁸, K. H. Hiller⁴², S. J. Hillier¹⁸, I. Hinchliffe¹⁵, E. Hines¹²², R. R. Hinman¹⁵, M. Hirose¹⁵⁸, D. Hirschebuehl¹⁷⁶, J. Hobbs¹⁴⁹, N. Hod¹⁰⁷, M. C. Hodgkinson¹⁴⁰, P. Hodgson¹⁴⁰, A. Hoecker³⁰, M. R. Hoefkamp¹⁰⁵, F. Hoenig¹⁰⁰, M. Hohlfeld⁸³, T. R. Holmes¹⁵, T. M. Hong¹²², L. Hooft van Huysduynen¹¹⁰, W. H. Hopkins¹¹⁶, Y. Horii¹⁰³, A. J. Horton¹⁴³, J.-Y. Hostachy⁵⁵, S. Hou¹⁵², A. Hoummada^{136a}, J. Howard¹²⁰, J. Howarth⁴², M. Hrabovsky¹¹⁵, I. Hristova¹⁶, J. Hrivnac¹¹⁷, T. Hryn'ova⁵, A. Hrynevich⁹³, C. Hsu^{146c}, P. J. Hsu^{152,o}, S.-C. Hsu¹³⁹, D. Hu³⁵, Q. Hu^{33b}, X. Hu⁸⁹, Y. Huang⁴², Z. Hubacek³⁰, F. Hubaut⁸⁵, F. Huegging²¹, T. B. Huffman¹²⁰, E. W. Hughes³⁵, G. Hughes⁷², M. Huhtinen³⁰, T. A. Hülsing⁸³, M. Hurwitz¹⁵, N. Huseynov^{65,b}, J. Huston⁹⁰, J. Huth⁵⁷, G. Iacobucci⁴⁹, G. Iakovidis²⁵, I. Ibragimov¹⁴², L. Iconomidou-Fayard¹¹⁷, E. Ideal¹⁷⁷, Z. Idrissi^{136e}, P. Iengo^{104a}, O. Igonkina¹⁰⁷, T. Iizawa¹⁷², Y. Ikegami⁶⁶, K. Ikematsu¹⁴², M. Ikeno⁶⁶, Y. Ilchenko^{31,p}, D. Iliadis¹⁵⁵, N. Ilic¹⁵⁹, Y. Inamaru⁶⁷, T. Ince¹⁰¹, P. Ioannou⁹, M. Iodice^{135a}, K. Iordanidou⁹, V. Ippolito⁵⁷, A. Irls Quiles¹⁶⁸, C. Isaksson¹⁶⁷, M. Ishino⁶⁸, M. Ishitsuka¹⁵⁸, R. Ishmukhametov¹¹¹, C. Issever¹²⁰, S. Istin^{19a}, J. M. Iturbe Ponce⁸⁴, R. Iuppa^{134a,134b}, J. Ivarsson⁸¹, W. Iwanski³⁹, H. Iwasaki⁶⁶, J. M. Izen⁴¹, V. Izzo^{104a}, B. Jackson¹²², M. Jackson⁷⁴, P. Jackson¹, M. R. Jaekel³⁰, V. Jain², K. Jakobs⁴⁸, S. Jakobsen³⁰, T. Jakoubek¹²⁷, J. Jakubek¹²⁸, D. O. Jamin¹⁵², D. K. Jana⁷⁹, E. Jansen⁷⁸, J. Janssen²¹,

M. Janus¹⁷¹, G. Jarlskog⁸¹, N. Javadov^{65,b}, T. Javůrek⁴⁸, L. Jeanty¹⁵, J. Jejelava^{51a,q}, G.-Y. Jeng¹⁵¹, D. Jennens⁸⁸, P. Jenni^{48,r}, J. Jentsch⁴³, C. Jeske¹⁷¹, S. Jézéquel⁵, H. Ji¹⁷⁴, J. Jia¹⁴⁹, Y. Jiang^{33b}, J. Jimenez Pena¹⁶⁸, S. Jin^{33a}, A. Jinaru^{26a}, O. Jinnouchi¹⁵⁸, M. D. Joergensen³⁶, P. Johansson¹⁴⁰, K. A. Johns⁷, K. Jon-And^{147a,147b}, G. Jones¹⁷¹, R. W. L. Jones⁷², T. J. Jones⁷⁴, J. Jongmanns^{58a}, P. M. Jorge^{126a,126b}, K. D. Joshi⁸⁴, J. Jovicevic¹⁴⁸, X. Ju¹⁷⁴, C. A. Jung⁴³, P. Jussel⁶², A. Juste Rozas^{12,n}, M. Kaci¹⁶⁸, A. Kaczmarska³⁹, M. Kado¹¹⁷, H. Kagan¹¹¹, M. Kagan¹⁴⁴, S. J. Kahn⁸⁵, E. Kajomovitz⁴⁵, C. W. Kalderon¹²⁰, S. Kama⁴⁰, A. Kamenshchikov¹³⁰, N. Kanaya¹⁵⁶, M. Kaneda³⁰, S. Kaneti²⁸, V. A. Kantserov⁹⁸, J. Kanzaki⁶⁶, B. Kaplan¹¹⁰, A. Kapliy³¹, D. Kar⁵³, K. Karakostas¹⁰, A. Karamaoun³, N. Karastathis¹⁰, M. J. Kareem⁵⁴, M. Karnevskiy⁸³, S. N. Karpov⁶⁵, Z. M. Karpova⁶⁵, K. Karthik¹¹⁰, V. Kartvelishvili⁷², A. N. Karyukhin¹³⁰, L. Kashif¹⁷⁴, G. Kasieczka^{58b}, R. D. Kass¹¹¹, A. Kastanas¹⁴, Y. Kataoka¹⁵⁶, A. Katre⁴⁹, J. Katzy⁴², K. Kawagoe⁷⁰, T. Kawamoto¹⁵⁶, G. Kawamura⁵⁴, S. Kazama¹⁵⁶, V. F. Kazanin¹⁰⁹, M. Y. Kazarinov⁶⁵, R. Keeler¹⁷⁰, R. Kehoe⁴⁰, M. Keil⁵⁴, J. S. Keller⁴², J. J. Kempster⁷⁷, H. Keoshkerian⁸⁴, O. Kepka¹²⁷, B. P. Kerševan⁷⁵, S. Kersten¹⁷⁶, R. A. Keyes⁸⁷, F. Khalil-zada¹¹, H. Khandanyan^{147a,147b}, A. Khanov¹¹⁴, A. Kharlamov¹⁰⁹, A. Khodinov⁹⁸, A. Khomich^{58a}, T. J. Khoo²⁸, G. Khoraiuli²¹, V. Khovanskiy⁹⁷, E. Khramov⁶⁵, J. Khubua^{51b,s}, H. Y. Kim⁸, H. Kim^{147a,147b}, S. H. Kim¹⁶¹, N. Kimura¹⁵⁵, O. Kind¹⁶, B. T. King⁷⁴, M. King¹⁶⁸, R. S. B. King¹²⁰, S. B. King¹⁶⁹, J. Kirk¹³¹, A. E. Kiryunin¹⁰¹, T. Kishimoto⁶⁷, D. Kisielewska^{38a}, F. Kiss⁴⁸, K. Kiuchi¹⁶¹, E. Kladiva^{145b}, M. Klein⁷⁴, U. Klein⁷⁴, K. Kleinknecht⁸³, P. Klimek^{147a,147b}, A. Klimentov²⁵, R. Klingenberg⁴³, J. A. Klinger⁸⁴, T. Klioutchnikova³⁰, P. F. Klok¹⁰⁶, E.-E. Kluge^{58a}, P. Kluit¹⁰⁷, S. Kluth¹⁰¹, E. Kneringer⁶², E. B. F. G. Knoops⁸⁵, A. Knue⁵³, D. Kobayashi¹⁵⁸, T. Kobayashi¹⁵⁶, M. Kobel⁴⁴, M. Kocian¹⁴⁴, P. Kodys¹²⁹, T. Koffas²⁹, E. Koffeman¹⁰⁷, L. A. Kogan¹²⁰, S. Kohlmann¹⁷⁶, Z. Kohout¹²⁸, T. Kohriki⁶⁶, T. Koi¹⁴⁴, H. Kolanoski¹⁶, I. Koletsou⁵, A. A. Komar^{96,*}, Y. Komori¹⁵⁶, T. Kondo⁶⁶, N. Kondrashova⁴², K. Köneke⁴⁸, A. C. König¹⁰⁶, S. König⁸³, T. Kono^{66,t}, R. Konoplich^{110,u}, N. Konstantinidis⁷⁸, R. Kopeliainsky¹⁵³, S. Koperny^{38a}, L. Köpke⁸³, A. K. Kopp⁴⁸, K. Korcyl³⁹, K. Kordas¹⁵⁵, A. Korn⁷⁸, A. A. Korol^{109,c}, I. Korolkov¹², E. V. Korolkova¹⁴⁰, O. Kortner¹⁰¹, S. Kortner¹⁰¹, T. Kosek¹²⁹, V. V. Kostyukhin²¹, V. M. Kotov⁶⁵, A. Kotwal⁴⁵, A. Kourkoumeli-Charalampidi¹⁵⁵, C. Kourkoumelis⁹, V. Kouskoura²⁵, A. Koutsman^{160a}, R. Kowalewski¹⁷⁰, T. Z. Kowalski^{38a}, W. Kozanecki¹³⁷, A. S. Kozhin¹³⁰, V. A. Kramarenko⁹⁹, G. Kramberger⁷⁵, D. Krasnopevtsev⁹⁸, M. W. Krasny⁸⁰, A. Krasznahorkay³⁰, J. K. Kraus²¹, A. Kravchenko²⁵, S. Kreiss¹¹⁰, M. Kretz^{58c}, J. Kretzschmar⁷⁴, K. Kreutzfeldt⁵², P. Krieger¹⁵⁹, K. Krizka³¹, K. Kroeninger⁴³, H. Kroha¹⁰¹, J. Kroll¹²², J. Kroseberg²¹, J. Krstic¹³, U. Kruchonak⁶⁵, H. Krüger²¹, N. Krumnack⁶⁴, Z. V. Krumshteyn⁶⁵, A. Kruse¹⁷⁴, M. C. Kruse⁴⁵, M. Kruskal²², T. Kubota⁸⁸, H. Kucuk⁷⁸, S. Kuday^{4c}, S. Kuehn⁴⁸, A. Kugel^{58c}, F. Kuger¹⁷⁵, A. Kuhl¹³⁸, T. Kuhl⁴², V. Kukhtin⁶⁵, Y. Kulchitsky⁹², S. Kuleshov^{32b}, M. Kuna^{133a,133b}, T. Kunigo⁶⁸, A. Kupco¹²⁷, H. Kurashige⁶⁷, Y. A. Kurochkin⁹², R. Kurumida⁶⁷, V. Kus¹²⁷, E. S. Kuwertz¹⁴⁸, M. Kuze¹⁵⁸, J. Kvita¹¹⁵, T. Kwan¹⁷⁰, D. Kyriazopoulos¹⁴⁰, A. La Rosa⁴⁹, J. L. La Rosa Navarro^{24d}, L. La Rotonda^{37a,37b}, C. Lacasta¹⁶⁸, F. Lacava^{133a,133b}, J. Lacey²⁹, H. Lacker¹⁶, D. Lacour⁸⁰, V. R. Lacuesta¹⁶⁸, E. Ladygin⁶⁵, R. Lafaye⁵, B. Laforge⁸⁰, T. Lagouri¹⁷⁷, S. Lai⁴⁸, H. Laier^{58a}, L. Lambourne⁷⁸, S. Lammers⁶¹, C. L. Lampen⁷, W. Lampl⁷, E. Lançon¹³⁷, U. Landgraf⁴⁸, M. P. J. Landon⁷⁶, V. S. Lang^{58a}, A. J. Lankford¹⁶⁴, F. Lanni²⁵, K. Lantzsch³⁰, S. Laplace⁸⁰, C. Lapoire³⁰, J. F. Laporte¹³⁷, T. Lari^{91a}, F. Lasagni Manghi^{20a,20b}, M. Lassnig³⁰, P. Laurelli⁴⁷, W. Lavrijsen¹⁵, A. T. Law¹³⁸, P. Laycock⁷⁴, O. Le Dortz⁸⁰, E. Le Guirriec⁸⁵, E. Le Menedeu¹², T. LeCompte⁶, F. Ledroit-Guillon⁵⁵, C. A. Lee^{146b}, S. C. Lee¹⁵², L. Lee¹, G. Lefebvre⁸⁰, M. Lefebvre¹⁷⁰, F. Legger¹⁰⁰, C. Leggett¹⁵, A. Lehan⁷⁴, G. Lehmann Miotto³⁰, X. Lei⁷, W. A. Leight²⁹, A. Leisos¹⁵⁵, A. G. Leister¹⁷⁷, M. A. L. Leite^{24d}, R. Leitner¹²⁹, D. Lellouch¹⁷³, B. Lemmer⁵⁴, K. J. C. Leney⁷⁸, T. Lenz²¹, G. Lenzen¹⁷⁶, B. Lenzi³⁰, R. Leone⁷, S. Leone^{124a,124b}, C. Leonidopoulos⁴⁶, S. Leontsinis¹⁰, C. Leroy⁹⁵, C. G. Lester²⁸, M. Levchenko¹²³, J. Levêque⁵, D. Levin⁸⁹, L. J. Levinson¹⁷³, M. Levy¹⁸, A. Lewis¹²⁰, A. M. Leyko²¹, M. Leyton⁴¹, B. Li^{33b,v}, B. Li⁸⁵, H. Li¹⁴⁹, H. L. Li³¹, L. Li⁴⁵, L. Li^{33e}, S. Li⁴⁵, Y. Li^{33c,w}, Z. Liang¹³⁸, H. Liao³⁴, B. Liberti^{134a}, P. Lichard³⁰, K. Lie¹⁶⁶, J. Liebal²¹, W. Liebig¹⁴, C. Limbach²¹, A. Limosani¹⁵¹, S. C. Lin^{152,x}, T. H. Lin⁸³, F. Linde¹⁰⁷, B. E. Lindquist¹⁴⁹, J. T. Linnemann⁹⁰, E. Lipeles¹²², A. Lipniacka¹⁴, M. Lisovsky⁴², T. M. Liss¹⁶⁶, D. Lissauer²⁵, A. Lister¹⁶⁹, A. M. Litke¹³⁸, B. Liu¹⁵², D. Liu¹⁵², J. Liu⁸⁵, J. B. Liu^{33b}, K. Liu^{33b,y}, L. Liu⁸⁹, M. Liu⁴⁵, M. Liu^{33b}, Y. Liu^{33b}, M. Livan^{121a,121b}, A. Lleres⁵⁵, J. Llorente Merino⁸², S. L. Lloyd⁷⁶, F. Lo Sterzo¹⁵², E. Lobodzinska⁴², P. Loch⁷, W. S. Lockman¹³⁸, F. K. Loebinger⁸⁴, A. E. Loevschall-Jensen³⁶, A. Loginov¹⁷⁷, T. Lohse¹⁶, K. Lohwasser⁴², M. Lokajicek¹²⁷, B. A. Long²², J. D. Long⁸⁹, R. E. Long⁷², K. A.Looper¹¹¹, L. Lopes^{126a}, D. Lopez Mateos⁵⁷, B. Lopez Paredes¹⁴⁰, I. Lopez Paz¹², J. Lorenz¹⁰⁰, N. Lorenzo Martinez⁶¹, M. Losada¹⁶³, P. Loscutoff¹⁵, X. Lou^{33a}, A. Lounis¹¹⁷, J. Love⁶, P. A. Love⁷², A. J. Lowe^{144,e}, F. Lu^{33a}, N. Lu⁸⁹, H. J. Lubatti¹³⁹, C. Luci^{133a,133b}, A. Lucotte⁵⁵, F. Luehring⁶¹, W. Lukas⁶², L. Luminari^{133a}, O. Lundberg^{147a,147b}, B. Lund-Jensen¹⁴⁸, M. Lungwitz⁸³, D. Lynn²⁵, R. Lysak¹²⁷, E. Lytken⁸¹, H. Ma²⁵, L. L. Ma^{33d}, G. Maccarrone⁴⁷, A. Macchiolo¹⁰¹, J. Machado Miguens^{126a,126b}, D. Macina³⁰, D. Madaffari⁸⁵, R. Madar³⁴, H. J. Maddocks⁷², W. F. Mader⁴⁴, A. Madsen¹⁶⁷, T. Maeno²⁵, A. Maevskiy⁹⁹, E. Magradze⁵⁴, K. Mahboubi⁴⁸, J. Mahlstedt¹⁰⁷, S. Mahmoud⁷⁴, C. Maiani¹³⁷, C. Maidantchik^{24a}, A. A. Maier¹⁰¹, A. Maio^{126a,126b,126d}, S. Majewski¹¹⁶, Y. Makida⁶⁶, N. Makovec¹¹⁷, B. Malaescu⁸⁰, Pa. Malecki³⁹

V. P. Maleev¹²³, F. Malek⁵⁵, U. Mallik⁶³, D. Malon⁶, C. Malone¹⁴⁴, S. Maltezos¹⁰, V. M. Malyshev¹⁰⁹, S. Malyukov³⁰, J. Mamuzic⁴², B. Mandelli³⁰, L. Mandelli^{91a}, I. Mandić⁷⁵, R. Mandrysch⁶³, J. Maneira^{126a,126b}, A. Manfredini¹⁰¹, L. Manhaes de Andrade Filho^{24b}, J. Manjarres Ramos^{160b}, A. Mann¹⁰⁰, P. M. Manning¹³⁸, A. Manousakis-Katsikakis⁹, B. Mansoulie¹³⁷, R. Mantifel⁸⁷, M. Mantoani⁵⁴, L. Mapelli³⁰, L. March^{146c}, G. Marchiori⁸⁰, M. Marcisovsky¹²⁷, C. P. Marino¹⁷⁰, M. Marjanovic¹³, F. Marroquim^{24a}, S. P. Marsden⁸⁴, Z. Marshall¹⁵, L. F. Marti¹⁷, S. Marti-Garcia¹⁶⁸, B. Martin⁹⁰, T. A. Martin¹⁷¹, V. J. Martin⁴⁶, B. Martin dit Latour¹⁴, H. Martinez¹³⁷, M. Martinez^{12.n}, S. Martin-Haugh¹³¹, A. C. Martyniuk⁷⁸, M. Marx¹³⁹, F. Marzano^{133a}, A. Marzin³⁰, L. Masetti⁸³, T. Mashimo¹⁵⁶, R. Mashinistov⁹⁶, J. Masik⁸⁴, A. L. Maslennikov^{109.c}, I. Massa^{20a,20b}, L. Massa^{20a,20b}, N. Massol⁵, P. Mastrandrea¹⁴⁹, A. Mastroberardino^{37a,37b}, T. Masubuchi¹⁵⁶, P. Mättig¹⁷⁶, J. Mattmann⁸³, J. Maurer^{26a}, S. J. Maxfield⁷⁴, D. A. Maximov^{109.c}, R. Mazini¹⁵², S. M. Mazza^{91a,91b}, L. Mazzaferro^{134a,134b}, G. Mc Goldrick¹⁵⁹, S. P. Mc Kee⁸⁹, A. McCarn⁸⁹, R. L. McCarthy¹⁴⁹, T. G. McCarthy²⁹, N. A. McCubbin¹³¹, K. W. McFarlane^{56.*}, J. A. McFayden⁷⁸, G. Mchedlidze⁵⁴, S. J. McMahon¹³¹, R. A. McPherson^{170.j}, J. Mechnich¹⁰⁷, M. Medinnis⁴², S. Meehan^{146a}, S. Mehlhase¹⁰⁰, A. Mehta⁷⁴, K. Meier^{58a}, C. Meineck¹⁰⁰, B. Meirose⁴¹, C. Melachrinou³¹, B. R. Mellado Garcia^{146c}, F. Meloni¹⁷, A. Mengarelli^{20a,20b}, S. Menke¹⁰¹, E. Meoni¹⁶², K. M. Mercurio⁵⁷, S. Mergelmeyer²¹, N. Meric¹³⁷, P. Mermoud⁴⁹, L. Merola^{104a,104b}, C. Meroni^{91a}, F. S. Merritt³¹, H. Merritt¹¹¹, A. Messina^{30.z}, J. Metcalfe²⁵, A. S. Mete¹⁶⁴, C. Meyer⁸³, C. Meyer¹²², J-P. Meyer¹³⁷, J. Meyer³⁰, R. P. Middleton¹³¹, S. Migas⁷⁴, S. Miglioranza^{165a,165c}, L. Mijović²¹, G. Mikenberg¹⁷³, M. Mikestikova¹²⁷, M. Mikuž⁷⁵, A. Milic³⁰, D. W. Miller³¹, C. Mills⁴⁶, A. Milov¹⁷³, D. A. Milstead^{147a,147b}, A. A. Minaenko¹³⁰, Y. Minami¹⁵⁶, I. A. Minashvili⁶⁵, A. I. Mincer¹¹⁰, B. Mindur^{38a}, M. Mineev⁶⁵, Y. Ming¹⁷⁴, L. M. Mir¹², G. Mirabelli^{133a}, T. Mitani¹⁷², J. Mitrevski¹⁰⁰, V. A. Mitsou¹⁶⁸, A. Miucci⁴⁹, P. S. Miyagawa¹⁴⁰, J. U. Mjörnmark⁸¹, T. Moa^{147a,147b}, K. Mochizuki⁸⁵, S. Mohapatra³⁵, W. Mohr⁴⁸, S. Molander^{147a,147b}, R. Moles-Valls¹⁶⁸, K. Möniq⁴², C. Monini⁵⁵, J. Monk³⁶, E. Monnier⁸⁵, J. Montejo Berlingen¹², F. Monticelli⁷¹, S. Monzani^{133a,133b}, R. W. Moore³, N. Morange⁶³, D. Moreno¹⁶³, M. Moreno Llácer⁵⁴, P. Morettini^{50a}, M. Morgenstern⁴⁴, M. Morii⁵⁷, V. Morisbak¹¹⁹, S. Moritz⁸³, A. K. Morley¹⁴⁸, G. Mornacchi³⁰, J. D. Morris⁷⁶, A. Morton⁵³, L. Morvaj¹⁰³, H. G. Moser¹⁰¹, M. Mosidze^{51b}, J. Moss¹¹¹, K. Motohashi¹⁵⁸, R. Mount¹⁴⁴, E. Mountricha²⁵, S. V. Mouraviev^{96.*}, E. J. W. Moyses⁸⁶, S. Muanza⁸⁵, R. D. Mudd¹⁸, F. Mueller¹⁰¹, J. Mueller¹²⁵, K. Mueller²¹, T. Mueller²⁸, D. Muenstermann⁴⁹, P. Mullen⁵³, Y. Munwes¹⁵⁴, J. A. Murillo Quijada¹⁸, W. J. Murray^{171,131}, H. Musheghyan⁵⁴, E. Musto¹⁵³, A. G. Myagkov^{130.aa}, M. Myska¹²⁸, O. Nackenhorst⁵⁴, J. Nadal⁵⁴, K. Nagai¹²⁰, R. Nagai¹⁵⁸, Y. Nagai⁸⁵, K. Nagano⁶⁶, A. Nagarkar¹¹¹, Y. Nagasaka⁵⁹, K. Nagata¹⁶¹, M. Nagel¹⁰¹, A. M. Nairz³⁰, Y. Nakahama³⁰, K. Nakamura⁶⁶, T. Nakamura¹⁵⁶, I. Nakano¹¹², H. Namasivayam⁴¹, G. Nanava²¹, R. F. Naranjo Garcia⁴², R. Narayan^{58b}, T. Nattermann²¹, T. Naumann⁴², G. Navarro¹⁶³, R. Nayyar⁷, H. A. Neal⁸⁹, P. Yu. Nechaeva⁹⁶, T. J. Neep⁸⁴, P. D. Nef¹⁴⁴, A. Negri^{121a,121b}, M. Negrini^{20a}, S. Nektarijevic¹⁰⁶, C. Nellist¹¹⁷, A. Nelson¹⁶⁴, S. Nemecek¹²⁷, P. Nemethy¹¹⁰, A. A. Nepomuceno^{24a}, M. Nessi^{30.ab}, M. S. Neubauer¹⁶⁶, M. Neumann¹⁷⁶, R. M. Neves¹¹⁰, P. Nevski²⁵, P. R. Newman¹⁸, D. H. Nguyen⁶, R. B. Nickerson¹²⁰, R. Nicolaidou¹³⁷, B. Nicquevert³⁰, J. Nielsen¹³⁸, N. Nikiforou³⁵, A. Nikiforov¹⁶, V. Nikolaenko^{130.aa}, I. Nikolic-Audit⁸⁰, K. Nikolopoulos¹⁸, P. Nilsson²⁵, Y. Ninomiya¹⁵⁶, A. Nisati^{133a}, R. Nisius¹⁰¹, T. Nobe¹⁵⁸, M. Nomachi¹¹⁸, I. Nomidis²⁹, S. Norberg¹¹³, M. Nordberg³⁰, O. Novgorodova⁴⁴, S. Nowak¹⁰¹, M. Nozaki⁶⁶, L. Nozka¹¹⁵, K. Ntekas¹⁰, G. Nunes Hanninger⁸⁸, T. Nunnemann¹⁰⁰, E. Nurse⁷⁸, F. Nuti⁸⁸, B. J. O'Brien⁴⁶, F. O'grady⁷, D. C. O'Neil¹⁴³, V. O'Shea⁵³, F. G. Oakham^{29.d}, H. Oberlack¹⁰¹, T. Obermann²¹, J. Ocariz⁸⁰, A. Ochi⁶⁷, I. Ochoa⁷⁸, S. Oda⁷⁰, S. Odaka⁶⁶, H. Ogren⁶¹, A. Oh⁸⁴, S. H. Oh⁴⁵, C. C. Ohm¹⁵, H. Ohman¹⁶⁷, H. Oide³⁰, W. Okamura¹¹⁸, H. Okawa¹⁶¹, Y. Okumura³¹, T. Okuyama¹⁵⁶, A. Olariu^{26a}, A. G. Olchevski⁶⁵, S. A. Olivares Pino⁴⁶, D. Oliveira Damazio²⁵, E. Oliver Garcia¹⁶⁸, A. Olszewski³⁹, J. Olszowska³⁹, A. Onofre^{126a,126c}, P. U. E. Onyisi^{31.p}, C. J. Oram^{160a}, M. J. Oreglia³¹, Y. Oren¹⁵⁴, D. Orestano^{135a,135b}, N. Orlando^{73a,73b}, C. Oropeza Barrera⁵³, R. S. Orr¹⁵⁹, B. Osculati^{50a,50b}, R. Ospanov⁸⁴, G. Otero y Garzon²⁷, H. Otono⁷⁰, M. Ouchrif^{136d}, E. A. Ouellette¹⁷⁰, F. Ould-Saada¹¹⁹, A. Ouraou¹³⁷, K. P. Oussoren¹⁰⁷, Q. Ouyang^{33a}, A. Ovcharova¹⁵, M. Owen⁵³, V. E. Ozcan^{19a}, N. Ozturk⁸, K. Pachal¹²⁰, A. Pacheco Pages¹², C. Padilla Aranda¹², M. Pagáčová⁴⁸, S. Pagan Griso¹⁵, E. Paganis¹⁴⁰, C. Pahl¹⁰¹, F. Paige²⁵, P. Pais⁸⁶, K. Pajchel¹¹⁹, G. Palacino^{160b}, S. Palestini³⁰, M. Palka^{38b}, D. Pallin³⁴, A. Palma^{126a,126b}, Y. B. Pan¹⁷⁴, E. Panagiotopoulou¹⁰, C. E. Pandini⁸⁰, J. G. Panduro Vazquez⁷⁷, P. Pani^{147a,147b}, N. Panikashvili⁸⁹, S. Panitkin²⁵, L. Paolozzi^{134a,134b}, Th. D. Papadopoulou¹⁰, K. Papageorgiou¹⁵⁵, A. Paramonov⁶, D. Paredes Hernandez¹⁵⁵, M. A. Parker²⁸, K. A. Parker¹⁴⁰, F. Parodi^{50a,50b}, J. A. Parsons³⁵, U. Parzefall⁴⁸, E. Pasqualucci^{133a}, S. Passaggio^{50a}, F. Pastore^{135a,135b.*}, Fr. Pastore⁷⁷, G. Pásztor²⁹, S. Patariaia¹⁷⁶, N. D. Patel¹⁵¹, J. R. Pater⁸⁴, T. Pauly³⁰, J. Pearce¹⁷⁰, L. E. Pedersen³⁶, M. Pedersen¹¹⁹, S. Pedraza Lopez¹⁶⁸, R. Pedro^{126a,126b}, S. V. Peleganchuk¹⁰⁹, D. Pelikan¹⁶⁷, H. Peng^{33b}, B. Penning³¹, J. Penwell⁶¹, D. V. Perepelitsa²⁵, E. Perez Codina^{160a}, M. T. Pérez García-Están¹⁶⁸, L. Perini^{91a,91b}, H. Pernegger³⁰, S. Perrella^{104a,104b}, R. Peschke⁴², V. D. Peshekhonov⁶⁵, K. Peters³⁰, R. F. Y. Peters⁸⁴, B. A. Petersen³⁰, T. C. Petersen³⁶, E. Petit⁴², A. Petridis^{147a,147b}, C. Petridou¹⁵⁵, E. Petrolu^{133a}, F. Petrucci^{135a,135b}, N. E. Pettersson¹⁵⁸, R. Pezoa^{32b}, P. W. Phillips¹³¹, G. Piacquadio¹⁴⁴, E. Pianori¹⁷¹,

A. Picazio⁴⁹, E. Piccaro⁷⁶, M. Piccinini^{20a,20b}, M. A. Pickering¹²⁰, R. Piegai²⁷, D. T. Pignotti¹¹¹, J. E. Pilcher³¹, A. D. Pilkington⁷⁸, J. Pina^{126a,126b,126d}, M. Pinamonti^{165a,165c.ac}, J. L. Pinfold³, A. Pingel³⁶, B. Pinto^{126a}, S. Pires⁸⁰, M. Pitt¹⁷³, C. Pizio^{91a,91b}, L. Plazak^{145a}, M.-A. Pleier²⁵, V. Pleskot¹²⁹, E. Plotnikova⁶⁵, P. Plucinski^{147a,147b}, D. Pluth⁶⁴, S. Poddar^{58a}, R. Poettgen⁸³, L. Poggioli¹¹⁷, D. Pohl²¹, M. Pohl⁴⁹, G. Polesello^{121a}, A. Policicchio^{37a,37b}, R. Polifka¹⁵⁹, A. Polini^{20a}, C. S. Pollard⁵³, V. Polychronakos²⁵, K. Pommès³⁰, L. Pontecorvo^{133a}, B. G. Pope⁹⁰, G. A. Popeneciu^{26b}, D. S. Popovic¹³, A. Poppleton³⁰, S. Pospisil¹²⁸, K. Potamianos¹⁵, I. N. Potrap⁶⁵, C. J. Potter¹⁵⁰, C. T. Potter¹¹⁶, G. Poulard³⁰, J. Poveda³⁰, V. Pozdnyakov⁶⁵, P. Pralavorio⁸⁵, A. Pranko¹⁵, S. Prasad³⁰, S. Prell⁶⁴, D. Price⁸⁴, J. Price⁷⁴, L. E. Price⁶, D. Prieur¹²⁵, M. Primavera^{73a}, S. Prince⁸⁷, M. Proissl⁴⁶, K. Prokofiev^{60c}, F. Prokoshin^{32b}, E. Protopapadaki¹³⁷, S. Protopopescu²⁵, J. Proudfoot⁶, M. Przybycien^{38a}, E. Ptacek¹¹⁶, D. Puddu^{135a,135b}, E. Pueschel⁸⁶, D. Poldon¹⁴⁹, M. Purohit^{25.ad}, P. Puzo¹¹⁷, J. Qian⁸⁹, G. Qin⁵³, Y. Qin⁸⁴, A. Quadt⁵⁴, D. R. Quarrie¹⁵, W. B. Quayle^{165a,165b}, M. Queitsch-Maitland⁸⁴, D. Quilty⁵³, A. Qureshi^{160b}, V. Radeka²⁵, V. Radescu⁴², S. K. Radhakrishnan¹⁴⁹, P. Radloff¹¹⁶, P. Rados⁸⁸, F. Ragusa^{91a,91b}, G. Rahal¹⁷⁹, S. Rajagopalan²⁵, M. Rammensee³⁰, C. Rangel-Smith¹⁶⁷, F. Rauscher¹⁰⁰, S. Rave⁸³, T. C. Rave⁴⁸, T. Ravenscroft⁵³, M. Raymond³⁰, A. L. Read¹¹⁹, N. P. Readioff⁷⁴, D. M. Rebuffi^{121a,121b}, A. Redelbach¹⁷⁵, G. Redlinger²⁵, R. Reece¹³⁸, K. Reeves⁴¹, L. Rehnisch¹⁶, H. Reisin²⁷, M. Relich¹⁶⁴, C. Rembser³⁰, H. Ren^{33a}, A. Renaud¹¹⁷, M. Rescigno^{133a}, S. Resconi^{91a}, O. L. Rezanova^{109.c}, P. Reznicek¹²⁹, R. Rezvani⁹⁵, R. Richter¹⁰¹, E. Richter-Was^{38b}, M. Ridel⁸⁰, P. Rieck¹⁶, J. Rieger⁵⁴, M. Rijssenbeek¹⁴⁹, A. Rimoldi^{121a,121b}, L. Rinaldi^{20a}, E. Ritsch⁶², I. Riu¹², F. Rizatdinova¹¹⁴, E. Rizvi⁷⁶, S. H. Robertson^{87.j}, A. Robichaud-Veronneau⁸⁷, D. Robinson²⁸, J. E. M. Robinson⁸⁴, A. Robson⁵³, C. Roda^{124a,124b}, L. Rodrigues³⁰, S. Roe³⁰, O. Røhne¹¹⁹, S. Rolli¹⁶², A. Romaniouk⁹⁸, M. Romano^{20a,20b}, E. Romero Adam¹⁶⁸, N. Rompotis¹³⁹, M. Ronzani⁴⁸, L. Roos⁸⁰, E. Ros¹⁶⁸, S. Rosati^{133a}, K. Rosbach⁴⁹, P. Rose¹³⁸, P. L. Rosendahl¹⁴, O. Rosenthal¹⁴², V. Rossetti^{147a,147b}, E. Rossi^{104a,104b}, L. P. Rossi^{50a}, R. Rosten¹³⁹, M. Rotaru^{26a}, I. Roth¹⁷³, J. Rothberg¹³⁹, D. Rousseau¹¹⁷, C. R. Royon¹³⁷, A. Rozanov⁸⁵, Y. Rozen¹⁵³, X. Ruan^{146c}, F. Rubbo¹², I. Rubinskiy⁴², V. I. Rud⁹⁹, C. Rudolph⁴⁴, M. S. Rudolph¹⁵⁹, F. Rühr⁴⁸, A. Ruiz-Martinez³⁰, Z. Rurikova⁴⁸, N. A. Rusakovich⁶⁵, A. Ruschke¹⁰⁰, H. L. Russell¹³⁹, J. P. Rutherford⁷, N. Ruthmann⁴⁸, Y. F. Ryabov¹²³, M. Rybar¹²⁹, G. Rybkin¹¹⁷, N. C. Ryder¹²⁰, A. F. Saavedra¹⁵¹, G. Sabato¹⁰⁷, S. Sacerdoti²⁷, A. Saddique³, H. F.-W. Sadrozinski¹³⁸, R. Sadykov⁶⁵, F. Safai Tehrani^{133a}, M. Saimpert¹³⁷, H. Sakamoto¹⁵⁶, Y. Sakurai¹⁷², G. Salamanna^{135a,135b}, A. Salamon^{134a}, M. Saleem¹¹³, D. Salek¹⁰⁷, P. H. Sales De Bruin¹³⁹, D. Salihagic¹⁰¹, A. Salnikov¹⁴⁴, J. Salt¹⁶⁸, D. Salvatore^{37a,37b}, F. Salvatore¹⁵⁰, A. Salvucci¹⁰⁶, A. Salzburger³⁰, D. Sampsonidis¹⁵⁵, A. Sanchez^{104a,104b}, J. Sánchez¹⁶⁸, V. Sanchez Martinez¹⁶⁸, H. Sandaker¹⁴, R. L. Sandbach⁷⁶, H. G. Sander⁸³, M. P. Sanders¹⁰⁰, M. Sandhoff¹⁷⁶, T. Sandoval²⁸, C. Sandoval¹⁶³, R. Sandstroem¹⁰¹, D. P. C. Sankey¹³¹, A. Sansoni⁴⁷, C. Santoni³⁴, R. Santonico^{134a,134b}, H. Santos^{126a}, I. Santoyo Castillo¹⁵⁰, K. Sapp¹²⁵, A. Saponov⁶⁵, J. G. Saraiva^{126a,126d}, B. Sarrazin²¹, G. Sartisohn¹⁷⁶, O. Sasaki⁶⁶, Y. Sasaki¹⁵⁶, K. Sato¹⁶¹, G. Sauvage^{5,*}, E. Sauvan⁵, G. Savage⁷⁷, P. Savard^{159.d}, C. Sawyer¹²⁰, L. Sawyer^{79.m}, D. H. Saxon⁵³, J. Saxon³¹, C. Sbarra^{20a}, A. Sbrizzi^{20a,20b}, T. Scanlon⁷⁸, D. A. Scannicchio¹⁶⁴, M. Scarcella¹⁵¹, V. Scarfone^{37a,37b}, J. Schaarschmidt¹⁷³, P. Schacht¹⁰¹, D. Schaefer³⁰, R. Schaefer⁴², J. Schaeffer⁸³, S. Schaepe²¹, S. Schaezel^{58b}, U. Schäfer⁸³, A. C. Schaffer¹¹⁷, D. Schaile¹⁰⁰, R. D. Schamberger¹⁴⁹, V. Scharf^{58a}, V. A. Schegelsky¹²³, D. Scheirich¹²⁹, M. Schernau¹⁶⁴, C. Schiavi^{50a,50b}, J. Schieck¹⁰⁰, C. Schillo⁴⁸, M. Schioppa^{37a,37b}, S. Schlenker³⁰, E. Schmidt⁴⁸, K. Schmieden³⁰, C. Schmitt⁸³, S. Schmitt^{58b}, B. Schneider¹⁷, Y. J. Schnellbach⁷⁴, U. Schnoor⁴⁴, L. Schoeffel¹³⁷, A. Schoening^{58b}, B. D. Schoenrock⁹⁰, A. L. S. Schorlemmer⁵⁴, M. Schott⁸³, D. Schouten^{160a}, J. Schovancova²⁵, S. Schramm¹⁵⁹, M. Schreyer¹⁷⁵, C. Schroeder⁸³, N. Schuh⁸³, M. J. Schultens²¹, H.-C. Schultz-Coulon^{58a}, H. Schulz¹⁶, M. Schumacher⁴⁸, B. A. Schumm¹³⁸, Ph. Schune¹³⁷, C. Schwanenberger⁸⁴, A. Schwartzman¹⁴⁴, T. A. Schwarz⁸⁹, Ph. Schwegler¹⁰¹, Ph. Schwemling¹³⁷, R. Schwienhorst⁹⁰, J. Schwindling¹³⁷, T. Schwindt²¹, M. Schwoerer⁵, F. G. Sciacca¹⁷, E. Scifo¹¹⁷, G. Sciolla²³, F. Scuri^{124a,124b}, F. Scutti²¹, J. Searcy⁸⁹, G. Sedov⁴², E. Sedykh¹²³, P. Seema²¹, S. C. Seidel¹⁰⁵, A. Seiden¹³⁸, F. Seifert¹²⁸, J. M. Seixas^{24a}, G. Sekhniaidze^{104a}, S. J. Sekula⁴⁰, K. E. Selbach⁴⁶, D. M. Seliverstov^{123.*}, N. Semprini-Cesari^{20a,20b}, C. Serfon³⁰, L. Serin¹¹⁷, L. Serkin⁵⁴, T. Serre⁸⁵, R. Seuster^{160a}, H. Severini¹¹³, T. Sfiligoj⁷⁵, F. Sforza¹⁰¹, A. Sfyrla³⁰, E. Shabalina⁵⁴, M. Shamim¹¹⁶, L. Y. Shan^{33a}, R. Shang¹⁶⁶, J. T. Shank²², M. Shapiro¹⁵, P. B. Shatalov⁹⁷, K. Shaw^{165a,165b}, A. Shcherbakova^{147a,147b}, C. Y. Shehu¹⁵⁰, P. Sherwood⁷⁸, L. Shi^{152.ae}, S. Shimizu⁶⁷, C. O. Shimmin¹⁶⁴, M. Shimojima¹⁰², M. Shiyakova⁶⁵, A. Shmeleva⁹⁶, D. Shoaleh Saadi⁹⁵, M. J. Shochet³¹, S. Shojaii^{91a,91b}, S. Shrestha¹¹¹, E. Shulga⁹⁸, M. A. Shupe⁷, S. Shushkevich⁴², P. Sicho¹²⁷, O. Sidiropoulou¹⁷⁵, D. Sidorov¹¹⁴, A. Sidoti^{20a,20b}, F. Siegert⁴⁴, Dj. Sijacki¹³, J. Silva^{126a,126d}, Y. Silver¹⁵⁴, D. Silverstein¹⁴⁴, S. B. Silverstein^{147a}, V. Simak¹²⁸, O. Simard⁵, Lj. Simic¹³, S. Simion¹¹⁷, E. Simioni⁸³, B. Simmons⁷⁸, D. Simon³⁴, R. Simoniello^{91a,91b}, P. Sinervo¹⁵⁹, N. B. Sinev¹¹⁶, G. Siragusa¹⁷⁵, A. Sircar⁷⁹, A. N. Sisakyan^{65.*}, S. Yu. Sivoklov⁹⁹, J. Sjölin^{147a,147b}, T. B. Sjursen¹⁴, H. P. Skottowe⁵⁷, P. Skubic¹¹³, M. Slater¹⁸, T. Slavicek¹²⁸, M. Slawinska¹⁰⁷, K. Sliwa¹⁶², V. Smakhtin¹⁷³, B. H. Smart⁴⁶, L. Smestad¹⁴, S. Yu. Smirnov⁹⁸, Y. Smirnov⁹⁸, L. N. Smirnova^{99.af}, O. Smirnova⁸¹, K. M. Smith⁵³, M. Smith³⁵, M. Smizanska⁷², K. Smolek¹²⁸, A. A. Snesarev⁹⁶

G. Snidero⁷⁶, S. Snyder²⁵, R. Sobie^{170,j}, F. Socher⁴⁴, A. Soffer¹⁵⁴, D. A. Soh^{152,ae}, C. A. Solans³⁰, M. Solar¹²⁸, J. Solc¹²⁸, E. Yu. Soldatov⁹⁸, U. Soldevila¹⁶⁸, A. A. Solodkov¹³⁰, A. Soloshenko⁶⁵, O. V. Solovyanov¹³⁰, V. Solovyev¹²³, P. Sommer⁴⁸, H. Y. Song^{33b}, N. Soni¹, A. Sood¹⁵, A. Sopczak¹²⁸, B. Sopko¹²⁸, V. Sopko¹²⁸, V. Sorin¹², D. Sosa^{58b}, M. Sosebee⁸, R. Soualah^{165a,165c}, P. Soueid⁹⁵, A. M. Soukharev^{109,c}, D. South⁴², S. Spagnolo^{73a,73b}, F. Spanò⁷⁷, W. R. Spearman⁵⁷, F. Spettel¹⁰¹, R. Spighi^{20a}, G. Spigo³⁰, L. A. Spiller⁸⁸, M. Spousta¹²⁹, T. Spreitzer¹⁵⁹, R. D. St. Denis^{53,*}, S. Staerz⁴⁴, J. Stahlman¹²², R. Stamen^{58a}, S. Stamm¹⁶, E. Stanecka³⁹, C. Stanescu^{135a}, M. Stanescu-Bellu⁴², M. M. Stanitzki⁴², S. Stapnes¹¹⁹, E. A. Starchenko¹³⁰, J. Stark⁵⁵, P. Staroba¹²⁷, P. Starovoitov⁴², R. Staszewski³⁹, P. Stavina^{145a,*}, P. Steinberg²⁵, B. Stelzer¹⁴³, H. J. Stelzer³⁰, O. Stelzer-Chilton^{160a}, H. Stenzel⁵², S. Stern¹⁰¹, G. A. Stewart⁵³, J. A. Stillings²¹, M. C. Stockton⁸⁷, M. Stoebe⁸⁷, G. Stoicea^{26a}, P. Stolte⁵⁴, S. Stonjek¹⁰¹, A. R. Stradling⁸, A. Straessner⁴⁴, M. E. Stramaglia¹⁷, J. Strandberg¹⁴⁸, S. Strandberg^{147a,147b}, A. Strandlie¹¹⁹, E. Strauss¹⁴⁴, M. Strauss¹¹³, P. Strizenec^{145b}, R. Ströhmer¹⁷⁵, D. M. Strom¹¹⁶, R. Stroynowski⁴⁰, A. Strubig¹⁰⁶, S. A. Stucci¹⁷, B. Stugu¹⁴, N. A. Styles⁴², D. Su¹⁴⁴, J. Su¹²⁵, R. Subramaniam⁷⁹, A. Succurro¹², Y. Sugaya¹¹⁸, C. Suhr¹⁰⁸, M. Suk¹²⁸, V. V. Sulin⁹⁶, S. Sultansoy^{4d}, T. Sumida⁶⁸, S. Sun⁵⁷, X. Sun^{33a}, J. E. Sundermann⁴⁸, K. Suruliz¹⁵⁰, G. Susinno^{37a,37b}, M. R. Sutton¹⁵⁰, Y. Suzuki⁶⁶, M. Svatos¹²⁷, S. Swedish¹⁶⁹, M. Swiatlowski¹⁴⁴, I. Sykora^{145a}, T. Sykora¹²⁹, D. Ta⁹⁰, C. Taccini^{135a,135b}, K. Tackmann⁴², J. Taenzer¹⁵⁹, A. Taffard¹⁶⁴, R. Tafirout^{160a}, N. Taiblum¹⁵⁴, H. Takai²⁵, R. Takashima⁶⁹, H. Takeda⁶⁷, T. Takeshita¹⁴¹, Y. Takubo⁶⁶, M. Talby⁸⁵, A. A. Talyshev^{109,c}, J. Y. C. Tam¹⁷⁵, K. G. Tan⁸⁸, J. Tanaka¹⁵⁶, R. Tanaka¹¹⁷, S. Tanaka¹³², S. Tanaka⁶⁶, A. J. Tanasijczuk¹⁴³, B. B. Tannenwald¹¹¹, N. Tannoury²¹, S. Tapprogge⁸³, S. Tarem¹⁵³, F. Tarrade²⁹, G. F. Tartarelli^{91a}, P. Tas¹²⁹, M. Tasevsky¹²⁷, T. Tashiro⁶⁸, E. Tassi^{37a,37b}, A. Tavares Delgado^{126a,126b}, Y. Tayalati^{136d}, F. E. Taylor⁹⁴, G. N. Taylor⁸⁸, W. Taylor^{160b}, F. A. Teischinger³⁰, M. Teixeira Dias Castanheira⁷⁶, P. Teixeira-Dias⁷⁷, K. K. Temming⁴⁸, H. Ten Kate³⁰, P. K. Teng¹⁵², J. J. Teoh¹¹⁸, F. Tepel¹⁷⁶, S. Terada⁶⁶, K. Terashi¹⁵⁶, J. Terron⁸², S. Terzo¹⁰¹, M. Testa⁴⁷, R. J. Teuscher^{159,j}, J. Therhaag²¹, T. Theveneaux-Pelzer³⁴, J. P. Thomas¹⁸, J. Thomas-Wilsker⁷⁷, E. N. Thompson³⁵, P. D. Thompson¹⁸, R. J. Thompson⁸⁴, A. S. Thompson⁵³, L. A. Thomsen³⁶, E. Thomson¹²², M. Thomson²⁸, W. M. Thong⁸⁸, R. P. Thun^{89,*}, F. Tian³⁵, M. J. Tibbetts¹⁵, R. E. Tisce Torres⁸⁵, V. O. Tikhomirov^{96,ag}, Yu. A. Tikhonov^{109,c}, S. Timoshenko⁹⁸, E. Tiouchichine⁸⁵, P. Tipton¹⁷⁷, S. Tisserant⁸⁵, T. Todorov^{5,*}, S. Todorova-Nova¹²⁹, J. Tojo⁷⁰, S. Tokár^{145a}, K. Tokushuku⁶⁶, K. Tollefson⁹⁰, E. Tolley⁵⁷, L. Tomlinson⁸⁴, M. Tomoto¹⁰³, L. Tompkins^{144,ah}, K. Toms¹⁰⁵, N. D. Topilin⁶⁵, E. Torrence¹¹⁶, H. Torres¹⁴³, E. Torró Pastor¹⁶⁸, J. Toth^{85,ai}, F. Touchard⁸⁵, D. R. Tovey¹⁴⁰, H. L. Tran¹¹⁷, T. Trefzger¹⁷⁵, L. Tremblet³⁰, A. Tricoli³⁰, I. M. Trigger^{160a}, S. Trincz-Duvoid⁸⁰, M. F. Tripiana¹², W. Trischuk¹⁵⁹, B. Trocmé⁵⁵, C. Troncon^{91a}, M. Trotter-McDonald¹⁵, M. Trovatelli^{135a,135b}, P. True⁹⁰, M. Trzebinski³⁹, A. Trzupek³⁹, C. Tsarouchas³⁰, J. C-L. Tseng¹²⁰, P. V. Tsiarehka⁹², D. Tsionou¹³⁷, G. Tsiopolitis¹⁰, N. Tsirintanis⁹, S. Tsiskaridze¹², V. Tsiskaridze⁴⁸, E. G. Tskhadadze^{51a}, I. I. Tsukerman⁹⁷, V. Tsulaia¹⁵, S. Tsuno⁶⁶, D. Tsybychev¹⁴⁹, A. Tudorache^{26a}, V. Tudorache^{26a}, A. N. Tuna¹²², S. A. Tuppuri^{20a,20b}, S. Turchikhin^{99,af}, D. Turecek¹²⁸, I. Turk Cakir^{4c}, R. Turra^{91a,91b}, A. J. Turvey⁴⁰, P. M. Tuts³⁵, A. Tykhonov⁴⁹, M. Tylmad^{147a,147b}, M. Tyndel¹³¹, I. Ueda¹⁵⁶, R. Ueno²⁹, M. Ughetto⁸⁵, M. Uglan¹⁴, M. Uhlenbrock²¹, F. Ukegawa¹⁶¹, G. Unal³⁰, A. Undrus²⁵, G. Unel¹⁶⁴, F. C. Ungaro⁴⁸, Y. Unno⁶⁶, C. Unverdorben¹⁰⁰, J. Urban^{145b}, P. Urquijo⁸⁸, P. Urrejola⁸³, G. Usai⁸, A. Usanova⁶², L. Vacavant⁸⁵, V. Vacek¹²⁸, B. Vachon⁸⁷, N. Valencic¹⁰⁷, S. Valentinetti^{20a,20b}, A. Valero¹⁶⁸, L. Valery³⁴, S. Valkar¹²⁹, E. Valladolid Gallego¹⁶⁸, S. Vallecorsa⁴⁹, J. A. Valls Ferrer¹⁶⁸, W. Van Den Wollenberg¹⁰⁷, P. C. Van Der Deijl¹⁰⁷, R. van der Geer¹⁰⁷, H. van der Graaf¹⁰⁷, R. Van Der Leeuw¹⁰⁷, N. van Eldik³⁰, P. van Gemmeren⁶, J. Van Nieuwkoop¹⁴³, I. van Vulpen¹⁰⁷, M. C. van Woerden³⁰, M. Vanadia^{133a,133b}, W. Vandelli³⁰, R. Vanguri¹²², A. Vaniachine⁶, F. Vannucci⁸⁰, G. Vardanyan¹⁷⁸, R. Vari^{133a}, E. W. Varnes⁷, T. Varol⁸⁶, D. Varouchas⁸⁰, A. Vartapetian⁸, K. E. Varvell¹⁵¹, F. Vazeille³⁴, T. Vazquez Schroeder⁵⁴, J. Veatch⁷, F. Veloso^{126a,126c}, T. Velz²¹, S. Veneziano^{133a}, A. Ventura^{73a,73b}, D. Ventura⁸⁶, M. Venturi¹⁷⁰, N. Venturi¹⁵⁹, A. Venturini²³, V. Vercesi^{121a}, M. Verducci^{133a,133b}, W. Verkerke¹⁰⁷, J. C. Vermeulen¹⁰⁷, A. Vest⁴⁴, M. C. Vetterli^{143,d}, O. Viazlo⁸¹, I. Vichou¹⁶⁶, T. Vickey^{146c,aj}, O. E. Vickey Boeriu^{146c}, G. H. A. Viehhauser¹²⁰, S. Viel¹⁵, R. Vigne³⁰, M. Villa^{20a,20b}, M. Villaplana Perez^{91a,91b}, E. Vilucchi⁴⁷, M. G. Vincter²⁹, V. B. Vinogradov⁶⁵, J. Virzi¹⁵, I. Vivarelli¹⁵⁰, F. Vives Vaque³, S. Vlachos¹⁰, D. Vladioiu¹⁰⁰, M. Vlasak¹²⁸, M. Vogel^{32a}, P. Vokac¹²⁸, G. Volpi^{124a,124b}, M. Volpi⁸⁸, H. von der Schmitt¹⁰¹, H. von Radziewski⁴⁸, E. von Toerne²¹, V. Vorobel¹²⁹, K. Vorobev⁹⁸, M. Vos¹⁶⁸, R. Voss³⁰, J. H. Vosseveld⁷⁴, N. Vranjes¹³⁷, M. Vranjes Milosavljevic¹³, V. Vrba¹²⁷, M. Vreeswijk¹⁰⁷, R. Vuillermet³⁰, I. Vukotic³¹, Z. Vykydal¹²⁸, P. Wagner²¹, W. Wagner¹⁷⁶, H. Wahlberg⁷¹, S. Wahrmund⁴⁴, J. Wakabayashi¹⁰³, J. Walder⁷², R. Walker¹⁰⁰, W. Walkowiak¹⁴², C. Wang^{33c}, F. Wang¹⁷⁴, H. Wang¹⁵, H. Wang⁴⁰, J. Wang⁴², J. Wang^{33a}, K. Wang⁸⁷, R. Wang¹⁰⁵, S. M. Wang¹⁵², T. Wang²¹, X. Wang¹⁷⁷, C. Wanotayaroj¹¹⁶, A. Warburton⁸⁷, C. P. Ward²⁸, D. R. Wardrope⁷⁸, M. Warsinsky⁴⁸, A. Washbrook⁴⁶, C. Wasicki⁴², P. M. Watkins¹⁸, A. T. Watson¹⁸, I. J. Watson¹⁵¹, M. F. Watson¹⁸, G. Watts¹³⁹, S. Watts⁸⁴, B. M. Waugh⁷⁸, S. Webb⁸⁴, M. S. Weber¹⁷, S. W. Weber¹⁷⁵, J. S. Webster³¹, A. R. Weidberg¹²⁰, B. Weinert⁶¹, J. Weingarten⁵⁴, C. Weiser⁴⁸, H. Weits¹⁰⁷, P. S. Wells³⁰, T. Wenaus²⁵, D. Wendland¹⁶, T. Wengler³⁰, S. Wenig³⁰, N. Wermes²¹, M. Werner⁴⁸, P. Werner³⁰, M. Wessels^{58a},

J. Wetter¹⁶², K. Whalen²⁹, A. White⁸, M. J. White¹, R. White^{32b}, S. White^{124a,124b}, D. Whiteson¹⁶⁴, D. Wicke¹⁷⁶, F. J. Wickens¹³¹, W. Wiedenmann¹⁷⁴, M. Wieler¹³¹, P. Wienemann²¹, C. Wiglesworth³⁶, L. A. M. Wiik-Fuchs²¹, A. Wildauer¹⁰¹, H. G. Wilkens³⁰, H. H. Williams¹²², S. Williams²⁸, C. Willis⁹⁰, S. Willocq⁸⁶, A. Wilson⁸⁹, J. A. Wilson¹⁸, I. Wingerter-Seez⁵, F. Winklmeier¹¹⁶, B. T. Winter²¹, M. Wittgen¹⁴⁴, J. Wittkowski¹⁰⁰, S. J. Wollstadt⁸³, M. W. Wolter³⁹, H. Wolters^{126a,126c}, B. K. Wosiek³⁹, J. Wotschack³⁰, M. J. Woudstra⁸⁴, K. W. Wozniak³⁹, M. Wu⁵⁵, S. L. Wu¹⁷⁴, X. Wu⁴⁹, Y. Wu⁸⁹, T. R. Wyatt⁸⁴, B. M. Wynne⁴⁶, S. Xella³⁶, D. Xu^{33a}, L. Xu^{33b,ak}, B. Yabsley¹⁵¹, S. Yacoob^{146b,al}, R. Yakabe⁶⁷, M. Yamada⁶⁶, Y. Yamaguchi¹¹⁸, A. Yamamoto⁶⁶, S. Yamamoto¹⁵⁶, T. Yamanaka¹⁵⁶, K. Yamauchi¹⁰³, Y. Yamazaki⁶⁷, Z. Yan²², H. Yang^{33e}, H. Yang¹⁷⁴, Y. Yang¹⁵², S. Yanush⁹³, L. Yao^{33a}, W-M. Yao¹⁵, Y. Yasu⁶⁶, E. Yatsenko⁴², K. H. Yau Wong²¹, J. Ye⁴⁰, S. Ye²⁵, I. Yeletsikh⁶⁵, A. L. Yen⁵⁷, E. Yildirim⁴², K. Yorita¹⁷², R. Yoshida⁶, K. Yoshihara¹²², C. Young¹⁴⁴, C. J. S. Young³⁰, S. Youssef²², D. R. Yu¹⁵, J. Yu⁸, J. M. Yu⁸⁹, J. Yu¹¹⁴, L. Yuan⁶⁷, A. Yurkewicz¹⁰⁸, I. Yusuff^{28,am}, B. Zabinski³⁹, R. Zaidan⁶³, A. M. Zaitsev^{130,aa}, A. Zaman¹⁴⁹, S. Zambito²³, L. Zanello^{133a,133b}, D. Zanzi⁸⁸, C. Zeitnitz¹⁷⁶, M. Zeman¹²⁸, A. Zemla^{38a}, K. Zengel²³, O. Zenin¹³⁰, T. Ženiš^{145a}, D. Zerwas¹¹⁷, D. Zhang⁸⁹, F. Zhang¹⁷⁴, J. Zhang⁶, L. Zhang¹⁵², R. Zhang^{33b}, X. Zhang^{33d}, Z. Zhang¹¹⁷, X. Zhao⁴⁰, Y. Zhao^{33d,117}, Z. Zhao^{33b}, A. Zhemchugov⁶⁵, J. Zhong¹²⁰, B. Zhou⁸⁹, C. Zhou⁴⁵, L. Zhou³⁵, L. Zhou⁴⁰, N. Zhou¹⁶⁴, C. G. Zhu^{33d}, H. Zhu^{33a}, J. Zhu⁸⁹, Y. Zhu^{33b}, X. Zhuang^{33a}, K. Zhukov⁹⁶, A. Zibell¹⁷⁵, D. Ziemska⁶¹, N. I. Zimine⁶⁵, C. Zimmermann⁸³, R. Zimmermann²¹, S. Zimmermann⁴⁸, Z. Zinonos⁵⁴, M. Ziolkowski¹⁴², L. Živković¹³, G. Zobernig¹⁷⁴, A. Zoccoli^{20a,20b}, M. zur Nedden¹⁶, G. Zurzolo^{104a,104b}, L. Zwalinski³⁰

¹ Department of Physics, University of Adelaide, Adelaide, Australia

² Physics Department, SUNY Albany, Albany, NY, USA

³ Department of Physics, University of Alberta, Edmonton, AB, Canada

⁴ (a) Department of Physics, Ankara University, Ankara, Turkey; (c) Istanbul Aydin University, Istanbul, Turkey;

(d) Division of Physics, TOBB University of Economics and Technology, Ankara, Turkey

⁵ LAPP, CNRS/IN2P3 and Université de Savoie, Annecy-le-Vieux, France

⁶ High Energy Physics Division, Argonne National Laboratory, Argonne, IL, USA

⁷ Department of Physics, University of Arizona, Tucson, AZ, USA

⁸ Department of Physics, The University of Texas at Arlington, Arlington, TX, USA

⁹ Physics Department, University of Athens, Athens, Greece

¹⁰ Physics Department, National Technical University of Athens, Zografou, Greece

¹¹ Institute of Physics, Azerbaijan Academy of Sciences, Baku, Azerbaijan

¹² Institut de Física d'Altes Energies and Departament de Física de la Universitat Autònoma de Barcelona, Barcelona, Spain

¹³ Institute of Physics, University of Belgrade, Belgrade, Serbia

¹⁴ Department for Physics and Technology, University of Bergen, Bergen, Norway

¹⁵ Physics Division, Lawrence Berkeley National Laboratory and University of California, Berkeley, CA, USA

¹⁶ Department of Physics, Humboldt University, Berlin, Germany

¹⁷ Albert Einstein Center for Fundamental Physics and Laboratory for High Energy Physics, University of Bern, Bern, Switzerland

¹⁸ School of Physics and Astronomy, University of Birmingham, Birmingham, UK

¹⁹ (a) Department of Physics, Bogazici University, Istanbul, Turkey; (b) Department of Physics, Dogus University, Istanbul, Turkey; (c) Department of Physics Engineering, Gaziantep University, Gaziantep, Turkey

²⁰ (a) INFN Sezione di Bologna, Bologna, Italy; (b) Dipartimento di Fisica e Astronomia, Università di Bologna, Bologna, Italy

²¹ Physikalisches Institut, University of Bonn, Bonn, Germany

²² Department of Physics, Boston University, Boston, MA, USA

²³ Department of Physics, Brandeis University, Waltham, MA, USA

²⁴ (a) Universidade Federal do Rio De Janeiro COPPE/EE/IF, Rio de Janeiro, Brazil; (b) Electrical Circuits Department, Federal University of Juiz de Fora (UFJF), Juiz de Fora, Brazil; (c) Federal University of Sao Joao del Rei (UFSJ), Sao Joao del Rei, Brazil; (d) Instituto de Fisica, Universidade de Sao Paulo, Sao Paulo, Brazil

²⁵ Physics Department, Brookhaven National Laboratory, Upton, NY, USA

²⁶ (a) National Institute of Physics and Nuclear Engineering, Bucharest, Romania; (b) Physics Department, National Institute for Research and Development of Isotopic and Molecular Technologies, Cluj Napoca, Romania; (c) University Politehnica Bucharest, Bucharest, Romania; (d) West University in Timisoara, Timisoara, Romania

- ²⁷ Departamento de Física, Universidad de Buenos Aires, Buenos Aires, Argentina
- ²⁸ Cavendish Laboratory, University of Cambridge, Cambridge, UK
- ²⁹ Department of Physics, Carleton University, Ottawa, ON, Canada
- ³⁰ CERN, Geneva, Switzerland
- ³¹ Enrico Fermi Institute, University of Chicago, Chicago, IL, USA
- ³² ^(a)Departamento de Física, Pontificia Universidad Católica de Chile, Santiago, Chile; ^(b)Departamento de Física, Universidad Técnica Federico Santa María, Valparaíso, Chile
- ³³ ^(a)Institute of High Energy Physics, Chinese Academy of Sciences, Beijing, China; ^(b)Department of Modern Physics, University of Science and Technology of China, Anhui, China; ^(c)Department of Physics, Nanjing University, Jiangsu, China; ^(d)School of Physics, Shandong University, Shandong, China; ^(e)Department of Physics and Astronomy, Shanghai Key Laboratory for Particle Physics and Cosmology, Shanghai Jiao Tong University, Shanghai; ^(f)Physics Department, Tsinghua University, 100084 Beijing, China
- ³⁴ Laboratoire de Physique Corpusculaire, Clermont Université and Université Blaise Pascal and CNRS/IN2P3, Clermont-Ferrand, France
- ³⁵ Nevis Laboratory, Columbia University, Irvington, NY, USA
- ³⁶ Niels Bohr Institute, University of Copenhagen, Copenhagen, Denmark
- ³⁷ ^(a)INFN Gruppo Collegato di Cosenza, Laboratori Nazionali di Frascati, Italy; ^(b)Dipartimento di Fisica, Università della Calabria, Rende, Italy
- ³⁸ ^(a)Faculty of Physics and Applied Computer Science, AGH University of Science and Technology, Kraków, Poland; ^(b)Marian Smoluchowski Institute of Physics, Jagiellonian University, Kraków, Poland
- ³⁹ The Henryk Niewodniczanski Institute of Nuclear Physics, Polish Academy of Sciences, Kraków, Poland
- ⁴⁰ Physics Department, Southern Methodist University, Dallas, TX, USA
- ⁴¹ Physics Department, University of Texas at Dallas, Richardson, TX, USA
- ⁴² DESY, Hamburg and Zeuthen, Germany
- ⁴³ Institut für Experimentelle Physik IV, Technische Universität Dortmund, Dortmund, Germany
- ⁴⁴ Institut für Kern- und Teilchenphysik, Technische Universität Dresden, Dresden, Germany
- ⁴⁵ Department of Physics, Duke University, Durham, NC, USA
- ⁴⁶ SUPA-School of Physics and Astronomy, University of Edinburgh, Edinburgh, UK
- ⁴⁷ INFN Laboratori Nazionali di Frascati, Frascati, Italy
- ⁴⁸ Fakultät für Mathematik und Physik, Albert-Ludwigs-Universität, Freiburg, Germany
- ⁴⁹ Section de Physique, Université de Genève, Geneva, Switzerland
- ⁵⁰ ^(a)INFN Sezione di Genova, Genoa, Italy; ^(b)Dipartimento di Fisica, Università di Genova, Genoa, Italy
- ⁵¹ ^(a)E. Andronikashvili Institute of Physics, Iv. Javakishvili Tbilisi State University, Tbilisi, Georgia; ^(b)High Energy Physics Institute, Tbilisi State University, Tbilisi, Georgia
- ⁵² II Physikalisches Institut, Justus-Liebig-Universität Giessen, Giessen, Germany
- ⁵³ SUPA-School of Physics and Astronomy, University of Glasgow, Glasgow, UK
- ⁵⁴ II Physikalisches Institut, Georg-August-Universität, Göttingen, Germany
- ⁵⁵ Laboratoire de Physique Subatomique et de Cosmologie, Université Grenoble-Alpes, CNRS/IN2P3, Grenoble, France
- ⁵⁶ Department of Physics, Hampton University, Hampton, VA, USA
- ⁵⁷ Laboratory for Particle Physics and Cosmology, Harvard University, Cambridge, MA, USA
- ⁵⁸ ^(a)Kirchhoff-Institut für Physik, Ruprecht-Karls-Universität Heidelberg, Heidelberg, Germany; ^(b)Physikalisches Institut, Ruprecht-Karls-Universität Heidelberg, Heidelberg, Germany; ^(c)ZITI Institut für technische Informatik, Ruprecht-Karls-Universität Heidelberg, Mannheim, Germany
- ⁵⁹ Faculty of Applied Information Science, Hiroshima Institute of Technology, Hiroshima, Japan
- ⁶⁰ ^(a)Department of Physics, The Chinese University of Hong Kong, Shatin, N.T., Hong Kong; ^(b)Department of Physics, The University of Hong Kong, Hong Kong; ^(c)Department of Physics, The Hong Kong University of Science and Technology, Clear Water Bay, Kowloon, Hong Kong, China
- ⁶¹ Department of Physics, Indiana University, Bloomington, IN, USA
- ⁶² Institut für Astro- und Teilchenphysik, Leopold-Franzens-Universität, Innsbruck, Austria
- ⁶³ University of Iowa, Iowa City, IA, USA
- ⁶⁴ Department of Physics and Astronomy, Iowa State University, Ames, IA, USA
- ⁶⁵ Joint Institute for Nuclear Research, JINR Dubna, Dubna, Russia
- ⁶⁶ KEK, High Energy Accelerator Research Organization, Tsukuba, Japan

- ⁶⁷ Graduate School of Science, Kobe University, Kobe, Japan
- ⁶⁸ Faculty of Science, Kyoto University, Kyoto, Japan
- ⁶⁹ Kyoto University of Education, Kyoto, Japan
- ⁷⁰ Department of Physics, Kyushu University, Fukuoka, Japan
- ⁷¹ Instituto de Física La Plata, Universidad Nacional de La Plata and CONICET, La Plata, Argentina
- ⁷² Physics Department, Lancaster University, Lancaster, UK
- ⁷³ ^(a) INFN Sezione di Lecce, Lecce, Italy; ^(b) Dipartimento di Matematica e Fisica, Università del Salento, Lecce, Italy
- ⁷⁴ Oliver Lodge Laboratory, University of Liverpool, Liverpool, UK
- ⁷⁵ Department of Physics, Jožef Stefan Institute and University of Ljubljana, Ljubljana, Slovenia
- ⁷⁶ School of Physics and Astronomy, Queen Mary University of London, London, UK
- ⁷⁷ Department of Physics, Royal Holloway University of London, Surrey, UK
- ⁷⁸ Department of Physics and Astronomy, University College London, London, UK
- ⁷⁹ Louisiana Tech University, Ruston, LA, USA
- ⁸⁰ Laboratoire de Physique Nucléaire et de Hautes Energies, UPMC and Université Paris-Diderot and CNRS/IN2P3, Paris, France
- ⁸¹ Fysiska institutionen, Lunds universitet, Lund, Sweden
- ⁸² Departamento de Física Teórica C-15, Universidad Autónoma de Madrid, Madrid, Spain
- ⁸³ Institut für Physik, Universität Mainz, Mainz, Germany
- ⁸⁴ School of Physics and Astronomy, University of Manchester, Manchester, UK
- ⁸⁵ CPPM, Aix-Marseille Université and CNRS/IN2P3, Marseille, France
- ⁸⁶ Department of Physics, University of Massachusetts, Amherst, MA, USA
- ⁸⁷ Department of Physics, McGill University, Montreal, QC, Canada
- ⁸⁸ School of Physics, University of Melbourne, Melbourne, VIC, Australia
- ⁸⁹ Department of Physics, The University of Michigan, Ann Arbor, MI, USA
- ⁹⁰ Department of Physics and Astronomy, Michigan State University, East Lansing, MI, USA
- ⁹¹ ^(a) INFN Sezione di Milano, Milan, Italy; ^(b) Dipartimento di Fisica, Università di Milano, Milan, Italy
- ⁹² B.I. Stepanov Institute of Physics, National Academy of Sciences of Belarus, Minsk, Republic of Belarus
- ⁹³ National Scientific and Educational Centre for Particle and High Energy Physics, Minsk, Republic of Belarus
- ⁹⁴ Department of Physics, Massachusetts Institute of Technology, Cambridge, MA, USA
- ⁹⁵ Group of Particle Physics, University of Montreal, Montreal, QC, Canada
- ⁹⁶ P.N. Lebedev Institute of Physics, Academy of Sciences, Moscow, Russia
- ⁹⁷ Institute for Theoretical and Experimental Physics (ITEP), Moscow, Russia
- ⁹⁸ National Research Nuclear University MEPhI, Moscow, Russia
- ⁹⁹ D.V. Skobeltsyn Institute of Nuclear Physics, M.V. Lomonosov Moscow State University, Moscow, Russia
- ¹⁰⁰ Fakultät für Physik, Ludwig-Maximilians-Universität München, Munich, Germany
- ¹⁰¹ Max-Planck-Institut für Physik (Werner-Heisenberg-Institut), Munich, Germany
- ¹⁰² Nagasaki Institute of Applied Science, Nagasaki, Japan
- ¹⁰³ Graduate School of Science and Kobayashi-Maskawa Institute, Nagoya University, Nagoya, Japan
- ¹⁰⁴ ^(a) INFN Sezione di Napoli, Naples, Italy; ^(b) Dipartimento di Fisica, Università di Napoli, Naples, Italy
- ¹⁰⁵ Department of Physics and Astronomy, University of New Mexico, Albuquerque, NM, USA
- ¹⁰⁶ Institute for Mathematics, Astrophysics and Particle Physics, Radboud University Nijmegen/Nikhef, Nijmegen, The Netherlands
- ¹⁰⁷ Nikhef National Institute for Subatomic Physics and University of Amsterdam, Amsterdam, The Netherlands
- ¹⁰⁸ Department of Physics, Northern Illinois University, De Kalb, IL, USA
- ¹⁰⁹ Budker Institute of Nuclear Physics, SB RAS, Novosibirsk, Russia
- ¹¹⁰ Department of Physics, New York University, New York, NY, USA
- ¹¹¹ Ohio State University, Columbus, OH, USA
- ¹¹² Faculty of Science, Okayama University, Okayama, Japan
- ¹¹³ Homer L. Dodge Department of Physics and Astronomy, University of Oklahoma, Norman, OK, USA
- ¹¹⁴ Department of Physics, Oklahoma State University, Stillwater, OK, USA
- ¹¹⁵ Palacký University, RCPTM, Olomouc, Czech Republic
- ¹¹⁶ Center for High Energy Physics, University of Oregon, Eugene, OR, USA
- ¹¹⁷ LAL, Université Paris-Sud and CNRS/IN2P3, Orsay, France

- 118 Graduate School of Science, Osaka University, Osaka, Japan
- 119 Department of Physics, University of Oslo, Oslo, Norway
- 120 Department of Physics, Oxford University, Oxford, UK
- 121 ^(a)INFN Sezione di Pavia, Pavia, Italy; ^(b)Dipartimento di Fisica, Università di Pavia, Pavia, Italy
- 122 Department of Physics, University of Pennsylvania, Philadelphia, PA, USA
- 123 Petersburg Nuclear Physics Institute, Gatchina, Russia
- 124 ^(a)INFN Sezione di Pisa, Pisa, Italy; ^(b)Dipartimento di Fisica E. Fermi, Università di Pisa, Pisa, Italy
- 125 Department of Physics and Astronomy, University of Pittsburgh, Pittsburgh, PA, USA
- 126 ^(a)Laboratorio de Instrumentacao e Fisica Experimental de Particulas-LIP, Lisbon, Portugal; ^(b)Faculdade de Ciências, Universidade de Lisboa, Lisbon, Portugal; ^(c)Department of Physics, University of Coimbra, Coimbra, Portugal; ^(d)Centro de Física Nuclear da Universidade de Lisboa, Lisbon, Portugal; ^(e)Departamento de Fisica, Universidade do Minho, Braga, Portugal; ^(f)Departamento de Fisica Teorica y del Cosmos and CAFPE, Universidad de Granada, Granada, Spain; ^(g)Dep Fisica and CEFITEC of Faculdade de Ciencias e Tecnologia, Universidade Nova de Lisboa, Caparica, Portugal
- 127 Institute of Physics, Academy of Sciences of the Czech Republic, Prague, Czech Republic
- 128 Czech Technical University in Prague, Prague, Czech Republic
- 129 Faculty of Mathematics and Physics, Charles University in Prague, Prague, Czech Republic
- 130 State Research Center Institute for High Energy Physics, Protvino, Russia
- 131 Particle Physics Department, Rutherford Appleton Laboratory, Didcot, UK
- 132 Ritsumeikan University, Kusatsu, Shiga, Japan
- 133 ^(a)INFN Sezione di Roma, Rome, Italy; ^(b)Dipartimento di Fisica, Sapienza Università di Roma, Rome, Italy
- 134 ^(a)INFN Sezione di Roma Tor Vergata, Rome, Italy; ^(b)Dipartimento di Fisica, Università di Roma Tor Vergata, Rome, Italy
- 135 ^(a)INFN Sezione di Roma Tre, Rome, Italy; ^(b)Dipartimento di Matematica e Fisica, Università Roma Tre, Rome, Italy
- 136 ^(a)Faculté des Sciences Ain Chock, Réseau Universitaire de Physique des Hautes Energies-Université Hassan II, Casablanca, Morocco; ^(b)Centre National de l'Énergie des Sciences Techniques Nucleaires, Rabat, Morocco; ^(c)Faculté des Sciences Semlalia, Université Cadi Ayyad, LPHEA-Marrakech, Marrakech, Morocco; ^(d)Faculté des Sciences, Université Mohamed Premier and LTPM, Oujda, Morocco; ^(e)Faculté des Sciences, Université Mohammed V-Agdal, Rabat, Morocco
- 137 DSM/IRFU (Institut de Recherches sur les Lois Fondamentales de l'Univers), CEA Saclay (Commissariat à l'Énergie Atomique et aux Énergies Alternatives), Gif-sur-Yvette, France
- 138 Santa Cruz Institute for Particle Physics, University of California Santa Cruz, Santa Cruz, CA, USA
- 139 Department of Physics, University of Washington, Seattle, WA, USA
- 140 Department of Physics and Astronomy, University of Sheffield, Sheffield, UK
- 141 Department of Physics, Shinshu University, Nagano, Japan
- 142 Fachbereich Physik, Universität Siegen, Siegen, Germany
- 143 Department of Physics, Simon Fraser University, Burnaby, BC, Canada
- 144 SLAC National Accelerator Laboratory, Stanford, CA, USA
- 145 ^(a)Faculty of Mathematics, Physics and Informatics, Comenius University, Bratislava, Slovak Republic; ^(b)Department of Subnuclear Physics, Institute of Experimental Physics of the Slovak Academy of Sciences, Kosice, Slovak Republic
- 146 ^(a)Department of Physics, University of Cape Town, Cape Town, South Africa; ^(b)Department of Physics, University of Johannesburg, Johannesburg, South Africa; ^(c)School of Physics, University of the Witwatersrand, Johannesburg, South Africa
- 147 ^(a)Department of Physics, Stockholm University, Stockholm, Sweden; ^(b)The Oskar Klein Centre, Stockholm, Sweden
- 148 Physics Department, Royal Institute of Technology, Stockholm, Sweden
- 149 Departments of Physics and Astronomy and Chemistry, Stony Brook University, Stony Brook, NY, USA
- 150 Department of Physics and Astronomy, University of Sussex, Brighton, UK
- 151 School of Physics, University of Sydney, Sydney, Australia
- 152 Institute of Physics, Academia Sinica, Taipei, Taiwan
- 153 Department of Physics, Technion: Israel Institute of Technology, Haifa, Israel
- 154 Raymond and Beverly Sackler School of Physics and Astronomy, Tel Aviv University, Tel Aviv, Israel
- 155 Department of Physics, Aristotle University of Thessaloniki, Thessaloniki, Greece
- 156 International Center for Elementary Particle Physics and Department of Physics, The University of Tokyo, Tokyo, Japan

- ¹⁵⁷ Graduate School of Science and Technology, Tokyo Metropolitan University, Tokyo, Japan
- ¹⁵⁸ Department of Physics, Tokyo Institute of Technology, Tokyo, Japan
- ¹⁵⁹ Department of Physics, University of Toronto, Toronto, ON, Canada
- ¹⁶⁰ ^(a)TRIUMF, Vancouver, BC, Canada; ^(b)Department of Physics and Astronomy, York University, Toronto, ON, Canada
- ¹⁶¹ Faculty of Pure and Applied Sciences, University of Tsukuba, Tsukuba, Japan
- ¹⁶² Department of Physics and Astronomy, Tufts University, Medford, MA, USA
- ¹⁶³ Centro de Investigaciones, Universidad Antonio Narino, Bogota, Colombia
- ¹⁶⁴ Department of Physics and Astronomy, University of California Irvine, Irvine, CA, USA
- ¹⁶⁵ ^(a)INFN Gruppo Collegato di Udine, Sezione di Trieste, Udine, Italy; ^(b)ICTP, Trieste, Italy; ^(c)Dipartimento di Chimica, Fisica e Ambiente, Università di Udine, Udine, Italy
- ¹⁶⁶ Department of Physics, University of Illinois, Urbana, IL, USA
- ¹⁶⁷ Department of Physics and Astronomy, University of Uppsala, Uppsala, Sweden
- ¹⁶⁸ Instituto de Física Corpuscular (IFIC) and Departamento de Física Atómica, Molecular y Nuclear and Departamento de Ingeniería Electrónica and Instituto de Microelectrónica de Barcelona (IMB-CNM), University of Valencia and CSIC, Valencia, Spain
- ¹⁶⁹ Department of Physics, University of British Columbia, Vancouver, BC, Canada
- ¹⁷⁰ Department of Physics and Astronomy, University of Victoria, Victoria, BC, Canada
- ¹⁷¹ Department of Physics, University of Warwick, Coventry, UK
- ¹⁷² Waseda University, Tokyo, Japan
- ¹⁷³ Department of Particle Physics, The Weizmann Institute of Science, Rehovot, Israel
- ¹⁷⁴ Department of Physics, University of Wisconsin, Madison, WI, USA
- ¹⁷⁵ Fakultät für Physik und Astronomie, Julius-Maximilians-Universität, Würzburg, Germany
- ¹⁷⁶ Fachbereich C Physik, Bergische Universität Wuppertal, Wuppertal, Germany
- ¹⁷⁷ Department of Physics, Yale University, New Haven, CT, USA
- ¹⁷⁸ Yerevan Physics Institute, Yerevan, Armenia
- ¹⁷⁹ Centre de Calcul de l'Institut National de Physique Nucléaire et de Physique des Particules (IN2P3), Villeurbanne, France
- ^a Also at Department of Physics, King's College London, London, UK
- ^b Also at Institute of Physics, Azerbaijan Academy of Sciences, Baku, Azerbaijan
- ^c Also at Novosibirsk State University, Novosibirsk, Russia
- ^d Also at TRIUMF, Vancouver, BC, Canada
- ^e Also at Department of Physics, California State University, Fresno, CA, USA
- ^f Also at Department of Physics, University of Fribourg, Fribourg, Switzerland
- ^g Also at Tomsk State University, Tomsk, Russia
- ^h Also at CPPM, Aix-Marseille Université and CNRS/IN2P3, Marseille, France
- ⁱ Also at Università di Napoli Parthenope, Naples, Italy
- ^j Also at Institute of Particle Physics (IPP), Victoria, Canada
- ^k Also at Particle Physics Department, Rutherford Appleton Laboratory, Didcot, UK
- ^l Also at Department of Physics, St. Petersburg State Polytechnical University, St. Petersburg, Russia
- ^m Also at Louisiana Tech University, Ruston, LA, USA
- ⁿ Also at Institutio Catalana de Recerca i Estudis Avancats, ICREA, Barcelona, Spain
- ^o Also at Department of Physics, National Tsing Hua University, Taiwan
- ^p Also at Department of Physics, The University of Texas at Austin, Austin TX, USA
- ^q Also at Institute of Theoretical Physics, Ilia State University, Tbilisi, Georgia
- ^r Also at CERN, Geneva, Switzerland
- ^s Also at Georgian Technical University (GTU), Tbilisi, Georgia
- ^t Also at O Chadai Academic Production, Ochanomizu University, Tokyo, Japan
- ^u Also at Manhattan College, New York, NY, USA
- ^v Also at Institute of Physics, Academia Sinica, Taipei, Taiwan
- ^w Also at LAL, Université Paris-Sud and CNRS/IN2P3, Orsay, France
- ^x Also at Academia Sinica Grid Computing, Institute of Physics, Academia Sinica, Taipei, Taiwan

- ^y Also at Laboratoire de Physique Nucléaire et de Hautes Energies, UPMC and Université Paris-Diderot and CNRS/IN2P3, Paris, France
- ^z Also at Dipartimento di Fisica, Sapienza Università di Roma, Rome, Italy
- ^{aa} Also at Moscow Institute of Physics and Technology State University, Dolgoprudny, Russia
- ^{ab} Also at Section de Physique, Université de Genève, Geneva, Switzerland
- ^{ac} Also at International School for Advanced Studies (SISSA), Trieste, Italy
- ^{ad} Also at Department of Physics and Astronomy, University of South Carolina, Columbia, SC, USA
- ^{ae} Also at School of Physics and Engineering, Sun Yat-sen University, Guangzhou, China
- ^{af} Also at Faculty of Physics, M.V. Lomonosov Moscow State University, Moscow, Russia
- ^{ag} Also at National Research Nuclear University MEPhI, Moscow, Russia
- ^{ah} Also at Department of Physics, Stanford University, Stanford CA, USA
- ^{ai} Also at Institute for Particle and Nuclear Physics, Wigner Research Centre for Physics, Budapest, Hungary
- ^{aj} Also at Department of Physics, Oxford University, Oxford, UK
- ^{ak} Also at Department of Physics, The University of Michigan, Ann Arbor, MI, USA
- ^{al} Also at Discipline of Physics, University of KwaZulu-Natal, Durban, South Africa
- ^{am} Also at University of Malaya, Department of Physics, Kuala Lumpur, Malaysia
- * Deceased